

On the fluctuations of the number of atoms in the condensate

Maciej B. Kruk^{1,3}, Piotr Kulik³, Malthe F. Andersen²,
Piotr Deuar¹, Mariusz Gajda¹, Krzysztof Pawłowski^{3,‡},
Emilia Witkowska¹, Jan J. Arlt², Kazimierz Rzążewski³

¹ Institute of Physics PAS, Aleja Lotników 32/46, 02-668 Warszawa, Poland

² Center for Complex Quantum Systems, Department of Physics and Astronomy, Aarhus University, Ny Munkegade 120, DK-8000 Aarhus C, Denmark.

³ Center for Theoretical Physics, Polish Academy of Sciences, Al. Lotników 32/46, 02-668 Warsaw, Poland.

E-mail: pawlowski@cft.edu.pl

February 2025

Abstract. Bose-Einstein condensation represents a remarkable phase transition, characterized by the formation of a single quantum subsystem. As a result, the statistical properties of the condensate are highly unique. In the case of a Bose gas, while the mean number of condensed atoms is independent of the choice of statistical ensemble, the microcanonical, canonical, or grand canonical variances differ significantly among these ensembles. In this paper, we review the progress made over the past 30 years in studying the statistical fluctuations of Bose-Einstein condensates. Focusing primarily on the ideal Bose gas, we emphasize the inequivalence of the Gibbs statistical ensembles and examine various approaches to this problem. These approaches include explicit analytic results for primarily one-dimensional systems, methods based on recurrence relations, asymptotic results for large numbers of particles, techniques derived from laser theory, and methods involving the construction of statistical ensembles via stochastic processes, such as the Metropolis algorithm. We also discuss the less thoroughly resolved problem of the statistical behavior of weakly interacting Bose gases. In particular, we elaborate on our stochastic approach, known as the hybrid sampling method. The experimental aspect of this field has gained renewed interest, especially following groundbreaking recent measurements of condensate fluctuations. These advancements were enabled by unprecedented control over the total number of atoms in each experimental realization. Additionally, we discuss the fluctuations in photonic condensates as an illustrative example of grand canonical fluctuations. Finally, we briefly consider the future directions for research in the field of condensate statistics.

Submitted to: *Rep. Prog. Phys.*

‡ Author to whom correspondence should be addressed.

Contents

1	Introduction	2
2	Fluctuations in the ideal gas	3
2.1	Archetype statistical ensembles	4
2.1.1	Microcanonical (MC)	4
2.1.2	Canonical (CN)	6
2.1.3	Grand Canonical (GC)	7
2.2	Bose-Einstein condensation	9
2.3	Fluctuations catastrophe	10
2.4	The Maxwell Demon (MD) rescue ensemble	12
2.5	Spectral classification	14
2.6	Historical survey	14
3	Modern frameworks for accounting fluctuations in bosonic systems	16
3.1	Stochastic ensemble sampling	16
3.2	Metropolis sampling in the classical fields approximation	17
3.3	Fock state sampling method	18
3.4	Dynamical ergodic approach and related methods	19
3.5	Master equation formulation	20
4	Role of interactions on particle number statistics	21
4.1	Bogolubov approximation	21
4.2	Anomalous fluctuations controversy	23
4.3	Beyond Bogoliubov	23
4.4	The Hybrid Sampling Method	25
5	Experiments	26
5.1	Experiments with atomic Bose gases	26
5.1.1	Relevant experimental developments	26
5.1.2	Challenges	27
5.1.3	Experimental Improvements	28
5.1.4	Experimental realization in ultracold Bose gases	28
5.1.5	Experimental results with ultracold gases	29
5.2	Experiments with Photons	31
6	Perspectives	31
7	Acknowledgments	33

1. Introduction

Fluctuations are an important property of quantum systems in general. In many cases they are well understood, however, the complete description of the fluctuations of interacting Bose gases remains an outstanding challenge. Since the field of ultracold gases is rapidly maturing, such systems are now at a state, where quantum-based sensor technology is approaching applications outside of laboratory environments, and the understanding of the fluctuations is ever more important.

In particular, Bose-Einstein condensates (BECs) have become a pivotal tool in advancing quantum simulations [1], and one might expect that a thorough understanding of their properties has been reached. Yet, despite significant theoretical efforts, the atom number fluctuations between the thermal and condensed components in an interacting Bose gas at relevant densities remain elusive. Ideally, such quantum systems can be characterized by all moments of their probability distribution, which have not yet been fully obtained for large interacting BECs [2, 3, 4, 5, 6].

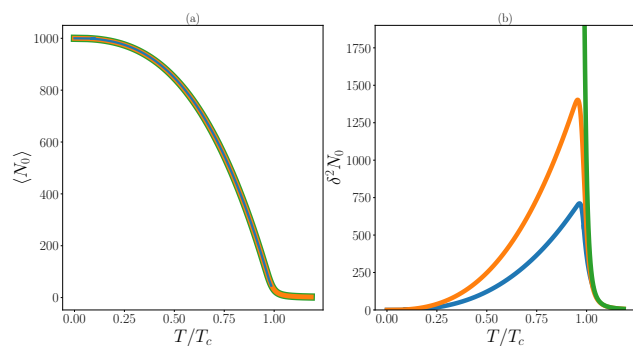


Figure 1. Illustration of the average number of condensed atoms (left) and its variance $\delta^2 N_0$ (right) as a function of temperature T in the three archetypical statistical ensembles. The choice of ensemble is irrelevant for $\langle N_0 \rangle$. On the other hand, when the temperature of an ultracold Bose gas is lowered towards the critical temperature T_c , a grand canonical ensemble (green) predicts unphysically large fluctuations. A canonical ensemble (orange) does not suffer from this problem and has fluctuations peaking just below T_c . A microcanonical ensemble shows the same temperature-dependent trend but with quantitatively lower fluctuations. Data for $N = 1000$ non-interacting atoms in an isotropic harmonic trap. The right panel is adopted from [7] (CC BY 4.0).

These fluctuations present a complex problem rich with intriguing challenges [6, 8, 9, 10, 11, 12]. In the forties of the last century, E. Schrödinger [13] was probably the first to note that the grand canonical ensemble implies unphysically large fluctuations of the condensate population below the critical temperature [14], a phenomenon known as the grand canonical catastrophe [15, 16]. This highlights one of the few cases where

different statistical ensembles yield vastly different results, necessitating the use of canonical or microcanonical approaches. See Fig. 1, which contrasts the enormous spread of condensate fluctuations between different ensembles with their good agreement for the mean condensate fraction.

Renewed interest in the statistics of the condensate was brought by the experimental discovery of BEC in ultracold atomic gases in 1995. The asymptotic expression for the variance of the condensate population in the noninteracting Bose gas under the canonical ensemble was derived by Politzer [2]. In parallel, numerical techniques were invented for the exact calculations for the finite number of particles [17]. While the canonical ensemble assumes an external reservoir exchanging energy with the system, an assumption invalid for isolated ultracold gases, nonetheless it provides a first intuitive understanding of the situation as shown in Fig. 1.

A description of experiments with ultracold atomic gases requires using the microcanonical ensemble, which is numerically challenging and has yet to be fully compared with experimental conditions. In the microcanonical ensemble, the partition function $\Gamma(E, N)$ —representing the number of ways to distribute energy E among N atoms—is key. Its computation for a noninteracting gas in a harmonic trap relates to the classical partition problem, extensively studied by mathematicians such as Leibniz and Bernoulli, with significant breakthroughs by Ramanujan and Hardy a century ago [18]. Notably, it was shown that canonical and microcanonical fluctuations coincide for large atom numbers in the noninteracting 1D gas [19, 20].

The 3D case for the microcanonical ensemble was not solved until 1997 [3], when a new ensemble, the Maxwell’s demon ensemble, was introduced. In this ensemble, the system exchanges particles with a reservoir while conserving energy, applying to the thermal cloud at low temperatures, where the BEC acts as the reservoir. This model provides an asymptotic expression for microcanonical fluctuations below the critical temperature T_c^0 of the noninteracting gas. The variance of the condensed atom number N_0 is then given by

$$\delta^2 N_0 = \left(\frac{\zeta(2)}{\zeta(3)} - \frac{3\zeta(3)}{4\zeta(4)} \right) N \left(\frac{T}{T_c^0} \right)^3, \quad (1)$$

as a function of temperature T and total atom number N where $\zeta(x)$ is the Riemann zeta function. The second term reflects the reduced fluctuations in the microcanonical ensemble compared to the canonical result, with a 61% reduction.

Of course, the ensemble description is physically meaningful only in the presence or with a history of interactions. Importantly, interactions are expected to alter condensate atom number fluctuations $\delta^2 N_0$.

In the homogeneous case, initial results indicated that interactions suppress fluctuations at low temperatures, due to strong atom pair correlations that limit the degrees of freedom [4, 5, 21]. Such interaction effects have been explored using various methods, including the Maxwell’s demon ensemble [22], number-conserving quasiparticle techniques [23, 24], and master-equation methods [25, 26], but most approaches either do not fully account for microcanonical conditions or are restricted to low temperatures [27] and small atom numbers.

Finally, under many conditions below T_c , the fluctuations are expected to scale *anomalously* with atom number $\delta^2 N_0 \propto N^{1+\gamma}$, with $\gamma \neq 0$ [4, 5] in stark contrast to most classical systems where the central limit theorem ensures normal scaling of the fluctuations $\delta^2 N \propto N$ due to the existence of a finite microscopic coherence length scale [21, 28].

The experimental characterization of BEC atom number fluctuations has long been a significant challenge, largely hindered by technical fluctuations in BEC experiments. However, this limitation was recently overcome [29], allowing for the experimental progress that led to the first ever observation of the fluctuations in the atomic BEC [30, 9], detailed at the end of this review. Notably, the measured fluctuations were significantly smaller than predicted by the canonical ensemble [9]. In parallel, significant theoretical progress has recently been made and the Fock state sampling and related hybrid sampling techniques bring the description of experimental systems into reach.

In this review we first describe in detail the baseline situation of the ideal gas in its many forms in Sec. 2, including a historical survey of results since the 1990s. Sec. 3 then reviews numerical approaches used to generate ensembles of samples/realizations for analysis of realistic finite-size cases, with particular attention on Monte Carlo approaches based on a Metropolis algorithm. Sec. 4 dives into the fascinating and not fully resolved topic of fluctuations in the weakly interacting condensates, along with again a historical survey of results since the 1990s. Sec. 5 outlines the recent remarkable experimental progress which has allowed direct measurement of the global condensate fluctuations. Finally we conclude and summarize the near- and mid-term future outlook of the topic in Sec. 6.

2. Fluctuations in the ideal gas

The ideal gas fluctuation behaviour underlies the whole topic, and across different dimensionalities, ensembles, and geometries demonstrates already many of the essential features and unusual results of condensate

fluctuation statistics, as well as the methodological difficulties involved. Therefore in the first half of the review its features and the methods that can be used to study it will be described in detail, concentrating on the results discovered since the 1990s till today.

2.1. Archetype statistical ensembles

Statistical mechanics provides a formalism allowing for the description of systems of large numbers of particles in the language of probability theory. It is based on the concept of statistical ensembles, i.e. a set of all possible states of the system subject to external constraints imposed on the system. Every ensemble is characterized by the corresponding partition functions, that determine statistical properties of the gas. To quantify the statistics we use throughout the review the probability distribution of the number of atoms outside condensate, denoted with $\mathcal{P}(N_{\text{ex}})$. Of particular interest are the low moments of the distribution

$$\langle N_{\text{ex}} \rangle = \sum_{N_{\text{ex}}} \mathcal{P}(N_{\text{ex}}) N_{\text{ex}} \quad (2)$$

$$\langle N_{\text{ex}}^2 \rangle = \sum_{N_{\text{ex}}} \mathcal{P}(N_{\text{ex}}) N_{\text{ex}}^2. \quad (3)$$

These statistical moments can be used to compute the average number of atoms in the condensate and the main subject of this review – the fluctuations:

$$\langle N_0 \rangle = N - \langle N_{\text{ex}} \rangle \quad (4)$$

$$\delta^2 N_0 = \delta^2 N_{\text{ex}} = \langle N_0^2 \rangle - \langle N_0 \rangle^2 \quad (5)$$

The last equation applies only in the absence of particle exchange with the environment and then expresses the fact that since the gas comprises only condensed and excited atoms, their fluctuations must be equal to each other. It does not hold in the grand canonical ensemble as will be discussed later.

In the formalism of statistical physics, many-body systems at thermal equilibrium can be described by several parameters, which can be divided into extensive ones, such as total energy E , number of particles N , and volume V , and corresponding intensive parameters, such as temperature T , chemical potential μ , and pressure p . Ultracold atomic gases, however, are typically trapped in a harmonic potential; they are not uniform, and their volume is not well defined. The role of the volume of the gas container, V , is replaced by the external trap frequency ω . In the following, we will focus on equilibrium systems, assuming that the trap frequency (or volume) is fixed. Therefore, we will omit the corresponding variables ω , or V from the formalism presented below, as they do not play a role.

We start by recalling the three archetypical ensembles for describing the ideal Bose gas, the microcanonical, canonical and grand canonical ensembles in

Sections 2.1.1, 2.1.2 and 2.1.3. We show the textbook definitions for particular partition functions and complement them with non-standard examples of their analytical evaluation relevant for BECs. The applications of the formalism to the fluctuations of the ideal Bose gas are presented in Section 2.2 and 2.4.

2.1.1. Microcanonical (MC) If the system is perfectly isolated, it is natural to assume that all (micro)states of the system consisting of N particles and having total energy E are equally probable. The statistical ensemble assigned to such a system is the microcanonical ensemble (MC). The uniform probability distribution assigned to every state of this ensemble is equal to $1/\Gamma(E, N)$ where $\Gamma(E, N)$ is the microcanonical partition function, equal to the number of all microstates that meet the constraints of energy and particle number. To give a more operational definition we assume that energy is coarse-grained, i.e. the entire range of energies is divided into energy shells $\Delta_E \ll E$ such, that the number of states N_Δ within a given interval is large $N_\Delta \gg 1$. For large systems, the final results do not depend on the particular choice of Δ_E . The microcanonical partition function is then:

$$\Gamma(E, N) = \sum_{\text{states}} \delta_{\Delta_E}(E - H_N), \quad (6)$$

where H_N is a Hamiltonian of the N -particles system, and, according to our discussion on coarse-graining, $\delta_{\Delta_E}(E - H_N) = 1$, if the energy of a given state is in the interval $[E - \Delta_E; E]$ and zero otherwise.

Knowledge of $\Gamma(E, N)$ alone does not suffice to determine the system's statistical properties directly. Specifically, fluctuations in the atom number within the condensate – the primary focus of this review – require an additional quantity $\Gamma_{\text{ex}}(E, N_{\text{ex}})$. This represents the total number of microstates with exactly N_{ex} atoms in excited states at energy E . The probability of observing exactly N_{ex} excited bosons is: $\mathcal{P}(E, N_{\text{ex}}) = \Gamma_{\text{ex}}(E, N_{\text{ex}})/\Gamma(E, N)$. (7)

This distribution is sufficient to compute the statistical properties of interest following Eqs. (2)-(4).

The calculation of the microcanonical partition function $\Gamma(E, N)$ or $\Gamma_{\text{ex}}(E, N_{\text{ex}})$ leads inevitably to combinatorial problems, which we illustrate in the conceptually simplest case of an ideal gas trapped in a one dimensional harmonic trap. In this case, the spectrum of a single particle is, in oscillatory units, $\epsilon_j = j$, ($j = 0, 1 \dots$)§. Therefore each microstate is just a set of N integers, being the N ordered values of occupied energy levels, i.e. $0 \leq \epsilon_{j_1} \leq \epsilon_{j_2} \leq \dots \leq \epsilon_{j_N}$, and obeying the constraint of fixed energy

$$E = \epsilon_{j_1} + \epsilon_{j_2} + \dots + \epsilon_{j_N}. \quad (8)$$

§ Without loss of generality we are omitting everywhere the shift $\hbar\omega/2$.

The partition function $\Gamma(E, N)$ is the number of the microstates with given energy and number of atoms, so here – the number of ways of writing the integer E as a sum of N non-negative integers, as in Eq. (8). Although the problem has a simple mathematical presentation via Eq. (8), still finding explicitly $\Gamma(E, N)$ is a challenging task, even numerically. It is related to a classic problem in the number theory called the “partition problem”, studied over centuries by many mathematicians, Leibnitz, Euler, Bernoulli, Hardy, Ramanujan to name a few [31]. The partition problem is to find the number of partitions $A(E)$ of an integer E into a sum of **any number of positive** integers $\epsilon_j^{(+)}$

$$E = \epsilon_{j_1}^{(+)} + \epsilon_{j_2}^{(+)} + \dots \quad (9)$$

In the context of our physical problem $\epsilon_j^{(+)}$ shall be interpreted as the occupied excited energy levels in one microstate. Finally Ramanujan and Hardy found the asymptotic (large E) solution $A(E) = \frac{e^{\pi\sqrt{2E/3}}}{4E\sqrt{3}}$ [18].

Note that the maximal number of terms on the right-hand side of Eq. (9) is E – this is a partition with all terms equal 1. This observation, if we interpret the terms as occupied excited energy levels, means that the number of excited atoms is limited, i.e. $N_{\text{ex}} \leq E$. As a consequence, if $N \geq E$, then at least $N - E$ atoms, however large N is, must occupy the 0-energy level, i.e. the ground state. This saturation of the number of excited atoms is reminiscent of the origin of Bose-Einstein condensation, which will be discussed later ¶. In the case of $N > E$, to every partition of the form Eq. (9), one can add $N_0 := N - N_{\text{ex}}$ zeros:

$$E = \underbrace{0 + 0 + \dots + 0}_{N_0 \text{ atoms at } \epsilon_0} + \underbrace{\epsilon_{j_1}^{(+)} + \dots + \epsilon_{j_{N_{\text{ex}}}}^{(+)}}_{N_{\text{ex}} \text{ excited atoms}} \quad (10)$$

to obtain a decomposition of the form of Eq. (8). This implies that for $N \geq E$, $\Gamma(E, N)$ does not depend on N and is just equal to $A(E)$.

Finding the statistics of the number of excited atoms, $\mathcal{P}(E, N_{\text{ex}})$, requires the function $\Gamma_{\text{ex}}(E, N_{\text{ex}})$. In the case of a 1D harmonic oscillator, $\Gamma_{\text{ex}}(E, N_{\text{ex}})$ is the number of ways of writing the energy E as a sum of exactly N_{ex} positive integers, known as the problem of restricted partitions. There are asymptotic formulas for $\Gamma_{\text{ex}}(E, N_{\text{ex}})$ in some specific cases [32, 33], but the general problem remains unsolved [34]. The $\Gamma_{\text{ex}}(E, N_{\text{ex}})$ can, however, be computed numerically using various recurrence relations, among which the

¶ The exact values can be easily evaluated using for instance Mathematica (function `PartitionP[]`).

¶ Strictly speaking, there is no condensation in a one dimensional system due to the lack of a critical temperature in the limit $N \rightarrow \infty$, but still the number of excited atoms is bounded for any finite fixed energy.

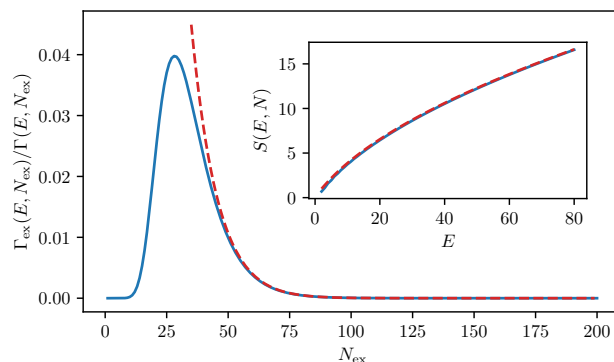


Figure 2. The microcanonical probability distribution of having N_{ex} atoms in a 1d harmonically trapped Bose gas: exact result (blue solid) obtained via Eq. (11) and asymptotic formulas for the number of restricted [33] partitions (dashed red). The inset shows comparison of the entropy $S(E, N) := k_B \ln \Gamma(E, N)$, where $\Gamma(E, N)$ is computed via exact method (blue line) or approximated with the asymptotic formula $A(E)$ [18] (red dashed line). Parameters $E = 200$ and $N > E$.

simplest – for the 1D harmonic oscillator – is:

$$\Gamma_{\text{ex}}(E, N_{\text{ex}}) = \Gamma_{\text{ex}}(E - 1, N_{\text{ex}} - 1) + \Gamma_{\text{ex}}(E - N_{\text{ex}}, N_{\text{ex}}). \quad (11)$$

Other recurrence relations for $\Gamma_{\text{ex}}(E, N_{\text{ex}})$ in this special case of a 1D gas in a harmonic potential are reported in [35]. Fig. 2 illustrates the accuracy of the asymptotic formulas of [33] and [18] by comparing them with exact results for entropy and probability distribution obtained with Eq. (11). Although the asymptotic formulas are sufficient to estimate entropy as a function of energy, and therefore also the temperature, they are not sufficiently accurate to give reliable statistics of N_{ex} . The analogy to number theory, and the results of mathematicians (e.g. Erdős [36]), allowed the Authors of [15] to study the fluctuations of the number of ground state atoms in the 1D harmonic potential analytically and show e.g. that $\Delta N_0/N \approx \frac{\pi}{\sqrt{6}} \frac{T}{\ln N} \frac{T}{T_0}$, with a characteristic temperature $T_0 := N/\ln N$. Further works [35] studied higher moments of the distribution $\mathcal{P}(E, N_{\text{ex}})$.

The above correspondence between the micro-canonical partition function and the classic problem in number theory is due to the simple spectrum of the 1D harmonic oscillator. In the case of a box, the problem reduces to finding the function $A_2(E)$, which represents the number of ways to partition E as a sum of squares. An asymptotic formula for $A_2(E)$ was first proposed by Hardy in his foundational 1918 paper [18]. This formula was later proved by E. Wright in 1934 [37] and subsequently simplified by R. Vaughan in 2015 [38]. It is:

$$A_2(E) \propto \exp\left(3\sqrt[3]{E}\Gamma(3/2)^2\zeta(3/2)^2/4\right) \quad (12)$$

In higher dimensions or for more complex spectra,

the problems of finding asymptotic solutions become increasingly difficult and less explored.

On the other hand there exist recurrence relations for Γ_{ex} for any energy spectrum. For instance, one can build on the recurrence relation for another object $\Gamma_{\text{ex}}(N, E, \varepsilon_j^c)$, the number of partitions of energy E into N terms, none of them exceeding ε_j^c . Here ε_j^c serves as the energy cut-off, limiting the available spectrum. The recurrence relation over the energy cut-off is [39]:

$$\Gamma_{\text{ex}}(N, E, \varepsilon_j^c) = \sum_{N_j=0}^N \Gamma_{\text{ex}}(N - N_j, E - N_j \varepsilon_j^c, \varepsilon_{j-1}^c) \binom{d(\varepsilon_j^c) + N_j - 1}{N_j - 1}. \quad (13)$$

The iterator N_j in the sum is the number of particles at the cut-off energy level ε_j^c . Due to the possible degeneracy $d(\varepsilon_j^c)$ of this level, the N_j atoms can be distributed in $\binom{d(\varepsilon_j^c) + N_j - 1}{N_j - 1}$ ways. The remaining $N - N_j$ atoms occupy levels not larger than ε_{j-1}^c and carry the energy $E - N_j \varepsilon_j^c$. The recurrence starts with $\Gamma_{\text{ex}}(N, E, \varepsilon_0) = \delta_{N,0} \delta_{E,0}$ and ends once ε_j^c reaches the total energy E , because $\Gamma_{\text{ex}}(N, E, E) \equiv \Gamma_{\text{ex}}(N, E)$.

The recurrence Eq. (13) is valid for any energy spectrum. The main challenges in using Eq. (13) are numerical complexity (scaling as $\mathcal{O}(E^2)$) and the necessity to deal with large and small numbers simultaneously⁺. Other recurrences of a similar complexity to Eq. (13) can be found in [17].

More generally, the task of finding $\Gamma(E, N)$ and $\Gamma_{\text{ex}}(E, N_{\text{ex}})$ is of relevance in many branches of science. It has been shown in [40], that the $D - 1$ dimensional case is related to the compact lattice animal problem discussed for instance in [41], further related to the Pott model (a generalization of the Ising Hamiltonian). The result can also be used to derive statistical properties of 1D fermions, using the concept of Fermion-Boson transmutation [42] (see also [43]). These and further analogies between very different systems have lead to the development of new numerical codes to compute partition functions [44] notwithstanding that the computation of the number of partitions is a hard numerical challenge belonging to the NP complexity class [45].

It turns out then, that the microcanonical ensemble, although conceptually the simplest one and directly related to many mathematical problems, is also the most difficult ensemble to use.

2.1.2. Canonical (CN) Now we turn to the situation when the system of interest can exchange energy, but

⁺ To evaluate the Eq. (13) we have used the C language MPFR numerical library for high-precision arithmetic.

not particles, with a heat-bath (a thermostat) of a constant temperature T . In equilibrium the system's temperature is obviously the same as the thermostat but its energy fluctuates. The ensemble of microstates corresponding to such an arrangement is known as the canonical ensemble (CN) with the partition function defined as:

$$\mathcal{Z}(\beta, N) = \sum_E e^{-\beta E} \Gamma(E, N), \quad (14)$$

where states contributing to a given microcanonical energy E are weighted with a Boltzmann factor $e^{-\beta E}$, with $\beta = 1/k_B T$ and Boltzmann constant k_B .

The Boltzmann factor decreases exponentially with energy, while the microcanonical partition function $\Gamma(E, N)$ grows exponentially. The product of the two has a maximum around the mean energy

$$\langle E \rangle = -\frac{\partial}{\partial \beta} \ln \mathcal{Z}(\beta, N), \quad (15)$$

as illustrated in Fig. 3. Therefore, the sum in Eq. (14), can be approximated by the integral:

$$\mathcal{Z}(\beta, N) \approx e^{\ln \Gamma(\langle E \rangle, N) - \langle E \rangle \beta} \int dE e^{-\frac{(E - \langle E \rangle)^2}{2\delta^2 E}}, \quad (16)$$

where $(\delta^2 E)^{-1} = (\partial^2 / \partial E^2) \ln \Gamma(\langle E \rangle) > 0$ is a squared width of the maximum of the energy distribution. If, in the limit of $N, E \rightarrow \infty$, the width of the distribution scales as $\delta^2 E \sim \mathcal{O}(\langle E \rangle)$, then:

$$\frac{\sqrt{\delta^2 E}}{\langle E \rangle} \sim \frac{1}{\sqrt{\langle E \rangle}}. \quad (17)$$

If this condition is met, the ensembles are considered to be equivalent (having in mind the thermodynamic limit). The criterion Eq. (17), is met if $\ln \Gamma(E, N)$ is an extensive function [46]. Then the whole sum in Eq. (14) is dominated by a single term, the one which corresponds to the mean energy given by Eq. (15). Taking the logarithm of both sides of Eq. (16) and maintaining the dominant terms, one finds that the partition functions of CN and MC ensembles are related:

$$\ln \Gamma(E, N) \approx \ln \mathcal{Z}(\beta, N) + E\beta, \quad (18)$$

where the canonical mean energy $\langle E \rangle$ equals the microcanonical energy, $\langle E \rangle = E$. In the above equation, β is not an independent variable, but depends on the energy according to Eq.(15), $\beta = \beta(E, N)$. Eq. (18) is then the Legendre transformation converting a function $\ln \mathcal{Z}(\beta, N)$ of variable β into a function $\ln \Gamma(E, N)$ that depends on the conjugate quantity, $E = -\partial(\ln \mathcal{Z})/\partial \beta$. Different discussions for the equivalence between ensembles can be found in [47].

A compact expression for the canonical partition function of an ideal gas can be obtained from the following form

$$\mathcal{Z}(\beta, N) = \sum_{N_1=0}^{\infty} \sum_{N_2=0}^{\infty} \dots e^{-\beta E} \delta_{\sum_j N_j, N}, \quad (19)$$

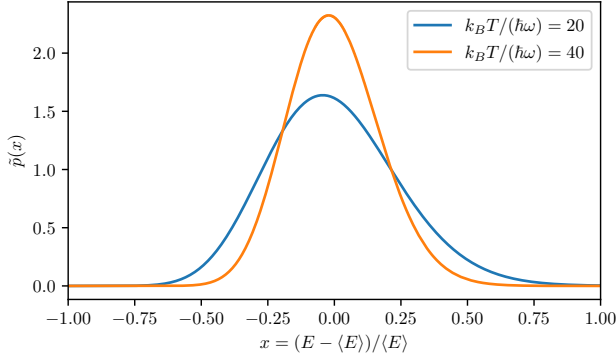


Figure 3. The probability distribution of microstates with energy E and $N = 100$ particles, $\mathcal{P}(E) = \Gamma e^{-\beta E} / \mathcal{Z}$, in a CN ensemble in a 1D harmonic trap given by Eq. (14). The figure illustrates the shrinking relative width of the energy distribution, shown using the normalised probability distribution $\tilde{p}(x) = \langle E \rangle \mathcal{P}(E(x))$ in the relative variable $x = (E - \langle E \rangle) / \langle E \rangle$.

where the Kronecker delta function enforces the condition of having exactly N atoms in the system, i.e. $N = \sum_{j=0}^{\infty} N_j$ with populations N_j of for the j th state. Since the gas is non-interacting, therefore the total energy E equals $\sum_j \epsilon_j N_j$, with the single-particle energies ϵ_j . Introducing an integral representation of the delta function, $\delta_{a,b} = \frac{1}{2\pi} \int_0^{2\pi} e^{ix(a-b)} dx$, one can calculate all sums over N_j :

$$\mathcal{Z}(\beta, N) = \frac{1}{2\pi} \int dx e^{-ixN} \prod_{j=1}^{\infty} \frac{1}{1 - e^{-(\beta\epsilon_j + ix)}}, \quad (20)$$

that simplify further due to the residue theorem for a complex variable $z = e^{ix}$:

$$\mathcal{Z}(\beta, N) = \sum_{j=1}^{\infty} e^{-\beta\epsilon_j(N-1)} \prod_{l \neq j} \frac{1}{1 - e^{-\beta(\epsilon_l - \epsilon_j)}}. \quad (21)$$

This final formula for the partition function (19) applies to any spectrum provided it is non-degenerate. A useful quantity is the partition function for the system of N atoms among which exactly N_{ex} are in the excited states. It can be computed similarly to the derivation presented above but with the Kronecker delta imposing the fixed number N_{ex} of excited bosons:

$$\mathcal{Z}_{\text{ex}}(\beta, N_{\text{ex}}) = \sum_{j=1}^{\infty} e^{-\beta\epsilon_j(N_{\text{ex}}-1)} \prod_{l \neq j} \frac{1}{1 - e^{-\beta(\epsilon_l - \epsilon_j)}}. \quad (22)$$

With this quantity one can compute the probability distribution $\mathcal{P}(\beta, N_{\text{ex}}) = \mathcal{Z}_{\text{ex}}(\beta, N_{\text{ex}}) / \mathcal{Z}(\beta, N)$ [48], and as a consequence also expectation values of the number of condensed and excited bosons, as well as their fluctuations. In this special case of a 1D harmonic oscillator, partition functions can be expressed in simpler form:

$$\mathcal{Z}(\beta, N) = \prod_{j=1}^N \frac{1}{1 - e^{-\beta j}} \quad (\text{for 1D h. o.}) \quad (23)$$

$$\mathcal{Z}_{\text{ex}}(\beta, N_{\text{ex}}) = e^{-\beta N_{\text{ex}}} \prod_{j=1}^{N_{\text{ex}}} \frac{1}{1 - e^{-\beta j}} \quad (\text{for 1D h. o.}) \quad (24)$$

The same approach can also be generalized to a 1D box with periodic boundary conditions under careful consideration of the double degeneracy of each excited state [49].

Another procedure for obtaining the canonical partition function uses directly the definition (14) with $\Gamma(E, N)$ obtained via methods described in Sec. 2.1.1. Yet another, quite efficient method to obtain $\mathcal{Z}(\beta, N)$ follows the recurrence relation (see the Appendix of [17] for a quick proof)

$$\mathcal{Z}(\beta, N) = \sum_{n=1}^N \mathcal{Z}(n\beta, 1) \mathcal{Z}(\beta, N - n), \quad (25)$$

that connects the “target” partition function with a smaller number of atoms $\mathcal{Z}(\beta, N - n)$, and a single particle partition for a low temperature $\mathcal{Z}(n\beta, 1)$. Finally $\mathcal{Z}(\beta, N)$ can be computed from the grand canonical partition function using contour integrals [2] as introduced in the next section.

2.1.3. Grand Canonical (GC) Thirdly, we consider a system in contact with a reservoir of both energy and particles. We assume that the reservoir has a constant temperature T , and particles can flow back and forth between the system and the reservoir. The energy cost of adding a particle to the system is given by the negative chemical potential μ , which is used to define the fugacity $z = e^{\beta\mu}$.

The grand canonical (GC) description does not introduce any constraints on the energy nor on the number of particles. All values are allowed, but Gibbs statistical weights $e^{\eta(\mu N - E)} = z^N e^{-\beta E}$ are introduced instead. The GC partition function $\Xi(\beta, z)$, that determines the probability distribution in the space of all microstates with an arbitrary energy and arbitrary number of particles, is defined as:

$$\Xi(\beta, z) = \sum_N z^N \mathcal{Z}(\beta, N), \quad (26)$$

where each term in the above sum is proportional to the probability of having N particles in the ensemble. The mean number of particles is controlled by the fugacity z , and in the thermodynamic limit:

$$\langle N \rangle = \frac{\partial}{\partial(\beta\mu)} \ln \Xi(\beta, \mu) = z \frac{\partial}{\partial z} \ln \Xi(\beta, z). \quad (27)$$

The entire distribution has a maximum at $N = \langle N \rangle$, if the value of the second derivative, $(\partial^2 / \partial(\beta\mu)^2) \ln \mathcal{Z}(\langle N \rangle)$ is negative, what is the usual case, see [46]. Then the derivative can be interpreted as $(\delta^2 N)^{-1}$. Moreover, because $(\delta^2 N)$ is extensive, the criterion of equivalence between the GC and CN ensembles takes the form:

$$\frac{\sqrt{\delta^2 N}}{\langle N \rangle} = \frac{1}{\sqrt{\langle N \rangle}}, \quad (28)$$

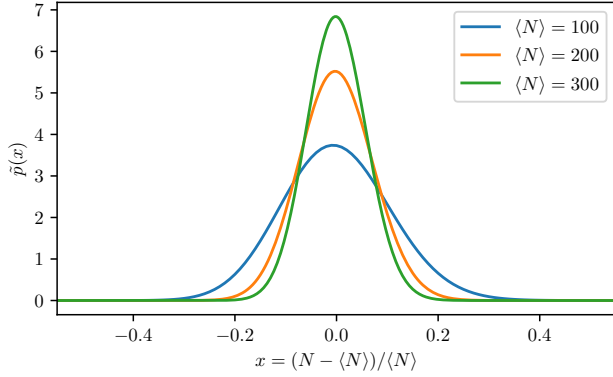


Figure 4. The narrowing of the probability distribution of microstates with N particles, $\mathcal{P}(N) = z^N \mathcal{Z}/\Xi$, in a 3D harmonic trap given by Eq. (26). We illustrate the shrinking particle number distribution $\tilde{p}(x)$ width (relative to the mean particle number) in the variable $x = (N - \langle N \rangle)/\langle N \rangle$, $\tilde{p}(x) = \langle N \rangle \mathcal{P}(N(x))$ for constant, uncondensed, $T/T_c > 1$. The chemical potential μ is fixed by the choice of $\langle N \rangle$.

i.e. in the limit of $\langle N \rangle \rightarrow \infty$ the probability distribution becomes a delta-like function focused on the mean number of particles, a trend shown in Fig. 4.

In such a case the canonical and grand canonical partition functions are related. The transformation from $\mathcal{Z}(\beta, N)$ into $\Xi(\beta, z)$ is the Legendre transformation:

$$\ln \mathcal{Z}(\beta, N) \approx \ln \Xi(\beta, z) - N \ln z. \quad (29)$$

As we will demonstrate in the next section, a Bose-Einstein condensate is a system in which this equivalence between different statistical ensembles is violated.

In contrast to the MC and CN formalisms, where determining partition functions analytically is possible only for a few special cases, obtaining the GC partition function is much simpler. This is because detailed constraints on the number of particles and energy are relaxed.

Summation over all single-particle energies ϵ_j in the spectrum can be substituted by summation over all one-particle states and corresponding occupation numbers N_j . For bosonic particles the N_j can take any integer value from zero to infinity. Had we considered fermionic particles, N_j could take only two values, zero or one. The energy of the system is $E = \sum_j N_j \epsilon_j$ and N is the sum of occupations of all states.

According to Eq. (26) we have:

$$\begin{aligned} \Xi(T, \mu) &= \sum_{N=0}^{\infty} \sum_{\{N_j\}_N} e^{-\sum_j N_j \beta(\epsilon_j - \mu)} = \quad (30) \\ &= \left(\sum_{N_0=0}^{\infty} \dots \right) \dots \left(\sum_{N_j=0}^{\infty} e^{-N_j \beta(\epsilon_j - \mu)} \right) \dots, \end{aligned}$$

where by $\{N_j\}_N$ we denote all sets of occupation numbers satisfying condition $\sum_j N_j = N$. From the above equation, by noticing that the terms in brackets are geometric series, we get:

$$\ln \Xi(\beta, z) = - \sum_{\epsilon_j} d(\epsilon_j) \ln(1 - z e^{-\beta \epsilon_j}), \quad (31)$$

where now summation goes over all energies and $d(\epsilon_j)$ is a factor accounting for their degeneracy [46].

We now focus on the most important case experimentally, the ideal gas in a 3D isotropic harmonic oscillator potential of frequency ω . As in Sec. 2.1.1 we shift the spectrum by the lowest energy (here $3\hbar\omega/2$) such that the ground state energy is 0, and we use oscillatory units for energy $\epsilon_0 = \hbar\omega$, dimensionless temperature $k_B T/\epsilon_0$.

The one-particle eigenenergies remain integers $\epsilon_j = j$ and the degeneracy of the energy state ϵ_j is $d(\epsilon_j) = (j+2)(j+1)/2$ (or $d(\epsilon_j) = j+1$ in 2D and $d(\epsilon_j) = 1$ in the 1D case).

The asymptotic expression for the GC partition function Ξ can be easily found. Using the Euler-MacLaurin formula to substitute summation over a discrete energy spectrum by integration and by noticing that $\ln(1-x) = -\sum_{l=0}^{\infty} \frac{x^l}{l}$ we have:

$$\ln \Xi(\beta, z) = -\ln(1-z) + \ln \Xi_{\text{ex}}(\beta, z), \quad (32)$$

where the term $\ln \Xi_{\text{ex}}(\beta, z)$ is the contribution from excited states:

$$\begin{aligned} \ln \Xi_{\text{ex}}(\beta, z) &\approx \sum_{l=0}^{\infty} \frac{z^l}{2l} \int_0^{\infty} d\epsilon_j e^{-l\beta\epsilon_j} (\epsilon_j + 2)(\epsilon_j + 1) \\ &\approx \frac{1}{\beta^3} g_4(z), \end{aligned} \quad (33)$$

The Bose function $g_\alpha(z)$ is defined as

$$g_\alpha(z) = \sum_{j=1}^{\infty} \frac{z^j}{j^\alpha}, \quad (34)$$

and the series is convergent for $0 \leq z \leq 1$ (if $\alpha > 1$). That is, over the physical range of variation of the fugacity $z = e^{\beta\mu}$ because the chemical potential for an ideal Bose gas is not larger than the one-particle ground state energy. If $\alpha > 1$, the values of $g_\alpha(z)$ at $z = 1$ are equal to the Riemann zeta function $g_\alpha(1) = \zeta(\alpha)$ and are finite. If $\alpha = 1$ then $g_1(z) = -\ln(1-z)$, and has a logarithmic divergence at $z = 1$. For $\alpha < 1$ the divergence is stronger. It is straightforward to check also that

$$z \frac{d}{dz} g_\alpha(z) = g_{\alpha-1}(z). \quad (35)$$

In (33) we omitted terms proportional to $1/\beta^2$ and $1/\beta$ because, as it will become clear soon, we are interested in the small β (i.e. large temperature) behaviour of $\ln \Xi(\beta, z)$. Combining the

two contributions, from the ground and excited states we have:

$$\ln \Xi(\beta, z) \approx -\ln(1-z) + \frac{1}{\beta^3} g_4(z). \quad (36)$$

The temperature and mean energy of the system are related:

$$\bar{E} = -\frac{\partial}{\partial \beta} \ln \Xi(\beta, z) = 3 \frac{g_4(z)}{\beta^4} \sim T^4, \quad (37)$$

which reminds one of the Stefan-Boltzmann law.

2.2. Bose-Einstein condensation

The textbook statistical description of a Bose-Einstein condensation is traditionally made within the GC ensemble following the very first ideas of A. Einstein [50, 46], and considers the thermodynamic limit of a D dimensional system in which the system size does not affect the intensive quantities,

$$\langle N \rangle \rightarrow \infty, \quad \beta \rightarrow 0, \quad \text{but } \langle N \rangle \beta^D = \text{const.} \quad (38)$$

In this formalism, and focusing on the ideal gas in a 3D isotropic harmonic oscillator potential as considered in 2.1.3, the mean number of particles $\langle N \rangle$ in the system depends on the temperature and the chemical potential/fugacity,

$$\langle N \rangle = \frac{z}{1-z} + \frac{1}{\beta^3} g_3(z), \quad (39)$$

see Eq.(27). The two terms on the right-hand side have physical interpretations: the mean occupation of the ground state and the mean occupation of all excited states, respectively:

$$\langle N_0 \rangle = \frac{z}{1-z}, \quad (40)$$

$$\langle N_{\text{ex}} \rangle = \frac{g_3(z)}{\beta^3}, \quad (41)$$

For a given inverse temperature β , the mean number of particles in excited states is limited by the value

$$\langle N_{\text{ex}} \rangle \leq \frac{g_3(1)}{\beta^3} = \frac{\zeta(3)}{\beta^3} = N_c. \quad (42)$$

Alternatively one can define a ‘critical’ value of $\beta = \beta_c$ as the temperature when maximal ‘capacity’ of excited states N_c is equal to the mean number of all particles, $\langle N \rangle$, in the system:

$$\beta_c = \frac{1}{T_c} = \left(\frac{\zeta(3)}{\langle N \rangle} \right)^{1/3}. \quad (43)$$

Combining Eq. (37) and Eq. (43) the mean energy of the system at the Bose-Einstein transition can be found:

$$E_c = 3 \frac{\zeta(4)}{\beta_c^4} = 3\zeta(4) \left(\frac{\langle N \rangle}{\zeta(3)} \right)^{4/3}. \quad (44)$$

It is convenient to rewrite equation Eq. (39) as:

$$\langle N \rangle \beta^3 = \langle N_0 \rangle (z) \beta^3 + g_3(z). \quad (45)$$

Equation (45) can be thought of as the equation determining a value of z for a given mean number of particles $\langle N \rangle$ (which now becomes a parameter of the system) and a temperature. In the thermodynamic limit (38) and above critical temperature the first term on the right-hand side of Eq.(45) vanishes, $\lim_{\beta \rightarrow 0} \langle N_0 \rangle (z) \beta^3 = 0$, because the fugacity z found from:

$$g_3(z) = \langle N \rangle \beta^3, \quad (46)$$

is $z < 1$, and consequently $\langle N_0 \rangle$ from Eq. (40) is finite (i.e. negligible in the thermodynamic limit). Below the critical temperature, i.e. for $\beta > \beta_c$, the fugacity must remain fixed at $z = 1$, in order to keep $\langle N \rangle \beta^3$ finite ($g_3(z > 1)$ diverges) and one obtains a non-zero mean fraction, $\lim_{\langle N \rangle \rightarrow \infty} \langle N_0 \rangle / \langle N \rangle > 0$, of particles in the ground state. This effect of sudden accumulation of a finite fraction of atoms in the ground state, usually observed while cooling the system down below critical temperature, is known as Bose-Einstein condensation. Equation (45) allows one to find the fraction of condensed particles:

$$\frac{\langle N_0 \rangle}{\langle N \rangle} = 1 - \left(\frac{T}{T_c} \right)^3. \quad (47)$$

The phase transition to the Bose-Einstein condensate is a direct consequence of a ‘finite capacity’ of excited states at fixed temperature. The above ‘textbook’ reasoning however, is loosely based on the assumption that the mean number of particles in the system remains constant or well controlled in this formulation also when temperature is decreased below the critical value. A potential problem with this, which we will return to in Sec. 2.3, is that $\langle N \rangle$ is extensive and not an original control parameter of the model formulated in (26) and (30), which was given in terms of only intensive parameters z and T . This leads to the following paradox: below T_c we found that fugacity is constant $z = 1$, therefore it cannot serve as a control knob in the model for the average number of particles, and the two-dimensional parameter space of systems with differing $\langle N \rangle$ and T is left underconstrained with only one control parameter T .

Bose-Einstein condensation depends on spatial dimensionality and on the shape of external trapping potential. This is because the phenomenon is sensitive to the density of states as we saw in Eq. (33). Calculations analogous to those presented above, allow one to find analytic expressions for the grand canonical partition function in the thermodynamic limit for dimensionalities $D = 2$ and $D = 1$:

$$\ln \Xi^{(D)}(\beta, z) \approx -\ln(1-z) + \frac{1}{\beta^D} g_{D+1}(z). \quad (48)$$

Based on this result, the relation between the fugacity and mean number of particles in the system, takes the form (compare Eq. (45)):

$$\langle N \rangle \beta^D = g_D(z) + \langle N_0 \rangle \beta^D. \quad (49)$$

If $\langle N_0 \rangle$ is finite, the second term in the right-hand side of the above equation can be neglected when passing to the thermodynamic limit (38). Evidently occupation of the ground state $\langle N_0 \rangle$ is finite in the limit of $N \rightarrow \infty$, hence $\langle N_0 \rangle / \langle N \rangle$ is negligible, as long as there exists a z solving the equation

$$\langle N \rangle \beta^D = g_D(z) \quad (50)$$

analogous to Eq.(46). In two dimensions, $g_2(z)$ is limited by the value $g_2(1) = \zeta(2) = \pi^2/6$. If $\langle N \rangle \beta^2 > \zeta(2)$, there is no solution of (50). For a fixed value of $\langle N \rangle$, there exists a critical temperature above which Eq. (50) is satisfied and all particles accumulate in the excited states:

$$\beta_c^{D=2} = \frac{1}{T_c^{D=2}} = \left(\frac{\zeta(2)}{\langle N \rangle} \right)^{1/2}. \quad (51)$$

If temperature decreases below the critical one and assuming that the mean number of particles in the system does not change, then because the capacity of excited states saturates at $N_c^{D=2}(T) = \zeta(2)/\beta^2$, the equation Eq.(49) can be solved with $z = 1$, and (51) giving a mean fraction of ground state particles that is finite:

$$\frac{\langle N_0 \rangle}{\langle N \rangle} = 1 - \left(\frac{T}{T_c^{D=2}} \right)^2. \quad (52)$$

This demonstrates the Bose-Einstein condensation of the ideal gas trapped in a harmonic potential in two dimensions. Interestingly, the same transition is not present in the uniform system trapped in a box (or in periodic boundary conditions).

In the presence of interactions, there the Kosterlitz-Thouless transition takes place instead, as measured for cold atoms in [51].

In the one-dimensional trap, the equation determining the fugacity z for a given $\langle N \rangle$ is:

$$\langle N \rangle \beta = \langle N_0 \rangle \beta - \ln(1 - z). \quad (53)$$

In the thermodynamic limit (38) the first term to the right-hand side vanishes if $\langle N_0 \rangle$ is finite.

As the logarithm is not bound, the fugacity can be found for any value of $\langle N \rangle \beta$, $z = 1 - e^{-\langle N \rangle \beta}$, without any need to place a finite fraction of particles, $\langle N_0 \rangle / \langle N \rangle$, in the ground state at nonzero temperature. Therefore, there is no Bose-Einstein phase transition in an ideal gas trapped in a 1D harmonic potential.

However, because the logarithm grows very slowly, if a system is finite there is still quite an appreciable occupation of the ground state, even at significantly nonzero temperature [52]. This occupation gradually increases as the temperature approaches zero. The characteristic value of the fugacity, at which $\langle N_0 \rangle$ is of the order of $\langle N \rangle$, $z/(1 - z) = \langle N \rangle$, equals $z = 1 - 1/\langle N \rangle$. Then Eq. (53) allows us to define (neglecting the first term in the right-hand side) a characteristic

temperature at which the population of the ground state becomes significant*:

$$\beta_c^{D=1} = \frac{1}{T_c^{D=1}} = \frac{\ln \langle N \rangle}{\langle N \rangle}. \quad (54)$$

By combining Eq.(53) and Eq.(54) the temperature dependence of the ground state occupation can be estimated:

$$\frac{\langle N_0 \rangle}{\langle N \rangle} = 1 - \frac{T}{T_c^{D=1}}. \quad (55)$$

The above picture is strongly modified by interactions. In [53], different regimes of quantum degeneracy of the 1D harmonically trapped system are identified: a true BEC condensate, a quasicondensate, and a gas of impenetrable bosons — the Tonks-Girardeau gas.

2.3. Fluctuations catastrophe

The GC description of Bose-Einstein condensation has a serious drawback, which leads to the conclusion that the GC formalism fails below the Bose-Einstein condensation temperature for known systems in the thermodynamic limit [14].

The fugacity in this limit is equal to one, $z = 1$, thus no longer plays the role of a parameter controlling the mean number of particles. All canonical ensembles with different N contribute then to the GC partition function with the same weights, because we have $z^N = 1^N = 1$. Therefore, the assumption that the number of particles (or mean number of particles) at and below the critical temperature remains well controlled while decreasing the temperature at constant $z = 1$, which is used on (45) to get (47), is not well justified.

This hidden but dubious assumption that one can swap around z and $\langle N \rangle$ in the GCE is fundamental for the textbook formulation of Bose-Einstein condensation. It lies behind Eq. (47), despite the fact that, when in the thermodynamic limit, the GC formalism does not provide any knobs to control the value of $\langle N \rangle$ after reaching or crossing the critical temperature.

Fluctuations of the ground state occupation $\delta^2 N_0 \equiv \langle N_0^2 \rangle - \langle N_0 \rangle^2$, serve as the magnifying glass for the problems of the grand canonical description of the Bose-Einstein condensation, and expose the poor control over N or $\langle N \rangle$ in the model. From the definition of the grand canonical partition function Eq. (30) it follows that the mean occupation $\langle N_i \rangle$ of one-particle states of energy ϵ_i , and its fluctuations (squared) $\delta^2 N_i$ are (compare Eq.(27)):

$$\langle N_i \rangle = - \frac{\partial \ln \Xi(\beta, \mu)}{\beta \partial \epsilon_i}, \quad (56)$$

$$\delta^2 N_i = \frac{\partial^2 \ln \Xi(\beta, \mu)}{\beta^2 \partial \epsilon_i^2} = \langle N_i \rangle (1 + \langle N_i \rangle). \quad (57)$$

* A similar characteristic transition temperature was defined in [52] via $\langle N \rangle \beta = \ln(2/\beta)$.

Eq. (57) is valid for all temperatures. If applied to the ground state occupation below the condensation temperature where $\langle N_0 \rangle \sim \langle N \rangle \gg 1$ we find that:

$$\delta^2 N_0 = \langle N_0 \rangle (\langle N_0 \rangle + 1) \approx \langle N_0 \rangle^2 \sim \langle N \rangle^2. \quad (58)$$

The fluctuations δN_0 are comparable to the total (mean) number of particles in the system. The result is extravagantly large and in fact conceptually suspicious, as has been extensively discussed in the literature [14, 54, 55, 56].

Fluctuations of the total number of particles can be obtained from:

$$\delta^2 N = \frac{\partial^2 \ln \Xi(\beta, \mu)}{\beta^2 \partial \mu^2} = \left(z \frac{\partial}{\partial z} \right)^2 \ln \Xi(\beta, z), \quad (59)$$

and consequently with division of the GC partition function into the ground state contribution and the excited particles term, Eq.(36), the two subsystems contribute:

$$\delta^2 N = \delta^2 N_0 + \delta^2 N_{\text{ex}}, \quad (60)$$

where $\delta^2 N_0$ is given by Eq.(58) while the second term of Eq.(60) gives fluctuations of the excited subsystem, the thermal cloud:

$$\delta^2 N_{\text{ex}} = \left(z \frac{\partial}{\partial z} \right)^2 \ln \Xi_{\text{ex}}(\beta, z) = \frac{g_2(z)}{\beta^3}. \quad (61)$$

Below the condensation temperature $T < T_c$ the fugacity equals to one, $z = 1$, and by substitution of quantities from Sec. 2.2 fluctuations of the number of particles in the thermal cloud can be written as:

$$\delta^2 N_{\text{ex}} = (\langle N \rangle - \langle N_0 \rangle) \frac{\zeta(2)}{\zeta(3)} = \langle N_{\text{ex}} \rangle \frac{\zeta(2)}{\zeta(3)}. \quad (62)$$

It becomes clear now, that the total number of particles in the system fluctuates excessively only because of the enormous fluctuations of the ground state, illustrated in Fig. 1 in green. The problem fluctuations are solely related to the fact, that while the total number of particles in the system described by the GC ensemble (GCE) is free to take on any value there is no associated energy cost for entering or leaving the ground state. Having seen this, we can revisit the conceptual problems of the GCE below T_c from other angles than the poor conditioning of $N, \langle N \rangle$ on $z = 1$. Another conceptually dubious element there is that such strongly fluctuating $\delta N \sim \langle N \rangle$ makes it difficult to define the “system” well in the presence of a particle reservoir. Separation of system from reservoir becomes then mostly an exercise in arbitrary labeling. For example, Ref. [14] points out and earlier [55] also intimated, that in the limit $V \rightarrow \infty$ of a subsystem included inside an even larger $V' \gg V$ volume of an ideal gas whose remaining parts are the “reservoir”, the properties of the smaller volume V subsystem tend to whenever condensation is present those of a canonical

ensemble not a GCE. This is ascribed to the off-diagonal long-range order. Hence the often espoused view that the GCE at least describes properly a “small section” of a larger ideal gas is a fallacy below T_c .

From another angle, it has been noted that in CN and MC ensembles relevant physical quantities such as condensate fluctuations $\delta N_0(T)$ become independent of N as N grows, apart from N determining the global condensation temperature. This makes the introduction of a particle reservoir at a given $T \ll T_c$ basically irrelevant, and any resulting fluctuations of quantities that are calculated can again be suspected to be merely a consequence of this spurious labeling problem between system and reservoir particles.

Yet another view is given in a recent work [12], which proposes removal of the GCE fluctuation catastrophe via gauge symmetry breaking arguments. There it is argued that no condensate fluctuations take place in a GCE because of an imperative for symmetry breaking, and instead any remaining large particle fluctuations lie in excited modes. The need for symmetry breaking was supported e.g. by the result that a small symmetry breaking parameter ε added to an ideal gas Hamiltonian provides the leading contribution to the mean ground state occupation $\langle N_0 \rangle \approx \varepsilon^2 V / \mu^2 - T / \mu + \dots$ in finite systems. i.e. the better known chemical potential contribution $z / (1 - z) \approx -T / \mu$ is sub-leading [12].

The discussion presented so far reveals that a straightforward description of the ideal Bose gas according to only classical statistical mechanics fails at sufficiently low temperatures. The assumption about the equivalence of ensembles, a pillar of equilibrium statistical mechanics, is no longer true. The main reason is that below the critical temperature, most particles occupy the single quantum state of zero energy, thus energy is no longer an extensive quantity. The chemical potential equals the ground state energy and does not control the number of particles in the system which leads to divergent fluctuations. Therefore, there is a need to determine a formalism of Bose-Einstein condensation for the ideal Bose gas with a well-defined total number of particles.

The standard solution the problems of the GCE below T_c has been to employ a formalism in which the total number of particles is fixed – the canonical (CN) and microcanonical (MC) descriptions. However, the constraint on the number of particles adds significant complexity to the problem. This challenge was addressed by H. David Politzer in [2], where the CN arrangement is assumed. In this scenario, the temperature is set by the heat reservoir, but the number of particles is constant, leading to explicitly imposed vanishing of its fluctuations, $\delta^2 N = 0$.

Consequently, the fluctuations of the condensate,

$\delta_{CN}^2 N_0$, can be deduced from the fluctuations of the thermal cloud:

$$\delta_{CN}^2 N_0 = \delta_{CN}^2 N_{\text{ex}}, \quad (63)$$

where, to stress that we address the CN formalism, labels are added. Assuming that Ξ_{ex} still provides a correct description of the thermal cloud which is in equilibrium with the ground state that acts as a reservoir of particles, the fluctuations of the number of particles in the excited subsystem can be obtained from the scheme of the grand canonical ensemble by Eq.(62). These when combined with Eq.(47) give:

$$\delta_{CN}^2 N_0 = N \frac{\zeta(2)}{\zeta(3)} \left(\frac{T}{T_c} \right)^3. \quad (64)$$

Note that the mean total number of particles appears only to compensate the $\langle N \rangle^{1/3}$ appearing in the condensation temperature T_c from (43). This remarkably straightforward result demonstrates that the relative fluctuations of the condensate are normal, i.e. $\sqrt{\delta_{CN}^2 N_0}/N \sim 1/\sqrt{N}$. Its scaling was previously shown in [57], and (64) can be compared to the orange numerical curve in Fig. 1.

Finally, it is worth remembering that a GC formulation may remain useful for finite-size systems under other physical conditions. For example, the GC is valid in systems such as the so-called photon condensates [58] in which there are real fluctuations of the number of particles in a system whose extent is well defined by other physical effects. Another case is the ‘‘grand’’ canonical formulation of [6] in which $\langle N_0 \rangle$ is made to determine an effective fugacity $z_{\text{eff}} = \langle N_0 \rangle / (\langle N_0 \rangle + 1)$ consistent with (40), which z then enters GC expressions for calculation of observables. Finally, it is believed that for the interacting gas, the equivalence of different ensembles can be restored.

2.4. The Maxwell Demon (MD) rescue ensemble

In this section we explore in depth the original idea of [2], that the ground state contribution should be excluded from the statistical description, which treats only the excited subsystem of the thermal cloud. Constraints on the total number of particles, necessary for realistic condensation should be imposed externally.

We focus on the region of energies below the transition to the Bose-Einstein condensation phase, where $E < E_c$ from (44) and $z = 1$. Guided by the idea of a statistical description of the Bose-Einstein condensate in terms of quantities related to the excited subsystem only, one classifies all microstates based on the abundance of particles in the excited states. The recall that the MC partition function can be organized as:

$$\Gamma(E, N) = \sum_{N_{\text{ex}}=0}^N \Gamma_{\text{ex}}(E, N_{\text{ex}}), \quad (65)$$

where by $\Gamma_{\text{ex}}(E, N_{\text{ex}})$ we denote the number of microstates with exactly N_{ex} excited particles, as discussed previously.

It is convenient to define the following partition function:

$$\Upsilon(E, z) = \sum_{N_{\text{ex}}=0}^{\infty} z^{N_{\text{ex}}} \Gamma_{\text{ex}}(E, N_{\text{ex}}). \quad (66)$$

Which for $z = 1$, becomes the MC partition in the thermodynamic limit of an infinite number of particles, $\Upsilon(E, z = 1) = \Gamma(E, N \rightarrow \infty)$. The $\Upsilon(E, z)$ provides a description of the excited subsystem exchanging particles with the reservoir of particles in the ground state of zero energy. This fourth statistical ensemble, introduced in [3], is known as the Maxwell Daemon (MD) ensemble. Since the transfer of atoms between ground and excited states is not accompanied by any energy transfer, $z = 1$, when a particle leaves or enters the thermal cloud, the others have to adjust their energies accordingly. These unusual correlations invoke the concept of the Maxwell Daemon, a hypothetical entity with knowledge of the energies of all particles, allowing it to control the exchange of atoms between the thermal cloud and the zero-energy condensate, thereby maintaining the total energy constant.

In the thermodynamic limit, the mean number of excited particles, as well as its fluctuations, depend solely on the energy E of the system. Taking the limit $z \rightarrow 1$ we obtain MC averages $\langle \cdot \rangle_{MC}$ for the excited states:

$$\langle N_{\text{ex}} \rangle_{MC} = z \frac{\partial}{\partial z} \ln \Upsilon(E, z) |_{z=1}, \quad (67)$$

$$\delta_{MC}^2 N_{\text{ex}} = \left(z \frac{\partial}{\partial z} \right)^2 \ln \Upsilon(E, z) |_{z=1}. \quad (68)$$

The fugacity z has to be set to one after differentiation.

The above equations do not depend on the total number of particles. This is because, in the thermodynamic limit, the excited subsystem does not have any means to learn about the occupation of the ground state. The ground state reservoir contributes neither to the energy nor to the entropy. Eqs.(67, 68) are defined in the whole possible energy range from zero to infinity.

To relate these results to a large but finite system with a condensate, we should impose a constraint on N . This can be done using the value of the energy at the condensation transition, $E_c(N)$ from Eq.(44), at which the mean number of excited bosons is equal to the externally known total number of particles:

$$\langle N_{\text{ex}}(E_c) \rangle_{MC} \equiv N. \quad (69)$$

The energy E cannot exceed this maximal excitation energy $E_c(N)$, limiting the domain of functions, $\langle N_{\text{ex}}(E) \rangle_{MC}$, and $\delta_{MC}^2 N_{\text{ex}}(E)$ to the interval $E \in [0, E_c]$. This also limits the maximal number of excited

particles to N . In particular then, expressions Eq.(67) and Eq.(68) are valid for finite systems at energies below and at the critical one.

The fact that the upper limit of summation in $\Gamma(E, N)$, Eq. (65), is finite as opposed to $\Upsilon(E, z)$, Eq. (66), where summation runs to infinity, does not play any role below the ‘‘restriction temperature’’ at which $E/\hbar\omega \rightarrow N$, that lies very close to and just below T_c [19]. The extra terms in Eq. (66) are negligible compared to the main contribution to the sum. This is because the relative width of the maximum at the $\Gamma(E, \langle N_{\text{ex}}(E_c) \rangle_{MC})$ tends to zero in the thermodynamic limit, as illustrated in Fig. 3.

By imposing a constraint on N , the mean occupation of the condensate as well as its fluctuations can be related to those of the thermal cloud:

$$\langle N_0 \rangle_{MC} = N - \langle N_{\text{ex}} \rangle_{MC}, \quad (70)$$

$$\delta_{MC}^2 N_0 = \delta_{MC}^2 N_{\text{ex}}, \quad (71)$$

as announced in Eqns. 5. This procedure excludes the condensate mode from the expression (57) for fluctuation of mode occupations which led to physically incorrect results (58). Application of the above formalism requires knowledge of the Maxwell Daemon partition function, given by Eq. (66). Directly obtaining it from the definition proves challenging due to the energy constraint. However, relaxing this constraint simplifies the problem. The partition function of the GC ensemble of excited particles is a generating function of the Maxwell Daemon partition, $\Upsilon(E, z)$:

$$\begin{aligned} \Xi_{\text{ex}}(\beta, z) &= \sum_E e^{-\beta E} \Upsilon(E, z) \\ &= \sum_E \sum_{N_{\text{ex}}} e^{-\beta E} z^{N_{\text{ex}}} \Gamma(E, N_{\text{ex}}). \end{aligned} \quad (72)$$

The function $\Xi_{\text{ex}}(\beta, z)$ can be interpreted as a canonical distribution for the MD ensemble. For example, in the case of particles in the 3D harmonic potential this function is given by Eq. (33), $\ln \Xi_{\text{ex}}(\beta, z) = g_4(z)/\beta^3$. The mean value of the critical temperature, critical energy or mean occupation of the condensate, are identical in the GC formalism discussed in Sec. 2.2. The CN formalism is based on $\Xi_{\text{ex}}(\beta, z)$, however, the fluctuation of the condensate, pathological in the GC ensemble, are normal in the CN formulation with $\Xi_{\text{ex}}(\beta, z)$, Eq. (64).

The MD partition function Υ can be related to Ξ_{ex} , via the Legendre transformation, in the same way as the MC partition Γ is related to the CN partition \mathcal{Z} . The terms of the sum in Eq. (72) have a pronounced maximum at an energy which can be obtained from:

$$-\frac{\partial}{\partial \beta} \ln \Xi_{\text{ex}}(\beta, z) = E, \quad (73)$$

and therefore, when the relative width of this maximum goes to zero in the thermodynamic limit,

the sum in Eq. (72) is dominated by the value of the largest term, and we have:

$$\ln \Upsilon(E, z) = \ln \Xi_{\text{ex}}(\beta, z) + \beta E. \quad (74)$$

The inverse temperature β can be obtained from Eq.(73), and thus it can be made dependent on the energy and fugacity $\beta = \beta(E, z)$.

The early attempts to determine fluctuations of the Bose-Einstein condensate in a 3D harmonic potential, [57], applied two consecutive Legendre transformations. The first one, to obtain the canonical partition function, $\ln \mathcal{Z}(\beta, N) \approx \ln \Xi(\beta, z) - N \ln z$, by relating fugacity to other parameters, $z = z(N, \beta)$. In the second step, the microcanonical distribution was associated with the canonical one, $\ln \Gamma(E, N) = \ln \mathcal{Z}(\beta, N) + \beta E$, by replacing β by the appropriate value of energy $\beta = \beta(E, N)$. This approach, utilizing the saddle point method twice, turned out to work only for small systems close to the critical temperature, because the singular contribution from the ground state made the grand canonical partition function not well behaved in the thermodynamic limit [59].

In contrast, Eq. (74), and Eq. (73) allow one to connect microcanonical fluctuations of the number of excited particles, $\delta_{MC}^2 N_{\text{ex}} = (z \frac{\partial}{\partial z})^2 \ln \Upsilon(E, z)|_{z=1}$, to their canonical counterpart, $\delta_{CN}^2 N_{\text{ex}} = (z \frac{\partial}{\partial z})^2 \ln \Xi_{\text{ex}}(\beta, z)|_{z=1}$:

$$\delta_{MC}^2 N_{\text{ex}} = \delta_{CN}^2 N_{\text{ex}} - \frac{\langle EN_{\text{ex}} \rangle_{CN}^2}{\delta_{CN}^2 E}, \quad (75)$$

Therefore, the fluctuations in the MC system are always smaller than those in the CN system because of nonvanishing correlations between the energy and number of excited particles in the system, $\langle EN_{\text{ex}} \rangle_{CN}^2$.

For example, the above general results can be applied to the specific case of particles in 3D harmonic potential. There the equation relating the MC energy to the CN temperature β has the form (37):

$$E = 3 \frac{g_4(z)}{\beta^4} \rightarrow \beta(z, E) = \left(\frac{3g_4(z)}{E} \right)^{1/4} \quad (76)$$

Thus the explicit form of $\ln \Upsilon(E, z)$, in the thermodynamic limit, using (33) in (74), is

$$\ln \Upsilon(E, z) = 4 \frac{g_4(z)}{\beta^3}. \quad (77)$$

With that in mind, obtaining the mean occupation and fluctuations of the Bose-Einstein condensate in the perfectly isolated system, i.e., in the microcanonical ensemble, is simply a matter of straightforward differentiation and application of the formula for the critical temperature (43), just having to remember that $\beta(z)$ as above in (76). This procedure gives:

$$\langle N_0 \rangle_{MC} = N \left(1 - \left(\frac{T}{T_c} \right)^3 \right) \quad (78)$$

$$\delta_{MC}^2 N_0 = N \left(\frac{\zeta(2)}{\zeta(3)} - \frac{3\zeta(3)}{4\zeta(4)} \right) \left(\frac{T}{T_c} \right)^3. \quad (79)$$

Therefore for a 3D harmonic trap the CN fluctuations, (64), are about 62% larger in standard deviation than the MC ones, as illustrated in Fig. 1, while the mean condensate fraction is unchanged. The variance ratio is

$$S = \frac{\delta_{MC}^2 N_0}{\delta_{CN}^2 N_0} = 0.39. \quad (80)$$

The Maxwell Daemon ensemble gives a correct description of the Bose system below the condensation temperature by fixing the glitches of the textbook description of the Bose-Einstein condensation of the ideal gas. It is also a powerful tool, allowing to study systems characterised, in principle, by any single-particle spectrum, see [17, 19].

2.5. Spectral classification

Remarkably general conclusions have been gleaned from an analysis based purely on the functional form of the energy spectrum in a trap in d dimensions, following [60]:

$$\epsilon_j = \hbar \sum_{l=1}^d \omega_l j_l^\sigma, \quad (81)$$

where $\sigma = 1$ for a harmonic trap with the energy scale $\hbar\omega_l$ and $\sigma = 2$ for a uniform gas in a box where $\hbar\omega_l \equiv h/(2mL_l^2)$, m is mass of boson and L_l the box size in the l direction. The condensate occupation for $d > \sigma$ is $\langle N_0 \rangle \propto N[1 - (T/T_c)^{d/\sigma}]$. However, perhaps the most wide-reaching conclusion of the spectral analysis is that there are several distinct trap/dimension regimes for the ultracold temperatures that lie in the range $\epsilon_1 \ll T \lesssim T_c$ [17, 19]:

(1) High-dimensional traps with $d > 2\sigma > 0$, in which condensate fluctuations are normal, Gaussian and follow the Central Limit Theorem (CLT) in the thermodynamic limit, but grow faster than linearly with temperature:

$$\delta^2 N_0 \propto N \left(\frac{T}{T_c} \right)^{d/\sigma} \quad (82)$$

Here the heat capacity is discontinuous at the transition temperature and $\delta N_{\text{ex}} = \delta N_0 \sim \sqrt{\langle N_{\text{ex}} \rangle}$ follow the square root law but in the number of excited particles N_{ex} not the total. In this regime MC fluctuations have the same scaling but a smaller prefactor than CN due to the energy constraint [3].

(2) Lower dimensional traps with $\sigma < d < 2\sigma$, in which condensate fluctuations are anomalously large, and non-Gaussian in the thermodynamic limit:

$$\delta^2 N_0 \propto N^{2\sigma/d} \left(\frac{T}{T_c} \right)^2. \quad (83)$$

Notably in the region $\sigma < d < 2\sigma$, a BEC already exists, but the fluctuations are anomalously non-Gaussian in the canonical ensemble, though still weaker

than the $\delta^2 N_0 \propto N^2$ found in the GCE. Heat capacities are continuous and $\delta N_{\text{ex}} = \delta N_0$ does not follow a square root law. In fact $\delta N_{\text{ex}} \sim \langle N_{\text{ex}} \rangle^{\sigma/d}$.

(3) In the regime $d < \sigma$ no condensate exists in the thermodynamic limit, but the scaling of fluctuations can be found as

$$\delta^2 N_0 \sim \sum_{j=1}^d \left(\frac{T}{\hbar\omega_j} \right)^2, \quad (84)$$

heat capacity is continuous and the fluctuations are far from a square root law $\delta N_{\text{ex}} \sim \langle N_{\text{ex}} \rangle$.

The boundary case of $d = 2\sigma$ contains a logarithmic dependence [19]

$$\delta^2 N_0 \propto N \left(\frac{T}{T_c} \right)^2 \log \left(\sqrt{N} \frac{T}{T_c} + \gamma + 1 \right), \quad (85)$$

with $\gamma \approx 0.5772$, Euler's constant. Remarkably, for low dimensional traps $d < 2\sigma$, not only do the same scaling exponents as above occur for both the CN and MC ensembles, but even the prefactors are the same [19]. The Maxwell daemon combined with a saddle point approximation allows to derive from physical grounds the famous Hardy and Ramanujan formula for the asymptotics of the partition number. More detail, such as CN prefactors, is given in [17].

2.6. Historical survey

To flesh out our coverage, we relate here a selection of results on fluctuations in the ideal gas, and their historical development since the 1990's. Some but not all of these results can be also found in the earlier topical reviews [14, 6, 56, 12].

Early work is described in detail in the extensive review of [14], including fluctuation results from Refs. [61, 60, 62, 63, 64, 65, 66], and we will not cover the results from this period in detail. Of particular note are a variety of recurrence relations that were reported by [67] (MC) and later [68, 69, 20, 17, 70], as well as the work of [69] which studied finite-size but large systems up to $N = 10^4$ numerically, and in particular found CN specific heats in 1D and 3D harmonic traps.

However, an explosion of work on condensate fluctuations occurred in the period 1996-1998 after the first experimental realizations of Bose-Einstein condensation. The early work [15] studied the MC fluctuations in a 1D harmonically trapped gas using asymptotic formulas from number theory and found several now well known features such as linear growth of δN_0 with T until a maximum just below T_c , localization of the N_0 distribution, as well as the great discrepancy with the GCE. Gajda *et al.* [57] applied the saddle point method to the (at the time) more experimentally accessible 3D trapped ideal gas in the MC, obtaining an analytic estimate of the full distribution $\mathcal{P}(N_0)$ and numerically investigating

fluctuations, confirming $\delta^2 N_0 \propto N$ and the presence of the peak below T_c .

A large part of the flurry of new results was based on the incisive idea of Politzer [2] to consider explicitly the counting statistics of the excited particles and derive condensate statistics as a consequence, as well as its later rigorous formulation by Navez [3] who introduced the concept of the Maxwell's Demon ensemble. In this latter paper it was used to rigorously study the relationship between MC and CN fluctuations, finding (79) in the 3D trap as well as the general relationships

$$\langle \delta^2 N_0 \rangle_{MC} = \langle \delta^2 N_0 \rangle_{CN} - \frac{\langle \delta N_0 \delta E \rangle_{CN}}{\langle \delta^2 E \rangle_{CN}} \quad (86)$$

and $\langle N_0 \rangle_{CN} = \langle N_0 \rangle_{MC}$ in the thermodynamic limit, as well as confirming qualitative agreement with finite- N condensates. Here $\langle N_{\text{ex}} \rangle = \langle N_0 \rangle$, so (86) equals (75). Higher terms of (86) were later determined in [71].

In parallel, [20] showed the presence of the now very well known and characteristic fluctuations peak below T_c in the CN for harmonic and box traps, the independence of δN_0 from N at low T , and the narrowing of the $\mathcal{P}(N_0)$ distribution. For a 1D harmonic trap they also demonstrated that the CN ideal gas system's Ginzburg-Landau functional shows behaviour characteristic of a weakly interacting Bose gas despite having no true interaction. Any particle that leaves the condensate must show up in the excited states, a process that resembles as if a collision had occurred. Values of δN_0 for the MC were in turn found by [72] after developing an appropriate numerical procedure. These showed the same characteristic independence of N at low T as in the CN (See Fig. 5). However, their functional dependence on T and N were found qualitatively similar but lower than the CN ones. [54] looked at MC fluctuations in harmonic traps and showed that their magnitude is essentially independent of N , indicating the dubious nature of a GC ensemble model.

The work [6] introduced a so-called ‘‘grand’’ canonical approximation to CN quantities in which the mean condensate occupation

$$\langle N_0 \rangle = N - \sum_{j \neq 0} \frac{1}{e^{\beta \varepsilon_j} - 1}, \quad (87)$$

is made to determine an effective fugacity $z_{N_0} = N_0 / (N_0 + 1)$ consistent with (40) which then enters GC expressions for observables. This leads to

$$\delta^2 N_0 = \sum_i \frac{e^{\beta \varepsilon_i} / z_{N_0}}{[e^{\beta \varepsilon_i} / z_{N_0} - 1]^2}. \quad (88)$$

The two concurrent works of Weiss & Wilkens [17] and Grossmann & Holthaus [19] in a focus issue of the 1st volume of *Optics Express* generalized and systematized fluctuation results to date, basing on the

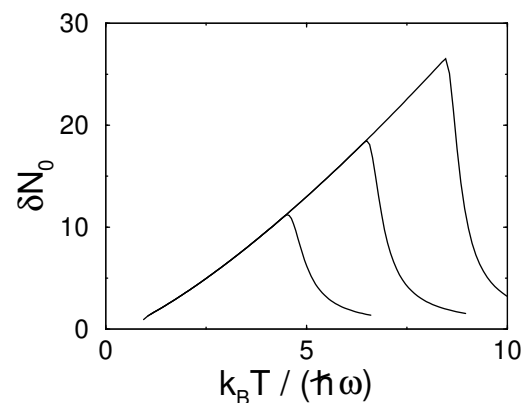


Figure 5. The change of microcanonical fluctuations $\delta_{MC} N_0$ with $N = 200, 500, 1000$ (left to right) for an ideal gas in a 3d harmonic trap. Note the perfect overlap at low T . Reproduced from [72] ©American Physical Society, DOI.

Used with permission.

Politzer idea [2] and the Maxwell Demon ensemble [3]. Notably, the essential dimensional classification based on (81) was developed in full for the CN and MC [19] ensembles, as described in Sec. 2.5, and very general results for prefactors in different geometries were provided. Ref. [17] also studied exact particle counting statistics and gave a lucid illustration of the fluctuations' dependence on T and N . The work in Ref. [19] drew attention to the fact that the condensate fluctuations never depend on total N but are instead tied to the excited population $\langle N_{\text{ex}} \rangle$, following the ‘‘expected’’ square root law $\delta N_0 \propto \sqrt{\langle N_{\text{ex}} \rangle}$ for high dimensional traps ($d > 2\sigma$) but growing faster than this like $\langle N_{\text{ex}} \rangle$ for lower dimensional trap spectra. This work also detailed the relationship of fluctuations to heat capacity and connected the topic to questions in number theory. Further investigation of these avenues as applied to harmonic traps was carried out in both CN and MC ensembles by [73] using the poles of a Zeta function, with particular attention paid to anisotropic harmonic traps and the link to integer partitioning.

The saddle point method used in many of the above studies to describe systems in the thermodynamic limit requires modification and care in the presence of a condensate. [71] describes this in detail, and finds general results for the CN ensemble that indicate that the crossover across the critical temperature occurs for many observables in an error-function-like manner that becomes a step function as $N \rightarrow \infty$.

In a new development, [74] introduced a master equation approach that has analogies to the quantum theory of a laser, as described in Sec. 3.5. This was soon developed further in [75] which provides many detailed results in the ideal gas, and additionally benchmarked in [76]. Follow on work [77] then [25] (and more rigorously [26]) extended this to weakly interacting

gases via a hybridization with the number-conserving Bogoliubov approach of [24], obtaining well behaved properties also at temperatures of the order of, and across T_c .

Other relevant later work includes a detailed study of the GC vs CN, plus also partially MC, ensembles near the critical temperature [78, 10] including consideration of universality classes, building on earlier work [79, 80]. The ensembles are found to disagree also in this region even in the thermodynamic limit. In related work, mesoscopic systems were found to exhibit non-Gaussian condensate statistics [81]. The ideal gas fluctuations were also re-analysed using a slightly different approach in [82, 83] as background for analysis of weakly interacting cases. Fluctuations were briefly treated for the case of non-extensive Tsallis statistics in [84]. A recent work considered the CN ideal gas in a 3d box at fixed total momentum [85], finding condensate fragmentation at the lowest temperatures, and approximately Gaussian distributions for the occupations of condensed modes.

Yukalov, in a series of works [56, 86, 28, 87], has argued that systems with “anomalous” fluctuations $\delta^2 N_0 \sim N^{a>1}$, e.g. ideal Bose gases with $2\sigma > d$ in the spectral classification, are unstable for thermodynamic reasons. They then discussed in depth in [87] the argument that only stable descriptions of systems possessing $\delta^2 N_0 \sim N^{a\leq 1}$ can fulfill the requirements of “representative” ensembles [88, 89, 90], and hence are indicated to submit to the principle of ensemble equivalence. A classification of this stability which is congruent with the spectral one of [17, 19] in Sec. 2.5 was rederived in [91]. On the other hand the analysis of [92] pointed to the anomalous fluctuations being tied to a broken U(1) gauge symmetry, and argues that it does not imply the instability of the system. There a random phase approximation restores U(1) gauge symmetry, and makes anomalous fluctuations absent.

Finally, recent work has also begun to look into condensate fluctuations in polariton condensates [93, 94, 95]. These are inherently open systems in which the total number of bosons, condensed or not, is not conserved, even on short timescales. Polariton number statistics in the steady (not equilibrium) state has been calculated and fluctuations analysed with the help of the Mandel $Q = \delta^2 N_0 / \langle N_0 \rangle - 1$ parameter known from quantum optics [96, 97].

3. Modern frameworks for accounting fluctuations in bosonic systems

In the previous section, we reviewed the definitions of statistical ensembles and highlighted the subtleties related to their inequivalence, particularly in the case of Bose-Einstein condensation. We also presented

approximate asymptotic formulas for condensate fluctuations in the case of an ideal gas. It might seem that the matter of the ideal gas is thus settled. Unfortunately, it turns out that asymptotic formulas do not apply to the description of current experiments, even when the interactions between particles are so weak that the system can be considered an ideal gas. The problem lies in the fact that statistical quantities, such as condensate fluctuations, converge very slowly to their asymptotic values. As shown in [98], even for $N = 100\,000$ atoms, the maximum fluctuations in a spherical trap differ from the asymptotic predictions of the fourth statistical ensemble by 20%. The discrepancy worsens for elongated traps (which are relevant in experiments). In an extreme case, in a 1D system, exact results [35] indicate that the asymptotic predictions regarding the probability distribution accurately reflect the true distribution only for N on the order of 10^{10} .

In practice, it is therefore necessary to compute statistical quantities for finite systems, which can usually be done only numerically. In this section, we present numerical techniques for generating statistical ensemble samples for a finite number of particles.

3.1. Stochastic ensemble sampling

The methods and the results concerning fluctuations of the Bose-Einstein condensate presented so far have two serious limitations. Firstly, they struggle to extend seamlessly to weakly interacting gases. Additionally, even for an ideal gas, numerical access to exact microcanonical fluctuations is restricted to a modest number of atoms, typically not more than 1000 in practice.

Instead, a number of alternative stochastic approaches have been developed to represent the complete phase space of the multiatom Hilbert space by an ensemble of unbiased samples. To do so one can generate numerous samples of configurations of the multiatom system, with their distribution constrained by a suitable control parameter. Among several approaches we focus here on those employing an occupation or classical field representation of atoms in modes as these are arguably the most flexible and most readily scalable to large but finite numbers $N \gg 1000$. In the following sections, we will outline three realizations of a Metropolis sampling approach: the first, based on a classical fields approximation, the second, known as the Fock States Sampling method, which models the phase space using a suitable set of number states below, and a hybrid approach that keeps the good features of both in Sec. 4.4. We will also describe the master equation approach in Sec. 3.5, and briefly mention the method of ergodic dynamical evolution of classical fields in Sec. 3.4.

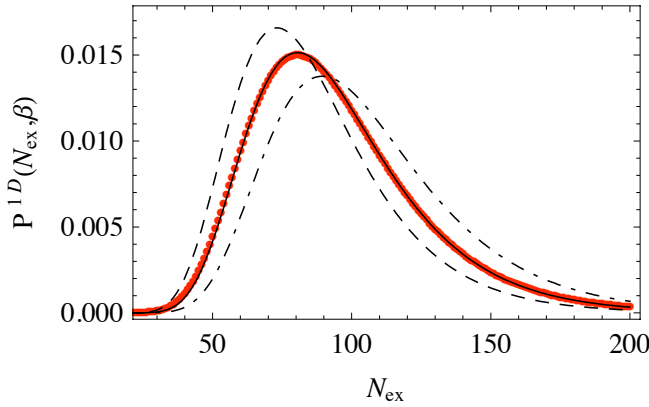


Figure 6. Probability distribution of having N_{ex} bosons outside the ground state of a 1D trap. Points represent the exact quantum distribution while lines are their classical field counterparts with $\hbar\omega j_{\text{max}} = 0.9k_{\text{B}}T$ (dotted-dashed line), $\hbar\omega j_{\text{max}} = k_{\text{B}}T$ (solid line), and $\hbar\omega j_{\text{max}} = 1.1k_{\text{B}}T$ (dashed line). $N = 1000$ and temperature $\hbar\omega\beta = 0.04$. Reprinted (figure) with permission from Witkowska, Gajda, Rzażewski [48], ©American Physical Society. Used with permission of all Authors of [48].

3.2. Metropolis sampling in the classical fields approximation

For equilibrium thermal states in the canonical ensemble, one employs the Boltzmann factor for the distribution. To construct the canonical set efficiently, one can apply the Metropolis algorithm [99], taking care of detailed balance conditions and thus defining a proper Markov chain that is subsequently sampled. Transition to the microcanonical ensemble then merely involves a straightforward post-selection from the canonical ensemble. For example, we can extract a subset of states with a well defined narrow energy range forming a representation of the microcanonical ensemble. Once these ensembles are established, calculating probability distributions for various variables becomes a direct averaging process over the samples.

The quantum theory of multiparticle systems finds a convenient formulation through the use of an atomic quantum field in 2nd quantization denoted as $\hat{\Psi}(\mathbf{r})$. We can expand the atomic field in the single particle states with wavefunctions $\phi_j(\mathbf{r})$ and annihilation operators \hat{a}_j :

$$\hat{\Psi}(\mathbf{r}) = \sum_j \phi_j(\mathbf{r}) \hat{a}_j \quad (89)$$

The classical field approximation, reviewed in detail in [100] and [101], applies to bosons and involves replacing operators \hat{a}_j of highly occupied single-particle states in (89) with complex amplitudes as per $\hat{a}_j \rightarrow \alpha_j$, while discarding other terms. This results in replacing the entire field operator with a complex

number wave function

$$\Psi(\mathbf{r}) = \sum_j \phi_j(\mathbf{r}) \alpha_j. \quad (90)$$

It corresponds to treating the wave aspects of the wavefunction analogously to classical electrodynamics for a photon field while discarding the “particle-like” effects, and becomes accurate as occupations become high enough. Notably, in thermal equilibrium, the highly occupied states correspond to those with the lowest energies, which are of most interest, especially for condensate fluctuations.

In order to generate a CN ensemble the probability (weight in the partition function) of any given classical field configuration $\vec{\alpha} = \{\alpha_j\}$ in the CN is

$$P_j(\alpha_j) = \frac{1}{Z_{\text{CFA}}(N, T)} \exp\left(-\frac{\sum_j \varepsilon_j |\alpha_j|^2}{k_{\text{B}}T}\right) \quad (91)$$

where $Z_{\text{CFA}}(N, T) = \sum_{\{\alpha_j\}} P(\{\alpha_j\})$ is the classical partition function and ε_j the energy of single-particle state j . The amplitudes α_j are subject to the constraint:

$$\sum_j |\alpha_j|^2 = N. \quad (92)$$

A Metropolis sampling algorithm for $\vec{\alpha}$ is readily implemented as described in [102]. Proposed updates take e.g. the form $\alpha_j \rightarrow \alpha_j + \delta_j$ with Gaussian complex noise δ_j whose amplitude is chosen for efficiency of the algorithm. One can update a single randomly chosen mode at a time or all together, correcting to preserve normalization (92). The procedure is also easily generalized to the GCE [103, 104, 105].

The classical fields approximation requires care, however, due to the appearance of a UV catastrophe in high energy modes. The set of modes should be terminated at single-particle energies of the order of $k_{\text{B}}T$ to avoid a preponderance of Rayleigh-Jeans distributed mode occupations ($\langle N_j \rangle \sim k_{\text{B}}T/\varepsilon_j$) in the high energy tails since the correct distribution is the Bose-Einstein one. Terminating the single-particle states at a cut-off can be a significant drawback as care becomes required to control the amount of influence the cutoff exerts [101, 106], especially as dimensionality grows [100]. For example, different energy cutoffs are optimal for different observables [107, 103, 108], and one must balance the mode cutoff in position and momentum space [109].

A benchmarking of the classical field representation in a one-dimensional harmonic trap (frequency ω) is illustrated in Fig. 6. For this geometry the classical field result can be found in closed form [110]:

$$\mathcal{P}(N_{\text{ex}}, T) = \frac{\xi^{N_{\text{ex}}}}{1 - \xi^N} \left(\frac{1 - \xi^{N_{\text{ex}}}}{1 - \xi^N} \right)^{j_{\text{max}} - 1} \quad (93)$$

where j_{\max} is the cut-off parameter (maximum value of j included), and $\xi := e^{-\frac{\hbar\omega}{k_B T}}$. As shown in Fig. 6, the result (93) coincides well with the exact distribution for the cut-off

$$E_{\max} = j_{\max} \hbar\omega = k_B T, \quad (94)$$

but the match degrades as the cutoff value is moved away from the optimal one.

3.3. Fock state sampling method

The fact that the classical fields approximation neglects the corpuscular nature of atoms makes it bear similarity to the pre-Planck approach to black body radiation, leading to a Rayleigh-Jeans distribution of mean occupations at high energy $\varepsilon_j \gtrsim k_B T$, and statistical outcomes plagued by an ultraviolet catastrophe if $E_{\max} \gg k_B T$. Similarly, restoring the corpuscular character of atoms is able to cure the ultraviolet divergence in our case. This crucial aspect is a distinctive feature of the Fock States Sampling (FSS) method developed recently [7] which we will now outline.

While an exact theory would demand the parametrization of the complete multiparticle Hilbert space (intractable for large systems), here one, opts for a model based on a skeleton of Fock states:

$$|N_0, N_1, \dots, N_K\rangle, \quad (95)$$

where N_j are occupations of single-particle orbitals (modes). The Markov chain framework encompasses all distributions of N atoms among the orbitals. Numerics impose an energy cut-off K in this context as well, yet, unlike a classical field representation the construction converges with $K \rightarrow \infty$, rendering results cut-off independent when the cut-off is suitably large. Since states (95) are the eigenstates of the Hamiltonian of the noninteracting gas, the Boltzmann factor for a canonical ensemble reads: $(N_j) = \exp\left(-\beta \sum_j N_j \varepsilon_j\right)$.

A Markov chain requires a choice of the Metropolis “dynamics” – proposed states and acceptance criteria, which must satisfy several mathematical conditions. First requirement is the the principle of detailed balance, i.e. that the probability of a transition must be equal to the probability of its reverse. Secondly, the “dynamics” may not leave any state unreachable by the algorithm. Numerically, the most efficient algorithms are found to be based on the properties of bosonic dynamical processes. The probability of proposing a new orbital should be equal for every atom. Thus, it should be proportional to the current number of atoms in a given mode. The probability of acceptance in a given mode should be proportional to the number of atoms in the mode plus one, imitating the well-known Bose enhancement factor known from stimulated and spontaneous processes, dating back to the relation of

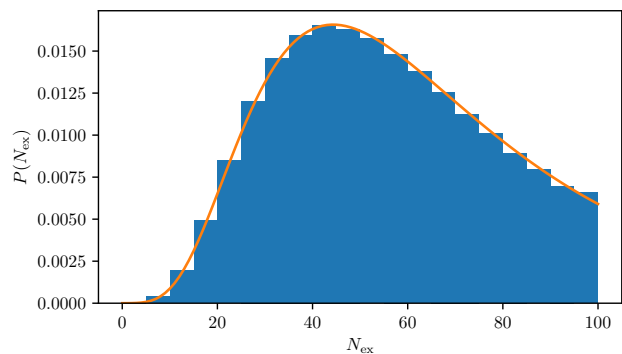


Figure 7. Distribution $\mathcal{P}(N_{\text{ex}})$ of the number of excited atoms for $N = 100$ bosons in a one-dimensional box with impenetrable walls for temperature $k_B T = 110\hbar^2/(2mL^2)$, where L is the width of the box. Blue histogram – FSS, solid orange line – exact calculation using (25).

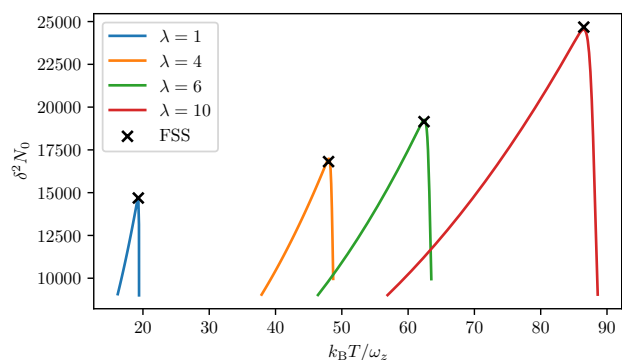


Figure 8. Fluctuations of BEC in a cloud of $N = 10000$ noninteracting atoms as a function of temperature in 3D traps with different aspect ratios λ . The solid lines are exact results obtained using (25). Results marked with black crosses were obtained via FSS method at the point of maximal fluctuations (most difficult to calculate).

A and B coefficients introduced by A. Einstein [111]. Thus, the probability of proposing a jump from orbital j to orbital l reads:

$$p_{j,l} \propto N_j (N_l + 1) \quad (96)$$

The algorithm is completed by a standard acceptance criterion. We draw a random number r from the interval $[0, 1]$ and accept the jump if $\exp(\beta [E(N_j) - E(N_l)]) \geq r$.

The quality of results obtained with the FSS method is illustrated in Fig. 7, which compares the FSS-produced histogram to the exact probability distribution of excited atoms confined in a one-dimensional box with impenetrable walls. Fig. 8 shows the temperature dependence of δN_0 for $N = 10000$ atoms in an elongated three-dimensional harmonic trap of various aspect ratios $\lambda = \omega_x/\omega_z = \omega_y/\omega_z$ as relevant for current experiment [9]. The exact results (solid lines) are obtained with the help of the recurrence

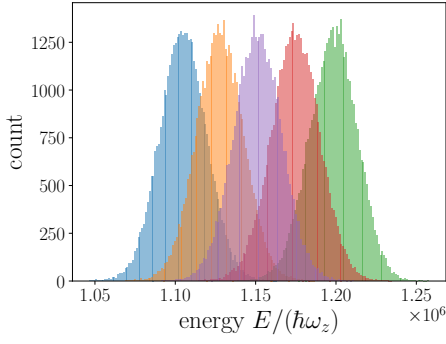


Figure 9. Histograms depicting the energy distributions of CN sets of states generated at different temperatures using the FSS method. The ensembles correspond to $N = 10^4$ atoms confined in a 3D harmonic trap with an aspect ratio $\lambda = 4$. The temperatures, shown from left (blue) to right (green), are $k_B T/\hbar\omega_z = 47.5, 47.75, 48, 48.25, 48.5$. Figure adopted from [7]. [CC BY 4.0](#).

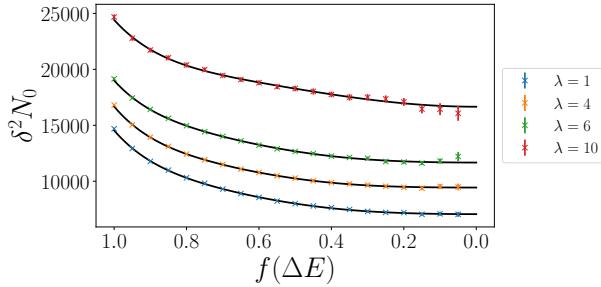


Figure 10. Dependence of condensate fluctuations on the energy window ΔE for $N = 10000$ atoms and different aspect ratios λ . $f(\Delta E)$ is the fraction of microstates that are within the energy window ΔE . Presented here is data obtained via postselection of FSS-generated states – crosses with uncertainties, and fitted high degree polynomials – solid black lines – to best estimate the MC limit.

relations (25), while the FSS results are marked with the stars. The agreement is excellent.

The above results also offer a practical avenue for deriving microcanonical fluctuations in systems with a large number of atoms, where the computational complexity of employing recurrence relations becomes prohibitive. In Fig. 9, the energy probability distributions at different temperatures in the CN ensemble are shown. Through a post-selection process one can selectively discard system copies lying outside a narrowing energy interval $E \in [\bar{E} - \Delta_E/2, \bar{E} + \Delta_E/2]$ around the distribution’s central energy \bar{E} . Although this decreases the number of retained copies, impacting statistical robustness, one can mitigate this effect by extrapolating results from larger intervals to estimate a well-defined fixed energy outcome. How this plays out can be seen in Fig. 10, where one also observes the continuum of ensembles between the CN and MC ensembles. [lier or later chapters](#).

Fig. 11 presents an experimentally important

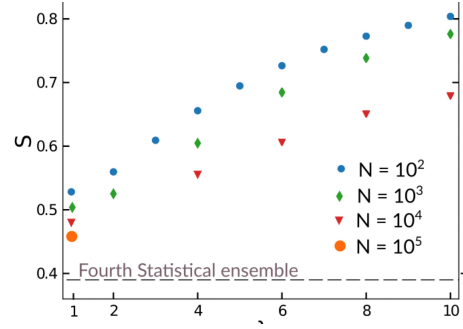


Figure 11. Ratio, S , between the calculated peak variance of the noninteracting BEC in the microcanonical and canonical ensembles as a function of the trap aspect ratio λ for $N = 10^2$ (blue points), $N = 10^3$ (green diamonds), $N = 10^4$ (red triangles) and $N = 10^5$ (purple square) atoms. The black dashed line corresponds to the asymptotic value estimated within the Maxwell’s demon ensemble (80). The three open symbols correspond to experimental points, presented in [9], with atom numbers $N = 8.8 \times 10^4 - 10.4 \times 10^4$. Figure reproduced from [9]. [CC BY 4.0](#).

quantity – $S = \delta_{MC}^2 N_0 / \delta_{CN}^2 N_0$, the ratio of maximal microcanonical fluctuations to canonical fluctuations. It is shown for various aspect ratios and increasing total numbers of atoms in a harmonic trap. Notably, even for a spherical trap with up to 100000 atoms, the calculated S exceeds significantly the $N \rightarrow \infty$ asymptotic value of 0.39, (80), as elucidated in [9].

3.4. Dynamical ergodic approach and related methods

A conceptually different, dynamical, approach to generate ensembles is also often used using evolution of classical field samples. For example, evolving a random field sample with total energy E and N particles in time via a Gross-Pitaevskii equation for the field (90),

$$i \frac{d\Psi(\mathbf{r})}{dt} = \left[-\frac{\nabla^2}{2} + V(\mathbf{r}) + g|\Psi(\mathbf{r})|^2 \right] \Psi(x) \quad (97)$$

with $V(\mathbf{r})$ the trapping potential and g the inter-particle interaction. Taking configurations at many consecutive times separated by an interval δt allows one to obtain microcanonical (MC) ensemble samples [112, 113, 114, 101] relying on an assumption of ergodicity. The conserved number of particles is

$$N = \int d^d \mathbf{r} |\Psi(\mathbf{r})|^2, \quad (98)$$

so we can see that a run will give at most an MC ensemble. Evolving a stochastic Gross-Pitaevskii equation in contact with a bath at temperature T and chemical potential μ through “growth” terms will generate GC samples [101, 115], whereas having contact with the bath via only “scattering” terms will generate CN samples [116]; A GC-type stochastic Gross-Pitaevskii equation modified by the addition of an appropriate restoring mechanism on N (sometimes

called a nonlinear chemical potential) can produce ensembles lying between CN and GC having a variance of N controlled by the user, for example to match actual variances produced by the preparation protocol in an experiment [117].

Under the right conditions it is also possible to go beyond classical field samples to a set of configurations that includes the effects of quantum fluctuations. For example when $N_{\text{ex}} \ll N$, Wigner distribution samples of a Bogoliubov description can be obtained [118, 119, 120], or a non-perturbative distribution of positive-P samples can be obtained via imaginary time evolution [121, 122], or under normal time dissipative evolution [123]. One can also generate number-phase Wigner samples [124, 125], and other varied schemes have also been proposed.

All the dynamical approaches rely on the presence of interactions to invoke ergodicity, unlike the Metropolis sampling and master equation formulations (below) that do not. However, the advantage of the ergodic approach for interacting systems is that it makes no hard-wired presuppositions about the one-particle basis states.

3.5. Master equation formulation

The master equation approach developed by Scully, Kocharovsky, and collaborators [74, 75] for finite N systems can provide a great deal of information about condensate and excited state fluctuations in a wide range of geometries, as well as analytic and numerical results for distribution functions or higher condensate moments. It bears similarity to the quantum model of the laser, and also to a class of stochastic Gross-Pitaevskii equation models for interacting gases that includes only “scattering” and not “growth” processes [116]. The approach has been reviewed in detail in [6]. Here we recapitulate the main essence of the model and salient results on condensate fluctuations.

The model starts with a trapped ideal gas system with boson modes \hat{a}_j ($j \geq 0$) of energy ε_j (occupations $\hat{N}_j = \hat{a}_j^\dagger \hat{a}_j$), in contact with a thermal reservoir of harmonic oscillator modes \hat{r}_ν with a dense energy spectrum having Bose-Einstein distributed mode occupations

$$\eta_\nu = \left[e^{\hbar\omega_\nu/k_B T} - 1 \right]^{-1}. \quad (99)$$

The reservoir-system interaction Hamiltonian in the interaction picture with coupling strengths $g_{\nu,kl}$ is given by

$$\hat{V} = \sum_\nu \sum_{l \geq 0, k > l} g_{\nu,kl} \hat{r}_\nu^\dagger \hat{a}_k \hat{a}_l^\dagger e^{-i(\hbar\omega_\nu - \varepsilon_k + \varepsilon_l)t} + \text{h.c.}, \quad (100)$$

which preserves particle number in the system, but not energy – thereby providing a canonical ensemble.

System modes k, l scatter off reservoir quanta which are annihilated or created. The total atom number is $N = N_0 + \sum_{j>0} N_j$. Assuming a large reservoir with a smooth dense energy spectrum, unchanged by the contact, and some auxiliary assumptions [75], one obtains the master equation for the reduced density operator of the system: I will use jump operator, to stress that this is typical Lindblad form). Then equation will be

$$\begin{aligned} \frac{d\hat{\rho}}{dt} = & \frac{\kappa}{2} \sum_{k>l} (\eta_{kl} + 1) \left[2\hat{C}_{kl} \hat{\rho} \hat{C}_{kl}^\dagger - \hat{C}_{kl}^\dagger \hat{C}_{kl} \hat{\rho} - \hat{\rho} \hat{C}_{kl}^\dagger \hat{C}_{kl} \right] \\ & + \frac{\kappa}{2} \sum_{k>l} \eta_{kl} \left[2\hat{C}_{kl}^\dagger \hat{\rho} \hat{C}_{kl} - \hat{C}_{kl}^\dagger \hat{C}_{kl} \hat{\rho} - \hat{\rho} \hat{C}_{kl}^\dagger \hat{C}_{kl} \right], \end{aligned}$$

where $\hat{C}_{kl} \equiv \hat{a}_l^\dagger \hat{a}_k$ is a jump operator.

Here the shorthand

$$\eta_{kl} = \left[e^{\hbar(\varepsilon_k - \varepsilon_l)/k_B T} - 1 \right]^{-1} \quad (101)$$

is used to indicate the reservoir occupation at an energy corresponding to the energy difference between levels k and l in the trap. Next, one assumes that the mean excited state occupations $\langle \hat{N}_{j>0} \rangle_{N_0}$ for a given condensate occupation N_0 are thermally distributed with temperature T for each N_0 value, i.e. $\propto \exp[-\sum_{j>0} \varepsilon_j N_j / k_B T]$.

It yields an equation of motion for the probabilities of condensate occupations:

$$\begin{aligned} \frac{dP_{N_0}}{dt} = & -\kappa \{ K_{N_0}(N_0 + 1)P_{N_0} - K_{N_0-1}N_0P_{N_0-1} \\ & + H_{N_0}N_0P_{N_0} - H_{N_0+1}(N_0 + 1)P_{N_0+1} \}, \quad (102) \end{aligned}$$

where $K_{N_0} = \sum_{l>0} (\eta_l + 1) \langle N_l \rangle_{N_0}$ and $H_{N_0} = \sum_{l>0} \eta_l (\langle N_l \rangle_{N_0} + 1)$ are cooling and heating rates, respectively. The sums are in terms of Bose-Einstein occupation factors (99) corresponding to energies $\omega_k = \varepsilon_k$. This yields the quite general equilibrium distribution

$$P_{N_0} = P_0 \prod_{j=1}^{N_0} \frac{K_{j-1}}{H_j}. \quad (103)$$

Closed-form results were obtained for two salient temperature regimes. At very low temperatures such that $\eta_j \ll 1$ and $\langle \hat{N}_j \rangle_{N_0} \ll 1$, one finds the condensate distribution to be governed by only one essential parameter

$$\mathcal{H} = \sum_{k>0} \eta_k = \sum_{k>0} \frac{1}{e^{\varepsilon_k/T} - 1} = \langle N_{\text{ex}} \rangle_{CN} \quad (104)$$

corresponding to the mean number of excited quanta as a function of T . This holds for $T \ll \varepsilon_1$ in general, and for a much wider temperature range in a harmonic trap. One has

$$P_{N_0} = \frac{1}{\mathcal{Z}} \frac{\mathcal{H}^{N-N_0}}{(N - N_0)!} \quad (105)$$

with the partition function \mathcal{Z} providing the normalization $\sum_{N_0} P_{N_0} = 1$. This leads to

$$\delta^2 N_0 = \mathcal{H} \left(1 - \frac{e^{-\mathcal{H}(\langle N_0 \rangle + 1)} \mathcal{H}^N}{\Gamma(N+1, \mathcal{H})} \right) \quad (106)$$

with $\Gamma(\alpha, x) = \int_x^\infty t^{\alpha-1} e^{-t} dt$ where $\langle N_0 \rangle = N - \mathcal{H} [1 + e^{-\mathcal{H}} \mathcal{H}^N / \Gamma(N+1, \mathcal{H})]$.

In more general higher temperatures a “quasi-thermal” distribution is assumed for

$$\langle N_{j>0} \rangle_{N_0} = \left(\frac{N - N_0}{\mathcal{H}} \right) \eta_j, \quad (107)$$

which differs from standard thermal mode occupations only by the prefactor that makes it satisfy $N = N_0 + \sum_{j>0} \langle N_j \rangle_{N_0}$. Now one obtains heating and cooling coefficients $K_{N_0} = (N - N_0)(1 + \bar{\eta})$ and $H_{N_0} = \mathcal{H} + (N - N_0)\bar{\eta}$ and the whole distribution is governed by two parameters: \mathcal{H} and the cross-correlation

$$\bar{\eta} = \frac{1}{N - N_0} \sum_{j>0} \eta_j \langle N_j \rangle_{N_0} = \frac{1}{\mathcal{H}} \sum_{j>0} \eta_j^2. \quad (108)$$

The probability distribution is binomial-related:

$$P_{N_0} = \frac{1}{\mathcal{Z}} \binom{N - N_0 - 1 + \mathcal{H}/\bar{\eta}}{N - N_0} \left(\frac{\bar{\eta}}{1 + \bar{\eta}} \right)^{N - N_0}.$$

The fluctuations are

$$\delta^2 N_0 2 = (1 + \bar{\eta})\mathcal{H} - P_0(\bar{\eta}N + \mathcal{H})(N - \mathcal{H} + \bar{\eta} + 1) - P_0^2(\bar{\eta}N + \mathcal{H})^2, \quad (109)$$

and the mean $\langle N_0 \rangle = N - \mathcal{H} + P_0(N\bar{\eta} + \mathcal{H})$ where

$$P_0 = \frac{1}{\mathcal{Z}} \left(\frac{(N + \mathcal{H}/\bar{\eta} - 1)!}{N!(\mathcal{H}/\bar{\eta} - 1)!} \right) \left(\frac{\bar{\eta}}{1 + \bar{\eta}} \right)^N \quad (110)$$

is the probability of having zero ground state atoms. In the thermodynamic limit $P_0 \rightarrow 0$, leaving us with just $\delta^2 N_0 = (1 + \bar{\eta})\mathcal{H}$ known previously [14]. Approximate expressions for $\mathcal{H}, \bar{\eta}$ in traps of various shape and dimensionality, in and not in the thermodynamic limit, are given in [6].

The formalism of the master equation has been also used to study the statistical properties of ultracold gases during different cooling techniques see for instance [126] that showed that the mean occupations in the stationary state of a laser-cooled ideal gas will resemble Bose-Einstein statistics.

4. Role of interactions on particle number statistics

We shift now from the secure domain of the ideal gas to the more challenging realm of fluctuations in a weakly interacting gas. We stress that there are no exact results in this case. We will start by recalling the main results of the Bogoliubov approximation for the weakly interacting gases with repulsive contact

interaction strength g , and follow by presenting more advanced modern approaches.

As background, one needs to keep in mind several global aspects of the system that change when interactions appear. One is that in a trapped system the shape, in particular the width, of the condensate mode can change drastically. At temperatures $T \ll T_c$ it is well described by the stationary solution of the GPE (97). Given sufficient central density n_0 such that $gn_0 \gg \hbar\omega$, the $T = 0$ condensate is quite well approximated by the Thomas-Fermi profile

$$\Psi(\mathbf{r}) = \sqrt{\frac{\mu - V(\mathbf{r})}{g}} \rightarrow \sqrt{\frac{\mu}{g}} \left[1 - \sum_{d=1}^D \left(\frac{x_d}{R_d} \right)^2 \right], \quad (111)$$

with Thomas-Fermi radii $R_d = (1/\hbar\omega_d)\sqrt{2n_0/m}$, and assumes negligible kinetic contribution. This shape and width change naturally strongly affects quantum fluctuations, including fluctuations of the lowest energy condensate mode. It is also crucial for the shift of T_c in trap.

A second aspect to keep in mind during the whole discussion to follow is that in lower dimensions a sufficiently large cloud will become a quasicondensate in which phase coherence is shorter than the cloud extent, and several low energy modes are highly occupied.

In the previous section, we reviewed several methods for calculating fluctuations in the number of condensed noninteracting bosons. We presented methods and results in different statistical ensembles and for various trapping potentials and different dimensionalities. Most of these results were exact.

Moving to weakly interacting gases in this section, brings us closer to realistic experimental conditions. Moreover, the statistics of the ideal gas would have no physical meaning without the weak collisions necessary for achieving thermal equilibrium. However, by entering the realm of weakly interacting gases, we move beyond exact results. To the best of our knowledge, no exact condensate fluctuations are known in closed form for any model of large systems with interactions.

4.1. Bogoliubov approximation

At very low temperatures, well below the critical temperature, we can use the Bogoliubov approximation, whose use for condensate fluctuations in ultracold atoms was initiated by Giorgini, Pitaevskii, and Stringari in [4]. In this approximation, the ultracold gas is divided into a stable condensate containing most of the atoms and a minority of uncondensed atoms represented by Bogoliubov quasiparticles. Thus, in the symmetry breaking Bogoliubov variant that we will use here, the atomic field operator is represented in the fol-

lowing form:

$$\hat{\Psi}(\mathbf{r}) = \sqrt{N} \varphi_0(\mathbf{r}) + \hat{\delta}(\mathbf{r}) \quad (112)$$

where $\varphi_0(\mathbf{r})$ stands for a condensate wave-function obtained via the stationary solution of the Gross-Pitaevskii equation and the quantum part $\hat{\delta}$ represents together the thermal and quantum depleted atoms that do not occupy the condensate mode. The fundamental assumptions then made are that terms $\mathcal{O}(\hat{\delta}^3)$ and higher in the Hamiltonian can be discarded because the overall condensate depletion is small ($T \ll T_c$). Further, in a stationary, equilibrium state terms $\mathcal{O}(\hat{\delta})$ turn out to be zero. The quantum part is conveniently diagonalized by a combination of the creation and annihilation operators of the Bogoliubov quasiparticles in modes labelled l :

$$\hat{\delta}(\mathbf{r}) = \sum_l u_l(\mathbf{r}) \hat{b}_l + v(\mathbf{r}) \hat{b}_l^\dagger, \quad (113)$$

where the u_l and v_l functions are obtained by solving the Bogoliubov-de Gennes equations which read

$$\begin{aligned} [\hat{K} + V(\mathbf{r}) + 2Ng|\varphi_0|^2 - \mu] u_l + Ng\varphi_0^2 v_l &= \hbar\omega_l u_l, \\ [\hat{K} + V(\mathbf{r}) + 2Ng|\varphi_0|^2 - \mu] v_l + Ng\varphi_0^2 u_l &= -\hbar\omega_l v_l \end{aligned} \quad (114)$$

where $\hat{K} = -\frac{\hbar^2 \Delta}{2m}$ is the kinetic energy, μ is the chemical potential, and $\hbar\omega_l$ the quasiparticle energies above the ground state. Notably, these excitations follow a spectrum that is phonon-like for $\hbar\omega_l \propto (1/\lambda_l)$ when $\hbar\omega \lesssim \mu$ and λ_l is a characteristic wavelength, and become particle like with $\hbar\omega_l \approx \hbar k_l^2/(2m)$ at high energies. The excitations and fluctuations have different properties in the two regimes.

To impose the bosonic commutation relations $[\hat{b}_l, \hat{b}_j] = 1$, one uses the constraint for u_l and v_l functions

$$\int |u_l(\mathbf{r})|^2 d^D r - \int |v_l(\mathbf{r})|^2 d^D r = 1. \quad (115)$$

The eigenvalue equations (114) are solved numerically, except for the uniform case which has plane wave solutions and $\omega = (k/2)\sqrt{k^2 + 4gn}$. The procedure is simplified if the problem has a symmetry. For instance for a spherically symmetric case the u_l and v_l functions are proportional to spherical harmonics and the diagonalization is reduced to a single, radial variable.

The excitations behave as independent quantum oscillators, and in the canonical ensemble, each oscillator is in thermal equilibrium. Then, we readily calculate the variance in the number of thermal atoms.

$$\begin{aligned} \delta^2 N_0 &= \delta^2 N_{\text{ex}} = \langle N_{\text{ex}}^2 \rangle - \langle N_{\text{ex}} \rangle^2 \\ N_{\text{ex}} &= \int \langle \hat{\delta}^\dagger(\mathbf{r}) \hat{\delta}(\mathbf{r}) \rangle d^D r = \sum_l \langle \hat{b}_l^\dagger \hat{b}_l + 1 \rangle \int d^D \mathbf{r} |v_l(\mathbf{r})|^2. \end{aligned} \quad (116)$$

Since the symmetry breaking variant of the Bogoliubov approximation (112) violates particle number conservation, as the temperature increases, the number of uncondensed atoms rises while the condensate remains undepleted. Thus, and also because of the removal of high order terms, this approximation yields reliable results only at very low temperatures when $N_{\text{ex}} \ll N$. We illustrate the relation between the Bogoliubov approximation and the exact result on a simple case of the noninteracting gas confined in a three dimensional one dimensional harmonic trap (see orange line in Fig. 13).

The pioneering Bogoliubov analysis of [4] for the interacting 3D Bose gas in a box found that $\delta^2 N_0 = 2\sqrt{\pi}(aN_0)^3 V$ even at $T = 0$, solely due to interactions (the so-called quantum fluctuations), where $g = 4\pi a \hbar^2/m$. At temperature,

$$\delta^2 N_0 \approx 0.105 \left(\frac{mT}{\hbar^2} \right)^2 V^{4/3} + \frac{k_B T m^2 c V}{3\pi^2 \hbar^3} \log \left(\frac{Vm^3 c^3}{\hbar^3} \right). \quad (117)$$

when $T \ll T_c$, and $c = \sqrt{gN_0/mV}$ is the speed of sound. The first term is half of the value in the ideal gas with periodic boundary conditions, and does not depend on the interaction a . The factor 2 between interacting and non-interacting cases was attributed to the choice of statistical ensemble in [4] or, the order of limits when going to thermodynamic limit and $g \rightarrow 0$ [127, 128]. Notably, both results shows super-Poissonian fluctuations $\delta^2 N_0 \approx V^{4/3} \propto N^{4/3}$. In a 3D harmonic trap on the other hand,

$$\delta^2 N_0 \propto \left(\frac{T}{T_c} \right)^2 \left(\frac{ma^2 T_c}{\hbar^2} \right)^{2/5} N^{4/3}. \quad (118)$$

exhibiting also a 4/3 power scaling but interestingly with a prefactor dependent on interaction, and no corresponding ideal gas term. Either way, scaling of fluctuations with a power greater than one in the size N or V indicates anomalously large fluctuations that according to the analysis of [87] would be expected to be unstable and not obey ensemble equivalence [87].

The subsequent work of Kocharovsky *et al* used the number-conserving Bogoliubov formalism of Girardeau and Arnowitt [129] to obtain fluctuations and higher moments of the condensate occupation [24, 23], including box and arbitrary potential traps. In particular, it was shown that the condensate statistics are never Gaussian, and that interactions suppress their magnitude, presumably for energetic reasons.

Other work studied 2D and quasi-2D trapped gases [130, 131] finding $\delta^2 N_0 \propto N^2$ plus extra terms $\mathcal{O}(N^{3/2})$, $\mathcal{O}(N)$ and arriving at the rather strange looking powers $\delta^2 N_0 \propto N^{22/15}$ for a 3D trapped gas [132] and $\delta^2 N_0 \propto N^{10/3}/(\ln N)^2$ for the 1D trapped case [133]. Some very simplified GCE models such as a single-mode condensate have also been studied [134].

It has also been found [8] that the difference between MC and CN fluctuations scales normally in N , so they become equivalent in the thermodynamic limit (but anomalous). This contrasts heavily with the trapped ideal gas for which MC and CN fluctuations stay different in the thermodynamic limit.

4.2. Anomalous fluctuations controversy

However, in contrast to all the above, the early work of Idziaszek *et al.* [22] found normal fluctuations $\delta^2 N_0 \sim N$ and later [86, 28] studied a symmetry-broken Bogoliubov description of the weakly interacting gas and investigated its thermodynamic considerations. They argued that fluctuations are normal $\delta^2 N_0 \leq \propto N$ in both CN and GCE, including arbitrarily nonuniform [135], or mesoscopic [91] cases. Hence they would be expected to be representative ensembles and obey ensemble equivalence [87].

This issue of whether the fluctuations of the weakly interacting gas as described by Bogoliubov are anomalous or not has been the source of a controversy with many studies indicating anomalous fluctuations as above, but others finding normal Gaussian fluctuations $\delta^2 N_0 \propto N$. On the anomalous side: Ref. [4] (extended to stronger interactions by [136]), then [24, 23], as well as a later CN analysis by [82] (box) [83] (harmonic trap): On the normal side [22], but also later work by [86, 28, 135, 91].

The matter was reassessed in the low temperature regime by Idziaszek in [8], recovering the anomalous scaling predictions in the particle-number-conserving and traditional, symmetry breaking nonconserving theory, and in a wide range of cases: both in MC and CN ensembles, in uniform and harmonically trapped gases in 3D. The review [6] has also argued for the presence of anomalous fluctuations.

A number of explanations for the two kinds of results for condensate fluctuations have been proposed. Ref. [83] has pointed to the difference arising from whether a perturbation theory approach is used (giving normal condensate fluctuations due to thermal atoms in single-particle excited orbitals) or a full Bogoliubov approach that describes primarily fluctuations due to collective excitations of low energy modes (anomalous condensate fluctuations). This interpretation is also confirmed by [8]. Nevertheless, Ref. [12], using a different analysis, argues that anomalous fluctuations are a result of inconsistent inclusion of higher order terms in the Bogoliubov calculations, and should not be present when $U(1)$ symmetry is broken. The earlier work of [92] pointed to anomalous fluctuations being tied to a broken $U(1)$ gauge symmetry, but also argued that appropriate use of the random phase approximation of [137] restores normal fluctuations. A further angle on the problem was provided by

[138] using a Bogoliubov-Popov approach which saw a crossover from anomalous to normal fluctuations for sufficiently large systems, though this same work also predicted unphysically large fluctuations near T_c .

Overall it appears that the controversy regarding anomalous or normal condensate fluctuations is convolved with the issue of whether a thermodynamic limit or an explicitly mesoscopic-size system is under consideration, but there are yet to be further aspects of the matter to understand.

4.3. Beyond Bogoliubov

Study of the statistics of interacting bosons beyond the regime of applicability of the Bogoliubov approximation is notoriously difficult. The exact result can be obtained in the thermodynamic limit of the 1D box, modelled by the Lieb-Liniger model [139, 140] – a rare example of a solvable model describing a quantum many-body system – plus its extension to nonzero temperature in the Yang-Yang model [141]. These are used as the baseline for a number of successful [142, 143, 144, 145] and ongoing studies of fluctuations such as [146]. Still, fluctuations of N_0 and ensemble (in)equivalence were not subjects of research by this route.

The statistics of an interacting Bose gas has been the subject of many studies based on various Monte-Carlo methods [147, 148] most of which were focused on the interaction-induced shift to the critical temperature (see the review [149]). The full statistics of 1D trapped gas has been computed in [150] in the canonical ensemble confirming the results of the Bogoliubov approximation at low temperature.

Returning to explicit studies of δN_0 , the work of [25] (and more rigorously [26], but arguably less accurately [151]) showed that one can hybridise the Bogoliubov approximation with the master equation method of [74], obtaining well-behaved properties also at temperatures of the order of, and across T_c . A complementary approach explicitly imposing CN restraints is presented in [151]. Fig. 12 shows the first four moments of N_0 in a 3D box in both ideal and interacting gases, as calculated with this approach.

Other works investigated various aspects of the problem. Refs. [152, 153, 154, 155] looked at 3D traps and boxes and found condensate fluctuations to depend on boundary conditions in mesoscopic systems and even in the thermodynamic limit; Refs. [152, 156] made also forays towards stronger interactions.

Condensate fluctuations in the interacting gas have also been studied via a completely independent constructive approach using a classical field representation of wavefunctions in the canonical ensemble, first in [102], which provided a constructive Metropolis algorithm. Another classical field approach are the er-

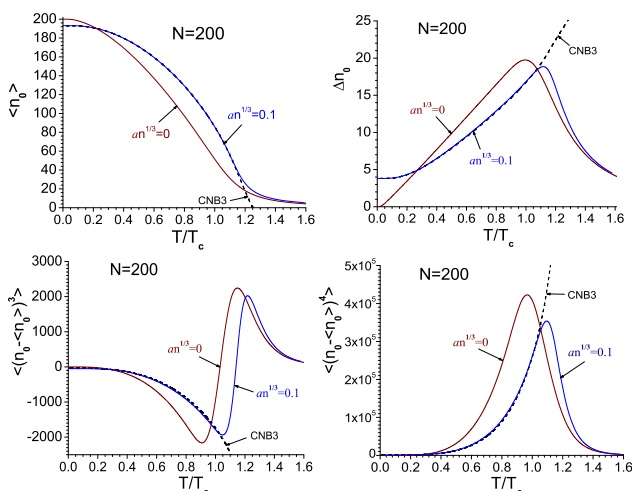


Figure 12. The first four moments of condensate occupation in a 3D box with $N = 200$ in both the ideal gas (brown solid) and the weakly interacting gas ($an^{1/3} = 0.1$, blue solid) as calculated using the hybrid master equation/quasiparticle approach [25]. The dashed “CNB3” lines refer to the interacting quasiparticle based approach in [24, 23]. Reproduced with permission from [25]. ©American Physical Society. Used with permission.

godic evolution methods described in Sec. 3.4. In [157] a harmonically trapped 1D gas was studied, and it was found that the peak fluctuations grow and shift to lower values of T/T_* as $g > 0$ grows (along with an overall reduction of $\langle N_0 \rangle$ for the same T/T_* , T_* being the characteristic transition temperature for the system). The same effect was seen for a 3D trap by [27] using a different approach with the help of recursion relations. However an opposite effect was reported for hard sphere pseudo-potentials [158].

Classical fields can also be easily applied to an interacting system with external particle exchange as in a grand canonical ensemble [115, 159], or intermediate ensembles [117] that better approach experimental levels of fluctuations. The latter study constructively confirmed from an independent angle that the introduction of interactions suppresses the extravagantly large fluctuations seen in the ideal gas in a GCE.

A separate topic of interest for which condensate fluctuations have been investigated despite the difficulties is the weakly attractively interacting gas. First [110] using a classical field approach for a 1D trapped system, found a small reduction of condensate fluctuations for weak attraction, turning into an increase as attraction became stronger. A later work used recursion relations [160] on Li^7 parameters of trapped finite-size condensates, finding δN_0 fluctuations reduced compared to the non-interacting case.

One should remark about the restoration of ensemble equivalence by interactions. It is generally

accepted that with sufficiently strong interactions the interactions energetically suppress any excessive number fluctuations [20] and equivalence between GC and CN ensembles are restored. This can take place even for objectively very weak interactions if the system is collectively large. The details of this matter have been, and continue to be, widely debated [20, 4, 22, 23, 28, 87, 6, 25, 125, 106, 161, 162, 78, 12, 163, 164, 165]. The review [6], chapter 6, gives some results regarding when ideal gas fluctuations transition to the interaction regime, using a Bogoliubov treatment. Refs. [10] and [11] give fairly recent summaries of the current understanding, [12] is a recent view on the grand canonical catastrophe or, as named there, incorrect use of the GCE. The practical importance of the matter relates intimately to the question of whether one needs to be careful with one’s choice of ensemble for theoretical or numerical calculations or whether it is fine to choose the most practically convenient one at one’s disposal.

Finally, in real experiments with ultracold atoms it can occur also that variation in particle number due to technical elements of the preparation makes the total number fluctuations significant but less than what would be predicted by the GCE. For example, [166] reported standard deviations $\delta N/N$ of about 20-35%. To experimentally investigate the fluctuations of N_0 the deviation needs to be lower, for a typical total number of atoms, than 0.2%. The newer experiments with strong focus on control over N report 0.01% [167] – see Sec. 5 for details.

Two further cases relevant with regard to intermediate ensembles are: (1) photonic BECs. Here the size of the particle reservoir with which they are in contact can be varied to experimentally study the crossover between the GCE and CE in a controlled way [58]. (2) the broad field of polaritonic condensates [93, 95] – here the system is very open in terms of particle exchange so that it can not be described as an equilibrium system even in its steady state. Methods to explicitly deal with such intermediate ensembles include averaging of CN ensemble results with N variation entered by hand, stochastic equations tailored to polariton physics [168, 94] or automatic control of the N variance while stochastically generating ensembles like in [117].

As we mentioned previously, the problem of fluctuations in the interacting Bose-gas is notoriously difficult. Most of the above-mentioned results were devoted to the canonical or grand canonical ensembles. On the other hand the recent experiment [9] reported fluctuations below the canonical one. In the next subsection we describe a recent advance – a stochastic method suitable for weakly interacting systems in a microcanonical ensemble.

4.4. The Hybrid Sampling Method

Among the methods described in Sec. 3 two in particular used a Metropolis sampling approach. In order to obtain the canonical ensemble in a wave picture (classical fields) or the complementary particle picture (Fock states sampling - FSS). Both scan the space of states to collect samples representative of the statistical ensemble from, a Markov chain constructed using the Boltzmann factor $e^{-\beta E}$ to determine the acceptance criterion in the Metropolis algorithm. Here E is the energy of the non-interacting Hamiltonian. Both methods can perfectly reproduce exact results in the ideal gas canonical ensemble, with the added benefit in FSS method of calculating the condensate statistics in the microcanonical ensemble.

At first glance, including the effect of weak collisions in both methods seems simple: ensure that the energy defining the Boltzmann factor includes the expectation value of the interaction Hamiltonian. However, applying this approach to the most relevant case of a harmonic traps yields different results for the classical fields and the FSS methods. According to the classical fields method, collisions increase fluctuations, while the FSS method indicates they decrease them.

In fact, both methods have serious drawbacks when applied to the interacting gas. The set of states in the FSS method contains only Fock states and lacks the vector space structure fundamental to coherent and entangled elements of quantum physics. There are no superpositions, no coherence. It works well for the ideal gas [7, 9] in which a hard-wired basis set does not pose a problem, but there is no provision for interference or repulsion between locally overlapping orbitals if interaction is introduced.

The classical fields method operates in a vector space, dealing very well with amplitudes, superpositions, and not relying strongly on basis choice. The condensate wave function, as defined via Onsager-Penrose criterion [169], can be computed post-factum by diagonalizing the one-particle density matrix, and subsequently the correct state occupation statistics can be calculated [100]. However, the classical fields method does not deal well with occupations in the high energy modes which decay too slowly as $k_B T / \varepsilon_j$ instead of the $1/(e^{\varepsilon_j \beta} - 1)$ required by full quantum mechanics in the particle-like regime. It is therefore plagued by the ultraviolet catastrophe, with results heavily dependent on the cut-off value, whose best though not ideal value must vary nontrivially with temperature and the coupling constant [110, 101, 108, 103]. The aim of this section is to present a hybrid sampling method, which combines the virtues of both methods: allowance of coherences and an adaptively shaped condensate wave function characteristic of the classical fields method, while preserving the absence of a neces-

sary cut-off as inherited from the FSS method.

The set of states used to model the canonical ensemble consists of all classical fields in consecutive single particle orbitals. In practical numerics, only a finite number of states is necessary, so we use a sufficiently high energy cut-off. Thus, each state $\Psi(\mathbf{r}) = \sum_{j=0}^{j_{\max}} \alpha_j \phi_j(\mathbf{r})$ is defined by a finite vector of complex amplitudes

$$\vec{\alpha} = (\alpha_0, \alpha_1, \dots, \alpha_{j_{\max}}), \quad (119)$$

just like in the classical fields approximation (90), but now, the occupation of each orbital is restricted to be an integer $N_j = |\alpha_j|^2$ with global constraint $\sum_j N_j = N$ - this like in the FSS approach.

In the hybrid method, each proposed update in the Markov chain consists of two substeps. First, we move one atom from orbital j to orbital l according to the FSS algorithm described in Sec. 3.3. Next, we rotate the phase of every nonzero (occupied) α_i . To do so one first adds a random noise

$$\alpha_i \mapsto \alpha_i + \delta \xi_i \quad (120)$$

where δ is a (optimally small, $|\delta| \ll 1$) parameter fixed mutation and ξ_i a complex Gaussian random number of variance one, and then normalizes to the original $|\alpha_i|$ that one had after moving one atom $j \rightarrow l$. Overall this produces smaller relative phase changes in highly occupied orbitals.

This way, we obtain a new state with a single atom transferred from orbital j to l and with randomly modified phases. As a next step, we calculate the expectation value of the Hamiltonian in each state:

$$H(\vec{\alpha}) = \sum_i E_i |\alpha_i|^2 + \frac{g}{2} \int d^D \mathbf{r} \left| \sum_i \alpha_i \phi_i(\mathbf{r}) \right|^4 \quad (121)$$

where with the notation of (90),

$$E_j = \int d^D \mathbf{r} \phi_j^*(\mathbf{r}) \left[-\frac{1}{2} \nabla^2 + V(\mathbf{r}) \right] \phi_j(\mathbf{r}). \quad (122)$$

We chose $\phi_j(\mathbf{r})$ as the single particle orbitals of the empty trap, but choices may depend on the problem, as usual in classical field methods.

The Boltzmann factor $e^{-\beta H(\vec{\alpha})}$ is used in the usual Metropolis algorithm manner to compare to a random number $r \in [0, 1)$ giving acceptance when $e^{-\beta H(\vec{\alpha})} \geq r$, cloning otherwise.

Once the canonical ensemble is constructed from sufficiently spaced Markov chain samples $\vec{\alpha}^{(\nu)}$, $\nu = 1, \dots, \mathcal{M}$, taking care to gather a large ensemble and discard the initial transient, the next step towards extracting the condensate [100] is the construction of the one-particle density matrix, which can be done directly in the orbital basis

$$\rho_1(\vec{\alpha}, \vec{\alpha}') = \langle \alpha_j^* \alpha_{j'} \rangle = \frac{1}{\mathcal{M}} \sum_{\nu=1}^{\mathcal{M}} \alpha_j^{(\nu)*} \alpha_{j'}^{(\nu)}. \quad (123)$$

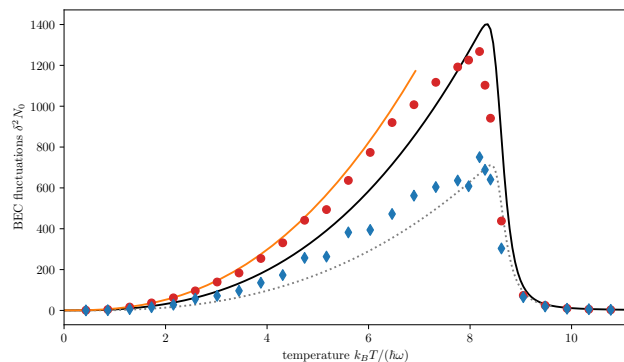


Figure 13. Fluctuations of the condensate atom number as a function of temperature in a 3D spherically harmonic trap with frequency $\omega = 2\pi \times 100$ Hz for $N = 1000$ Rubidium atoms (assumed scattering length $a = 81.8$ Bohr radii) Solid black line – exact canonical fluctuations for the noninteracting gas (25); dotted grey line – exact microcanonical fluctuations for the noninteracting gas; solid orange line – canonical fluctuations calculated with the Bogoliubov approximation; red circles – hybrid method, canonical ensemble (note the near perfect agreement with Bogoliubov approximation at low temperatures); blue diamonds – hybrid method, microcanonical ensemble.

According to the Onsager-Penrose definition, the dominant eigenvalue $\lambda_0 = N_0$ is the condensate fraction. The corresponding eigenvector $(\alpha_{0,0}, \alpha_{0,1}, \dots, \alpha_{0,j_{\max}})$ determines the condensate wavefunction $\psi_0(\mathbf{r}) = \sum_{j=0} \alpha_{0j} \phi_j(\mathbf{r})$. Then the probability distribution of condensate occupation in the CN is represented by a histogram $\mathcal{P}(N_0^{(\nu)})$ of projections of the individual samples $\vec{\alpha}^{(\nu)}$ onto condensate:

$$N_0^{(\nu)} = \sum_j \left| \alpha_j^{(\nu)*} \alpha_{0,j} \right|^2. \quad (124)$$

As explained in Sec. 3.3, the postselection process on $H(\vec{\alpha}^{(\nu)}) \in [\bar{E} - \Delta_E/2; \bar{E} + \Delta_E/2]$ allows us to also extract the microcanonical statistics at energy \bar{E} .

We demonstrate the utility of the hybrid method with the physically relevant results shown in Fig. 13. Specifically, we consider $N = 1000$ rubidium atoms confined in a 3D spherically symmetric harmonic trap with a frequency of $\omega/2\pi = 100$ Hz. The data are represented as follows: black solid lines correspond to results for a non-interacting gas in the canonical ensemble, while black dotted lines show the microcanonical results for the same non-interacting gas. Both of these results are exact. The results for the interacting gas were obtained using the hybrid method. Red circles represent canonical data, while blue diamonds denote microcanonical data. The orange dotted lines correspond to the benchmark of the (particle non-conserving) Bogoliubov approximation. The hybrid CN and Bogoliubov results align at low temperatures. We see that in this case, interactions reduce the maximum fluctuations observed in the canonical ensemble. Notably, while interacting CN

results in this regime with large N and T might also be obtained using a master equation approach, this is the only current approach that gives MC fluctuations in this regime (barring a basic classical field ergodic method which would have large cutoff-dependent systematics in 3d).

The methods just discussed have been used for some comparisons with experimental results, but their number remains limited and the comparisons have been quite noisy. One significant reason for this is the scarcity of experimental data: to date, only one group has achieved the necessary precision in measuring fluctuations in the number of condensed atoms. Additionally, the large number of atoms typically involved in such experiments poses significant challenges for the current theoretical/numerical methods.

5. Experiments

In the following, we review the experimental progress in addressing the measurement of condensate fluctuations.

The experimental realization of weakly interacting BECs introduced a new framework for studying many-particle quantum systems. However, until recently the experimental investigation of BEC population statistics was limited to the first moment, and higher moments, such as BEC atom number fluctuations, remained inaccessible due to technical noise. The considerable theoretical interest in number fluctuations discussed in this review crucially necessitates the experimental exploration of this fundamental feature.

Two recent experimental developments have allowed for a deeper investigation of the fluctuations in Bose gases. On the one hand, atomic BECs have made considerable progress in stability by using active monitoring and feedback techniques. This has allowed for a suppression of the technical noise contributions, revealing the inherent microcanonical fluctuations [9]. On the other hand, the creation of photonic BECs [170] has provided access to non-interacting Bose gases which realize the grand canonical scenario. We will emphasize the former case since recent theoretical progress has focused on the interacting Bose gas.

5.1. Experiments with atomic Bose gases

5.1.1. Relevant experimental developments Until recently, primarily the number of particles in a BEC, corresponding to the first moment of the statistical distribution had been investigated [171, 172, 173]. This provided access to the fraction of condensed atoms as a function of temperature and thus allowed for evaluation of the critical temperature [174, 175]. Typically, the ideal gas model already captures its general behavior in experiments with ultracold atoms. The

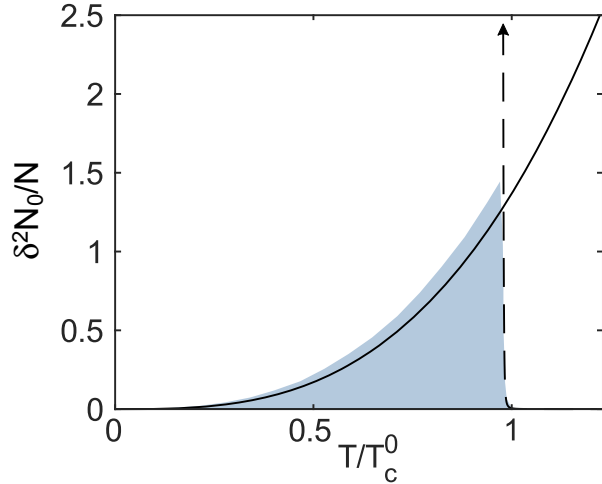


Figure 14. Limiting cases of the expected fluctuations in experimental realizations, for the case of an ideal gas with $N \sim 5 \times 10^5$ in an isotropic harmonic trap. At the critical temperature T_c^0 a grand canonical ensemble calculation predicts unphysically large fluctuations (dashed line). Below T_c^0 the leading CN contribution of Eq. (64) provides a good estimate of the fluctuations [2, 3] (solid line). An exact numerical calculation [17] shows how these two expressions serve as limiting cases in the two temperature regions (shaded area). Reproduced from [30] ©American Physical Society. Used with permission.

agreement is improved by the inclusion of corrections for interactions and finite size effects [176]. Importantly, interactions induce a shift of the critical temperature, which can be understood intuitively; A positive scattering length causes the atoms to repel each other, reducing the central density in a ultracold cloud, which in turn reduces the critical temperature for condensation. Note however, that higher order corrections push the shift in the opposite direction [177]. A more detailed comparison between experiment and theory can be achieved by treating the interactions between the condensate atoms and the thermal atoms with self-consistent methods. Detailed experimental investigations of the condensate fraction were reported in [171, 172, 173, 175]. The observation of beyond mean-field contributions to both the shift in the critical temperature and the condensate fractions was reported in [174, 178]. A wide array of experiments have also probed local density fluctuations, some of the first being [179, 180]. However, local fluctuations do not provide a way to extract the fluctuations of the number of atoms in the ground state mode – which is nonlocal.

The first time the statistical properties of a Bose gas were considered experimentally was a seminal experiment showing the sub-Poissonian number statistics in such a gas [181]. These measurements were conducted for very low total atom numbers $50 < N < 3000$ at low temperatures. In the

regime $N < 400$ they showed sub-Poissonian statistics with $\delta^2 N/N < 1$ as expected from analogy to Fig. 14. However, the experiment did not distinguish between condensed and thermal atoms and thus it remained unclear whether the effects of the evaporation process or the inherent fluctuations of the condensed atom number had been observed.

Importantly, fluctuations in BECs are also caused by nonequilibrium phenomena that go beyond standard statistical ensembles. In particular, phase fluctuations typically occur in BECs at high temperature, especially in elongated or low-dimensional clouds [182, 183], and lead to density modulations after time-of-flight (TOF) imaging [184]. Furthermore, studies have investigated the dynamical behaviour of the condensate fraction when crossing the phase transition. Wolswijk *et al.* [185] measured fluctuations of condensate fraction in an Na^{23} during evaporative cooling as it took the gas below T_c . They found exponential decay of the fluctuations at a rate somewhat slower than the condensate growth rate.

5.1.2. Challenges The challenges for the experimental observation of fluctuations in a typical quantum gas experiment are directly evident from fluctuation calculations illustrated by Fig. 14. Consider a sample with total atom number $N \sim 5 \times 10^5$. If the peak fluctuations are of the order of \sqrt{N} , this means that the standard deviation of the BEC atom number N_0 has to be measured at a level of $\delta N_0 \approx 700$. However, any drift in the temperature T and atom number N also leads to a change in N_0 . The stability requirements for N and T can be estimated from the well-known ideal-gas result Eq. (47) for the condensate atom number, $N_0 = N - \text{const.} \times T^3$. To first order the variation in N_0 for low condensate fraction is then $\delta N_0 \sim N(\frac{\delta N}{N} - 3\frac{\delta T}{T})$. The relative stability of N and T must thus meet the condition $\frac{\delta N}{N} < 0.14\%$ and $\frac{\delta T}{T} < 0.05\%$. In principle, this can be achieved in two ways. Either the experiment inherently meets the stability criteria, or alternatively, it may be possible to post select data within a small range of N and T in an experiment with large shot-to-shot fluctuations but very good imaging allowing for precise determination of N , N_0 and T . Recent work has shown that only the first option is possible [186], since post-selection adds an ambiguity to the measured ensemble precluding the identification of fluctuations. Additionally, the post-selection method would require a very large number of realizations due to the variation of N and N_0 by 10% in typical experiments. Therefore, the active stabilization of the experiment was chosen in recent experimental realizations outlined below.

In addition to preparation, experimental noise is present in the measurement and estimation of

the atom numbers. Noise sources include, but are not limited to, shot noise in imaging light, camera noise, optical imperfections, fitting uncertainties, light frequency variations, the probabilistic distribution of a finite number of atoms, and the effects of interactions between atoms on the distributions used to extract the thermal and BEC atom numbers individually. Moreover, these noise sources have a complex dependency on both atom numbers and temperature. These effects have to be taken into account to an appropriate extent when the atom number fluctuations are measured [186].

5.1.3. Experimental Improvements To improve the preparation noise in the experiment with active stabilization it is necessary to extract information about the system non-destructively. The dark-field Faraday imaging (DFFI) technique reported in [187] is well suited for this task. The technique exploits the Faraday rotation effect of the polarization of light traversing an atomic sample. By using far-detuned probe light, the absorption of light is limited and the atomic sample is left relatively unaltered. In [29], the probe light was linearly polarized and the non-rotated light was diverted towards a beam dump by a polarizer. Consequently, only the rotated probe light passes the polarizer and was detected on a CCD camera. This then allowed for spatially resolved non-destructive images of ultracold clouds and in particular for the extraction of the atom number. This dark-field Faraday imaging approach was also shown to yield a precision that surpasses the atom-shot-noise [167] for appropriate imaging conditions.

By adding an active feedback mechanism to the DFFI technique, the atom number in a single shot can be decreased in a controlled manner and thus the atom numbers can be stabilized at the cost of slightly fewer atoms. This method was demonstrated in [29] where the radio frequency (rf) evaporation in a magnetic trap was controlled in real-time in response to the DFFI signal. The stabilization method was later implemented in [30] to achieve the first measurements on the atom number fluctuations in partly condensed BECs.

5.1.4. Experimental realization in ultracold Bose gases In the following, we briefly outline the experimental steps used in the recent observations of fluctuations in BECs [30, 9, 186]. To initiate the experiments $\approx 10^9$ ^{87}Rb atoms were captured and cooled in a magneto-optical trap. The cloud was then optically pumped into the $|F = 2, m_F = 2\rangle$ state and transferred to a harmonic magnetic trap with axial frequency ω_a and radial frequency ω_ρ . In this trap, further rf evaporative cooling was performed to lower the temperature of the sample. This sequence is prone to technical

fluctuations that can obscure the observation of atom number fluctuations. To address this, the stabilization procedure outlined above was initiated when the cloud contained $\sim 4 \times 10^6$ atoms at a temperature of $14 \mu\text{K}$. The cloud was probed using minimally destructive Faraday imaging [187, 167] to determine the atom number in that particular experimental realization. This number was then corrected with a weak rf pulse of controlled duration which removed excess atoms. Subsequently, a second Faraday measurement verified the outcome, thereby achieving a relative stability of atom number at the 10^{-4} level [29]. For the final cooling step towards BEC, a tightly compressed magnetic trap with a high collision rate was used. In its most compressed state, the trap's aspect ratio was $\lambda = 174$, which can cause significant phase fluctuations across the cloud that evolve into density modulations during time of flight, complicating precise atom number and temperature determination [184]. To mitigate this, the trap was decompressed for measurements, reducing the aspect ratio to values between $4.5 < \lambda < 10$, where the phase coherence length exceeds the condensate length along the long axis. In the final stage, BECs were produced by forced evaporation at a radio frequency corresponding to the desired BEC temperature. To ensure thermal equilibrium, the BEC was held at the final frequency for 800 ms, followed by another 400 ms without rf radiation, before the trap was switched off. The cloud was then probed after a time-of-flight expansion using resonant absorption imaging on the $|F = 2\rangle \rightarrow |F' = 3\rangle$ cycling transition. A measurement consisted of 4 images used to reduce undesired imaging artifacts. Image 1 contained atoms, image 2 had no atoms, and image 3 and 4 had no imaging light but were otherwise taken under the same conditions as image 1 and 2. Image 3 was subtracted from image 1 and image 4 from image 2 to remove dark counts from the camera.

Great care was taken to mitigate imaging effects on the detected atom number. This includes calibration of the effective saturation intensity [188, 189, 190, 191], the radius of the thermal cloud fitting region [192], and the effects of the imaging photons on the cloud [193, 194]. Effects of imaging induced Doppler shifts were also considered [195, 189]. The focusing of the imaging system was optimized by following previously developed methods [196]. The imaging light parameters were optimized to minimize noise according to earlier work [197, 198, 195, 199]. Techniques to reduce shot noise and imaging fringes were considered [200, 201, 202, 203]. It proved especially important to keep the imaging duration short to avoid any movement during the image. Keeping the duration between images short reduces the fringes caused by oscillations in optical elements when

comparing the images with and without atoms.

To determine the BEC atom number in each image, the wings of the cloud are fitted with a Bose-enhanced thermal distribution reduced to the two-dimensional column density from which the temperature is obtained. The fitted distribution is subtracted from the image, and the BEC atom number N_0 is obtained by integration of the remaining column density.

However, the variance cannot be determined directly from N_0 , since small remaining drifts of the magnetic offset field lead to minor temperature variations with a median standard deviation of ~ 3 nK. This drift is eliminated by subtracting a linear fit of the condensate number as a function of the total atom number [30] and determine the residuals η_i , where i indicates the order in time. The BEC atom number variance is then given by a two-sample variance of the residuals

$$\delta^2 N_0 = \frac{1}{2} \langle (\eta_{i+1} - \eta_i)^2 \rangle. \quad (125)$$

Thus, this two-sample variance contains the BEC fluctuations and detection noise, but excludes slow technical drifts. This evaluation technique is commonly called the *correlation method*.

The peak fluctuations are determined by a fit to $\delta^2 N_0$ based on the theoretical expectation illustrated in Figs. 1 (b), 5, and 14. Specifically the fit function mimics the asymptotic behavior of the fluctuations in a non-interacting gas $\delta^2 N_0 = \zeta(2) \left(\frac{k_B}{\hbar\bar{\omega}}\right)^3 T^3$, where $\bar{\omega}$ is the geometric mean of the trapping frequencies [2]. Moreover, the fluctuations decay in near step-like manner close to the critical temperature, which we model with a Heaviside step function $\Theta(T_p - T)$, where T_p is the temperature at the peak fluctuations. To account for small temperature drifts the expression is furthermore convolved with a normal distribution $\mathcal{N}(T, \sigma_T)$ centered on the temperature T with a standard deviation σ_T given by the median of the measured temperature variation. Thus, fit model is given by

$$\delta^2 N_0(T) = (f * g)(T) + \mathcal{O} \quad (126)$$

where f and g are given by

$$f(T) = \delta N_{0,p}^2 \left(\frac{T}{T_p}\right)^3 \Theta(T_p - T),$$

$$g(T) = \mathcal{N}(T, \sigma_T).$$

The three fit parameters are the peak atom number variance $\delta N_{0,p}^2$, T_p and an offset \mathcal{O} which accounts for experimental noise [30]. They constitute the final result of an experiment at a given initial atom number and trap configuration. A more refined fit has recently been explored in [186].

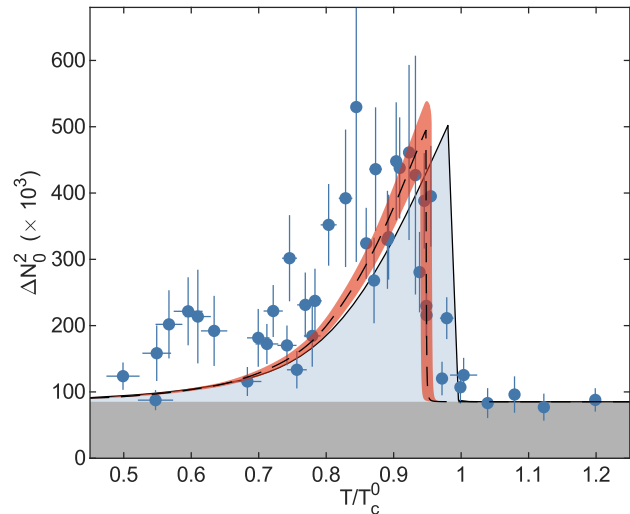


Figure 15. Variance of the BEC atom number, constituting the first detection of BEC atom number fluctuations. The dashed line is a fit to the data (see text) where shading indicates the confidence bound on the fit. The data is compared to a prediction in a non-interacting gas (light blue shading). Gray shading indicates a fitted offset due to technical fluctuations. Reproduced from [30] ©American Physical Society. Used with permission.

5.1.5. Experimental results with ultracold gases The first observation of atom number fluctuation in a BEC according to the methods outlined above succeeded in 2019 [30]. The stabilization technique based on Faraday imaging enabled the preparation of ultracold thermal clouds at the shot noise level, eliminating numerous technical noise sources. In the data analysis, the *correlation method* was utilized to accurately determine both the fluctuations and the sample temperature.

This allowed for the observation of the distinctive signature of the fluctuations, namely a sudden increase in fluctuations of the condensate atom number near the critical temperature as shown in Fig. 15. Note that these initial experiments employed a less refined fit function than outlined above. Nonetheless, they captured both the size of the peak fluctuations and the shift of the critical temperature due to interactions in the system.

These initial experiments raised the question whether the effects of interaction and the appropriate thermodynamic ensemble can be identified. This was investigated by measuring the peak fluctuations for various atom numbers and trap geometries [9] as shown in Fig. 16. Most significantly, the study showed a reduction in observed peak atom number fluctuations by 27% with respect to predictions for a canonical non-interacting gas. This reduction is expected in the microcanonical case and thus underscores the microcanonical nature of the system. The experiment

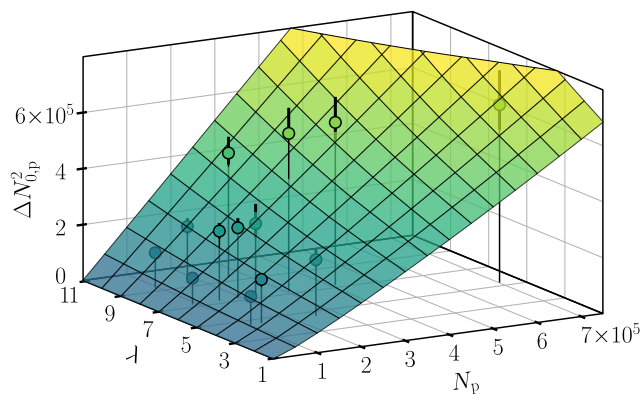


Figure 16. Peak variance of the BEC atom number as a function of N_p and trap aspect ratio λ . The experimental data was compared to a theoretical expectation for the non-interaction canonical ensemble, scaled to the data in a fitting procedure (see text). Reproduced from [9]. [CC BY 4.0](#)

also showed anomalous scaling of fluctuations with atom number, which was attributed to the interplay between dimensional and interaction effects. These results were accompanied by simulations showing the microcanonical reduction of fluctuations and the dependence on trapping geometry and atom number. This work advanced the field by demonstrating the critical role of the microcanonical ensemble in describing fluctuations and thus highlighted the path towards the interpretation of future experiments with ultracold gases.

The most recent work on fluctuations in degenerate Bose gases analysed the correlations between the thermal and the BEC atom number [186] in a partially condensed Bose gas. If only fundamental fluctuations were present, one would naturally expect a perfect anticorrelation. The possible observation of such a correlation thus served as a motivation for the investigations.

To allow for a comparison of the variances in the thermal and the condensed cloud, a comprehensive model of the noise sources was developed. This allowed for a distinction between noise contributions due to the preparation, the image analysis and the inherent fluctuations. The three largest noise contributions in the analysis procedure were identified as the effect of the image fitting technique, the effect of the binomial distribution of atoms in each pixel, and the effect of the variation of the imaging laser frequency. These uncertainties, together with several smaller contributions, were included in the analysis of atom number fluctuation results for the thermal and BEC components as shown in Fig. 17. This led to a temperature-dependent offset of the variance due to all technical noise sources and complicated the analysis, in particular since the technical noise features a slow increase starting at the critical temperature.

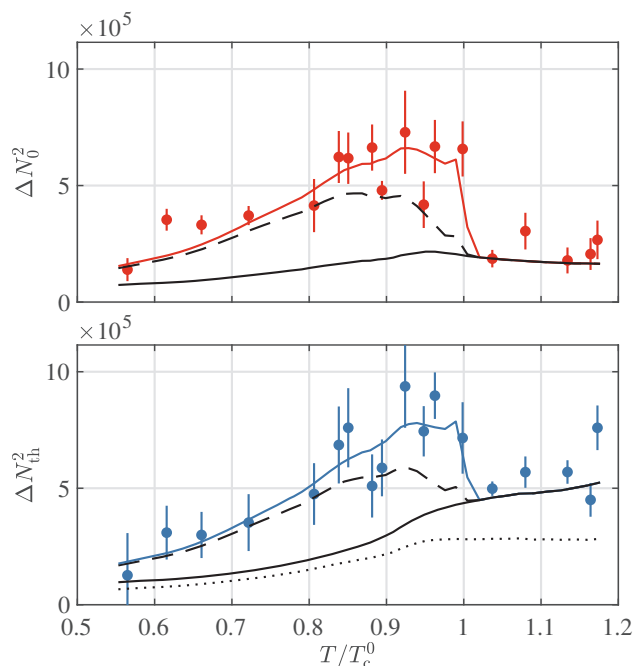


Figure 17. Fluctuations in BECs and the corresponding thermal clouds. Upper panel: Variance of the BEC atom number as a function of temperature. The variance due to estimation errors (full black line), and total technical noise (dashed black line) are indicated. The colored line shows the total fitted variance. Lower panel: Variance of the thermal atom number shown with the same contributions to the variance. In addition, a dotted line indicates the estimation error extracted from the Monte Carlo simulation. Reproduced from [186]. [CC BY 4.0](#).

In total the analysis provided an improved value of the peak BEC atom number fluctuations, $\delta N_{p,0}^2 = (3.7 \pm 7) \times 10^5$ near the critical temperature for the specific experimental parameters, representing a 41% reduction compared to Ref. [9] and further supports the microcanonical nature of the fluctuations.

The noise analysis also revealed that the *correlation method* to extract the variance leads to an artificial anticorrelation between the thermal and BEC atom numbers. Hence, the measurement of atom number fluctuations in the thermal cloud as shown in Fig. 17 can not be considered an independent observation of fluctuations but presents a complementary method to obtain fluctuation data.

These recent achievements highlight the potential for more refined experiments, including larger atomic samples to approach the thermodynamic limit, and improved measurement techniques to reduce uncertainties. This research provides a foundation for an improved understanding the complex interplay of quantum statistics, interactions, and ensemble constraints in Bose gases.

5.2. Experiments with Photons

Photonic Bose-Einstein condensates in dye microcavities [170] provide access to the investigation of condensate statistics in different ensembles from atomic condensates. The photonic condensates can have access to controlled heat and particle reservoirs in the dye molecules resulting in systems described by canonical or grand canonical ensembles. In particular photonic condensates are often compared to lasers, but the two systems exhibit some fundamentally different properties with fluctuations being one of them.

Early theoretical investigations of photonic condensates in the grand canonical ensemble showed fluctuations above Poisson-like behaviour and increased fluctuations compared to atomic experiments [204]. Shortly after, fluctuations in photonic condensates were observed experimentally [205]. The experiment yielded both the fluctuations and the probability distributions of photonic condensates for different condensate fractions. The observations found the expected unusually large fluctuations and a comparison with the non-interacting grand canonical predictions found a good agreement in the measured range.

Theoretical calculations of the effects of contact interactions in photonic condensates were carried out [206] and compared to the experimental results from [205]. The result was a good agreement with the experiment but stressed the importance of a systematic, experimental investigation of the interaction strength. Further theoretical investigation of the effect of weak interactions in experimentally accessible few-particle systems were carried out with two different models in [58]. The resulting fluctuations for grand canonical ensembles were still much higher than for canonical ensembles. It was also found that the typical textbook treatment using the ideal gas model differed significantly from even weakly interacting systems.

The fluctuation-dissipation theorem which connects the thermal fluctuations in a system to its response to external perturbations were experimentally investigated in [207] using photonic condensates. The response and the fluctuations of the photonic condensates were measured separately and compared. The result was good agreement with the theorem and demonstrated the thermal nature of the photonic condensate system.

The dynamics of fluctuations in open photonic condensate systems were theoretically and experimentally investigated in [208]. It was found that the precise behaviour of the fluctuations depended sensitively on the openness of the system and further study of the effect of interactions between system and environment was encouraged.

The experimental results with photonic conden-

states in [205, 207] demonstrate their versatility in statistical remeasurements and the complementarity to atomic condensate experiments in investigation of different thermodynamical regimes.

6. Perspectives

This review provides a comprehensive overview of the current theoretical understanding and experimental results on the condensate fluctuations in quantum degenerate Bose gases. We highlighted the available theoretical approaches with a special focus on the role of the ensemble choice. We discussed the important experimental progress made recently using two experimental platforms based on ultracold atom and photons in dye filled microcavities. Thus this work also updates previous reviews covering related topics [14, 6, 56, 12].

As we have seen in previous sections, numerous questions remain, providing opportunities for further investigation. In the following we first outline the perspectives for future experimental work and then discuss the next steps to be taken in theoretical development.

Based on the available techniques of producing highly stable Bose-Einstein condensates it should be possible to examine the higher moments of the fluctuations as shown theoretically in Fig. 12. However, the measurement of higher moments requires considerably more data and consequently a longer period in which the atom number and trap parameters are kept stable. Another avenue based on the existing experimental methods is the investigation of lower dimensional systems such as quasi-1D or quasi-2D systems where BECs can be produced with standard techniques. If the stabilization technique is combined with the use of Feshbach resonances to tune the interaction strength a realization close to the case of the ideal gas may even be possible.

Another fascinating possibility is to explore fluctuations in experiments which can count individual atoms. In such experiments with small BECs it may be possible to freeze the entire ensemble and record each atom's position. Steps towards this goal have been taken in 2D systems recently [209, 210, 211] yielding the promise that exact counting experiments of fluctuations are on the horizon.

Moreover, the investigation of fluctuations can be extended to the growing number of available ultracold quantum systems. This includes multi component systems consisting of different atomic species or atoms in a number of quantum states [212]. In such quantum mixtures of ultracold gases the situation becomes yet more complicated due to the mutual interaction of the components. Alternatively, other

interactions within a single component have become experimentally accessible, particular long range dipole-dipole interactions [213]. These systems are currently under intense experimental scrutiny, and they would be a prime candidate to investigate the effect of such long range interaction on the fluctuations in a quantum gas. This study can be done together by both experiment and theory with established methods for weakly interacting gases.

On the theoretical side, a similarly large number of questions remain unanswered. One direction of investigation is ensemble (in)equivalence. As discussed in Secs. 2 and 3, different ensembles lead to different results when it comes to condensate fluctuations in the ideal gas, even in the thermodynamic limit. This may change drastically for interacting systems. Interactions make density fluctuations energetically unfavourable, and it is expected that condensate fluctuations will become ensemble-independent. A definitive understanding of the anomalous fluctuation controversy in weakly interacting gases, such as the conditions under which the various results become valid as the thermodynamic limit is approached, has also not been fully reached.

The Lieb-Liniger (LL) model [139, 140, 141], a solvable model of a 1D homogeneous gas of atoms interacting via a delta potential, provides a natural system for obtaining rigorous results in this context. While fluctuation results exist for the LL gas at finite temperature [214, 146, 145], they neither address N_0 fluctuations nor differences between statistical ensembles. Even within a given ensemble, the role of interactions in anomalous fluctuations remains controversial and requires unambiguous resolution. Another promising avenue for widening the topic lies in studying quantum statistics across different physical systems, including multicomponent condensates. Dipolar gases, known for exhibiting quantum droplets [215, 216] and supersolids [217, 218] have emerged as a highly active area of research in ultracold atoms. While some results exist on thermal effects in dipolar Bose-Einstein condensates (BECs), including changes in the BEC fraction at finite temperature [219, 220, 221, 222, 223, 224], the fluctuations of the number of condensed atoms have not yet been investigated. Of particular interest are the gas-droplet transition and the self-cooling mechanism observed in quantum droplets [225]. Beyond the thermodynamic equilibrium state, significant attention has been devoted to atoms in resonant cavities and interacting via photon-mediated interactions [226, 227, 228], or polaritonic BECs [229, 230, 231], where dynamical equilibrium can lead to novel phenomena.

Statistical properties of ultracold gases depend

strongly on the experimental protocols of cooling and thermalization [9] and ultimately, none of the typically used paradigmatic ensembles fits the reality perfectly. Therefore, some intermediate ensembles should be used, either by relaxing the constraint on the extensive variables [117], post-selection, or studying dynamics of an open system mimicking cooling processes [126]. Apart from this experiment matching need, there appear to be fundamental theoretical questions related to the system in equilibrium, but subject to other constraints. Here, the notion of the Gibbs ensemble has been used, with great success overall in recent years [232].

The research areas outlined above require the development of more sophisticated numerical methods. Even for the ideal gas, the calculation of statistics for experimentally relevant systems containing several hundred thousand atoms remains computationally challenging. Importantly, as shown in Figure 11 the thermodynamic limit is not achieved even for such large systems. Advances in methods for open quantum systems, generalizations of the Fock state sampling method of (FSSM), and new techniques within the framework of generalized hydrodynamics are expected to have a significant impact.

Finally, as experimental precision increases, it becomes crucial to consider the practical consequences of ensemble dependence. Experimental observations indicate a reduction in BEC fluctuations by 27% compared to canonical predictions. The question arises: do other quantities, such as magnetization (fraction of subcomponents in a multicomponent condensate), phase correlations, density-density correlations, or recombination rates, also exhibit ensemble dependence in finite systems? Low-temperature results [233] demonstrate that the rate of phase collapse can exhibit different scalings with the total number of atoms across different statistical ensembles. This finding highlights the importance of selecting the correct statistical ensemble in applications such as interferometry to ensure trustworthy results.

The experimental and theoretical findings available to date have made significant contributions to the understanding of quantum statistical mechanics. The reduction in fluctuations and the observed scaling behavior offer critical insights into the unique properties of isolated quantum systems.

This research also sets benchmarks for future studies, particularly in extending the analysis to higher moments of the fluctuation distribution and exploring time-dependent dynamics. Moreover, the theoretical methods and results will guide further investigations into interaction effects and their role in fluctuation phenomena.

7. Acknowledgments

We acknowledge support from the (Polish) National Science Center Grants No. 2021/43/B/ST2/01426 (K. R. and P. K.), 2018/31/B/ST2/01871 (P. D.), 2022/45/N/ST2/03511 (M. B. K.). M. F. A. and J. J. A. acknowledge support from the Danish National Research Foundation through the Center of Excellence “CCQ” (DNRF152) and by the Novo Nordisk Foundation NERD grant (Grantno. NNF22OC0075986). K.P. acknowledges support from the (Polish) National Science Center Grant No. 2024/53/B/ST2/02161.

Bibliography

- [1] Immanuel Bloch, Jean Dalibard, and Sylvain Nascimbène. Quantum simulations with ultracold quantum gases. *Nat. Phys.*, 8(4):267–276, apr 2012.
- [2] H. David Politzer. Condensate fluctuations of a trapped, ideal Bose gas. *Phys. Rev. A*, 54(6):5048–5054, dec 1996.
- [3] Patrick Navez, Dmitri Bitouk, Mariusz Gajda, Zbigniew Idziaszek, and Kazimierz Rzażewski. Fourth statistical ensemble for the Bose-Einstein condensate. *Phys. Rev. Lett.*, 79(10):1789–1792, sep 1997.
- [4] S. Giorgini, L. P. Pitaevskii, and S. Stringari. Anomalous fluctuations of the condensate in interacting Bose gases. *Phys. Rev. Lett.*, 80(23):5040–5043, jun 1998.
- [5] F. Meier and W. Zwerger. Anomalous condensate fluctuations in strongly interacting superfluids. *Phys. Rev. A*, 60(6):5133–5135, dec 1999.
- [6] Vitaly V. Kocharovskiy, Vladimir V. Kocharovskiy, Martin Holthaus, C.H. Raymond Ooi, Anatoly Svidzinsky, Wolfgang Ketterle, and Marlan O. Scully. Fluctuations in ideal and interacting Bose-Einstein condensates: From the laser phase transition analogy to squeezed states and Bogoliubov quasiparticles. In *Advances In Atomic, Molecular, and Optical Physics*, pages 291–411. Elsevier, 2006.
- [7] Maciej Bartłomiej Kruk, Dawid Hryniuk, Mick Kristensen, Toke Vibel, Krzysztof Pawłowski, Jan Arlt, and Kazimierz Rzażewski. Microcanonical and canonical fluctuations in atomic Bose-Einstein condensates – Fock state sampling approach. *SciPost Phys.*, 14:036, 2023.
- [8] Zbigniew Idziaszek. Microcanonical fluctuations of the condensate in weakly interacting Bose gases. *Phys. Rev. A*, 71:053604, May 2005.
- [9] M.B. Christensen, T. Vibel, A.J. Hilliard, M.B. Kruk, K. Pawłowski, D. Hryniuk, K. Rzażewski, M.A. Kristensen, and J.J. Arlt. Observation of microcanonical atom number fluctuations in a Bose-Einstein condensate. *Phys. Rev. Lett.*, 126(15):153601, apr 2021.
- [10] V. V. Kocharovskiy, Vl. V. Kocharovskiy, and S. V. Tarasov. Bose-Einstein condensation in mesoscopic systems: The self-similar structure of the critical region and the nonequivalence of the canonical and grand canonical ensembles. *JETP Letters*, 103(1):62–75, 2016.
- [11] Hugo Touchette. Equivalence and nonequivalence of ensembles: Thermodynamic, macrostate, and measure levels. *Journal of Statistical Physics*, 159(5):987–1016, 2015.
- [12] V I Yukalov. Particle fluctuations in systems with Bose-Einstein condensate. *Laser Physics*, 34(11):113001, oct 2024.
- [13] Erwin Schrödinger. *Statistical Thermodynamics*. Dover Publications, New York, 1989.
- [14] Robert M Ziff, George E Uhlenbeck, and Mark Kac. The ideal Bose-Einstein gas, revisited. *Phys. Rep.*, 32(4):169–248, sep 1977.
- [15] Siegfried Grossmann and Martin Holthaus. Microcanonical fluctuations of a Bose system’s ground state occupation number. *Phys. Rev. E*, 54(4):3495–3498, oct 1996.
- [16] Martin Holthaus, Eva Kalinowski, and Klaus Kirsten. Condensate fluctuations in trapped Bose gases: Canonical vs. microcanonical ensemble. *Ann. Phys.*, 270(1):198–230, nov 1998.
- [17] Christoph Weiss and Martin Wilkens. Particle number counting statistics in ideal Bose gases. *Opt. Express*, 1(10):272, nov 1997.
- [18] G. H. Hardy and S. Ramanujan. Asymptotic formulae in combinatory analysis. *Proc. London Math. Soc.*, 17:75–115, 1918.
- [19] Siegfried Grossmann and Martin Holthaus. Maxwell’s demon at work: Two types of Bose condensate fluctuations in power-law traps. *Opt. Express*, 1(10):262, nov 1997.
- [20] Martin Wilkens and Christoph Weiss. Particle number fluctuations in an ideal Bose gas. *Journal of Modern Optics*, 44(10):1801–1814, 1997.
- [21] W. Zwerger. Anomalous fluctuations in phases with a broken continuous symmetry. *Phys. Rev. Lett.*, 92:027203, Jan 2004.
- [22] Zbigniew Idziaszek, Mariusz Gajda, Patrick Navez, Martin Wilkens, and Kazimierz Rzażewski. Fluctuations of the weakly interacting Bose-Einstein condensate. *Phys. Rev. Lett.*, 82:4376–4379, May 1999.
- [23] V. V. Kocharovskiy, Vl. V. Kocharovskiy, and Marlan O. Scully. Condensate statistics in interacting and ideal dilute Bose gases. *Phys. Rev. Lett.*, 84:2306–2309, Mar 2000.
- [24] V. V. Kocharovskiy, Vl. V. Kocharovskiy, and Marlan O. Scully. Condensation of N bosons. III. analytical results for all higher moments of condensate fluctuations in interacting and ideal dilute Bose gases via the canonical ensemble quasiparticle formulation. *Phys. Rev. A*, 61:053606, April 2000.
- [25] Anatoly A. Svidzinsky and Marlan O. Scully. Condensation of N interacting bosons: A hybrid approach to condensate fluctuations. *Phys. Rev. Lett.*, 97:190402, November 2006.
- [26] Anatoly A. Svidzinsky and Marlan O. Scully. Condensation of N bosons: Microscopic approach to fluctuations in an interacting Bose gas. *Phys. Rev. A*, 82:063630, Dec 2010.
- [27] Satadal Bhattacharyya and Barnali Chakrabarti. Condensate fluctuation and thermodynamics of mesoscopic Bose-Einstein condensates: A correlated many-body approach. *Phys. Rev. A*, 93:023636, 2016.
- [28] V. I. Yukalov. No anomalous fluctuations exist in stable equilibrium systems. *Phys. Lett. A*, 340(5-6):369–374, jun 2005.
- [29] M. Gajdacz, A. J. Hilliard, M. A. Kristensen, P. L. Pedersen, C. Klempt, J. J. Arlt, and J. F. Sherson. Preparation of ultracold atom clouds at the shot noise level. *Phys. Rev. Lett.*, 117:073604, August 2016.
- [30] M.A. Kristensen, M.B. Christensen, M. Gajdacz, M. Iglicki, K. Pawłowski, C. Klempt, J.F. Sherson, K. Rzażewski, A. J. Hilliard, and J. J. Arlt. Observation of atom number fluctuations in a Bose-Einstein condensate. *Phys. Rev. Lett.*, 122(16):163601, apr 2019.
- [31] George E. Andrews. *205Chapter 9 Partitions. In Combinatorics: Ancient and Modern*. Oxford University Press, 06 2013.
- [32] G. Szekeres. AN ASYMPTOTIC FORMULA IN THE

- THEORY OF PARTITIONS. *The Quarterly Journal of Mathematics*, 2(1):85–108, 01 1951.
- [33] G. Szekeres. SOME ASYMPTOTIC FORMULAE IN THE THEORY OF PARTITIONS (II). *Q. J. Math.*, 4(1):96–111, January 1953.
- [34] Walter Bridges. Partitions into distinct parts with bounded largest part. *Res. number theory*, 6(4):1–19, December 2020.
- [35] C. Weiss and M. Holthaus. Asymptotics of the number partitioning distribution. *Europhys. Lett.*, 59(4):486, August 2002.
- [36] Paul Erdős and Joseph Lehner. The distribution of the number of summands in the partitions of a positive integer. *Duke Math. J.*, 8(2):335–345, June 1941.
- [37] E. Maitland Wright. Asymptotic partition formulae. III. Partitions into k -th powers. *Acta Math.*, 63(none):143–191, January 1934.
- [38] Robert C. Vaughan. Squares: Additive questions and partitions. *Int. J. Number Theory*, 11(05):1367–1409, April 2015.
- [39] Z. Idziaszek. *Kwantowe fluktuacje zimnych gazów atomowych*. PhD thesis, Centrum Fizyki Teoretycznej PAN, 2001.
- [40] D. P. Bhatia, M. A. Prasad, and D. Arora. Asymptotic results for the number of multidimensional partitions of an integer and directed compact lattice animals. *J. Phys. A: Math. Gen.*, 30(7):2281, April 1997.
- [41] F. Y. Wu, G. Rollet, H. Y. Huang, J. M. Maillard, Chin-Kun Hu, and Chi-Ning Chen. Directed compact lattice animals, restricted partitions of an integer, and the infinite-state potts model. *Phys. Rev. Lett.*, 76:173–176, Jan 1996.
- [42] K. Schönhammer and V. Meden. Fermion–boson transmutation and comparison of statistical ensembles in one dimension. *Am. J. Phys.*, 64(9):1168–1176, September 1996.
- [43] Anna Kubasiak, Jarosław K. Korbicz, Jakub Zakrzewski, and Maciej Lewenstein. Fermi-Dirac statistics and the number theory. *Europhys. Lett.*, 72(4):506, October 2005.
- [44] Rovenchak Andriy. Partition Function Formalism in the Problem of Multidimensional Integer Partitions. *CMST*, 16(2):187–190, 2010.
- [45] Stephan Mertens. Phase transition in the number partitioning problem. *Phys. Rev. Lett.*, 81:4281–4284, Nov 1998.
- [46] Kerson Huang. *Statistical Mechanics*. John Wiley & Sons, 2 edition, 1987.
- [47] R. K. Pathria. *Statistical Mechanics*. Butterworth-Heinemann, 2 edition, 1996.
- [48] Emilia Witkowska, Mariusz Gajda, and Kazimierz Rzażewski. Bose statistics and classical fields. *Phys. Rev. A*, 79:033631, Mar 2009.
- [49] Maciej Kruk, Maciej Lebek, and Kazimierz Rzażewski. Statistical properties of cold bosons in a ring trap. *Phys. Rev. A*, 101:023622, Feb 2020.
- [50] Albert Einstein. Quantentheorie des einatomigen idealen Gases. In *Albert Einstein: Akademie-Vorträge*, volume 6, pages 237–244. Wiley-VCH Verlag GmbH & Co. KGaA, Weinheim, FRG, sep 1924.
- [51] Zoran Hadzibabic, Peter Krüger, Marc Cheneau, Baptiste Battelier, and Jean Dalibard. Berezinskii–Kosterlitz–Thouless crossover in a trapped atomic gas. *Nature*, 441:1118–1121, June 2006.
- [52] Wolfgang Ketterle and N. J. van Druten. Bose-Einstein condensation of a finite number of particles trapped in one or three dimensions. *Phys. Rev. A*, 54:656–660, 1996.
- [53] D. S. Petrov, G. V. Shlyapnikov, and J. T. M. Walraven. Regimes of quantum degeneracy in trapped 1d gases. *Phys. Rev. Lett.*, 85:3745–3749, Oct 2000.
- [54] Siegfried Grossmann and Martin Holthaus. From number theory to statistical mechanics: Bose-Einstein condensation in isolated traps. [arXiv, cond-mat/9709045](https://arxiv.org/abs/cond-mat/9709045), 1997.
- [55] James R. Johnston. Coherent States in Superfluids: The Ideal Einstein-Bose Gas. *American Journal of Physics*, 38(4):516–528, 04 1970.
- [56] V I Yukalov. Principal problems in Bose-Einstein condensation of dilute gases. *Laser Physics Letters*, 1(9):435, aug 2004.
- [57] Mariusz Gajda and Kazimierz Rzażewski. Fluctuations of Bose-Einstein condensate. *Phys. Rev. Lett.*, 78:2686–2689, Apr 1997.
- [58] Christoph Weiss and Jacques Tempere. Grand-canonical condensate fluctuations in weakly interacting Bose-Einstein condensates of light. *Phys. Rev. E*, 94:042124, 2016.
- [59] Martin Holthaus and Eva Kalinowski. Universal renormalization of saddle-point integrals for condensed bose gases. *Phys. Rev. E*, 60:6534–6537, Dec 1999.
- [60] SR deGroot, GJ Hooyman, and CA Tenseldam. On the Bose-Einstein condensation. *Proceedings Of The Royal Society Of London Series A-Mathematical And Physical Sciences*, 203(1073):266–286, 1950.
- [61] M. Fierz. Über die statistischen schwankungen in einem kondensierenden system. *Helv. Phys. Acta*, 29:47, 1956.
- [62] RB Dingle. The Bose-Einstein statistics of particles, with special reference to the case of low temperatures. *Proceedings Of The Cambridge Philosophical Society*, 45(2):275–287, 1949.
- [63] RB Dingle. Theories of Helium ii. *Advances In Physics*, 1(2):111–168, 1952.
- [64] AR Fraser. The condensation of a perfect Bose-Einstein gas .2. *Philosophical Magazine*, 42(325):165–175, 1951.
- [65] EH Hauge. Fluctuations in ground state occupation number of ideal Bose gas. *Physica Norvegica*, 4(1):19–&, 1970.
- [66] F. Reif. *Fundamentals in Thermal Physics*. McGraw-Hill, ew York, 1965.
- [67] P.T. Landsberg. *Thermodynamics—with Quantum Statistical Illustrations*. Interscience Publishers, 250 Fifth Avenue, New York, 1961.
- [68] Peter Borrmann and Gert Franke. Recursion formulas for quantum statistical partition functions. *Journal of Chemical Physics*, 98:2484–2485, 1993.
- [69] F Brosens, J.T Devreese, and L.F Lemmens. Canonical Bose-Einstein condensation in a parabolic well. *Solid State Communications*, 100(2):123–127, 1996.
- [70] K. C. Chase, Aram Z. Mekjian, and Larry Zamick. Canonical and microcanonical ensemble approaches to Bose-Einstein condensation: The thermodynamics of particles in harmonic traps. *The European Physical Journal B - Condensed Matter and Complex Systems*, 8:281–285, 1999.
- [71] Martin Holthaus and Eva Kalinowski. The saddle-point method for condensed Bose gases. *Annals of Physics*, 276(2):321–360, 1999.
- [72] Siegfried Grossmann and Martin Holthaus. Fluctuations of the particle number in a trapped Bose-Einstein condensate. *Phys. Rev. Lett.*, 79:3557–3560, Nov 1997.
- [73] Martin Holthaus, Eva Kalinowski, and Klaus Kirsten. Condensate fluctuations in trapped Bose gases: Canonical vs. microcanonical ensemble. *Annals of Physics*, 270(1):198–230, 1998.
- [74] Marlan O. Scully. Condensation of n bosons and the laser phase transition analogy. *Phys. Rev. Lett.*, 82:3927–3931, May 1999.
- [75] V. V. Kocharovskiy, Marlan O. Scully, Shi-Yao Zhu, and M. Suhail Zubairy. Condensation of N bosons.

- II. nonequilibrium analysis of an ideal Bose gas and the laser phase-transition analogy. *Phys. Rev. A*, 61:023609, Jan 2000.
- [76] Martin Holthaus, Kishore T. Kapale, Vitaly V. Kocharovskiy, and Marlan O. Scully. Master equation vs. partition function: canonical statistics of ideal Bose–Einstein condensates. *Physica A: Statistical Mechanics and its Applications*, 300(3):433–467, 2001.
- [77] M. O. Scully and A. A. Svidzinsky. Condensation of n bosons iv: a simplified bogoliubov master equation analysis of fluctuations in an interacting bose gas. *Journal of Modern Optics*, 53(16-17):2399–2418, 2006.
- [78] S. V. Tarasov, V. V. Kocharovskiy, and V. V. Kocharovskiy. Grand canonical versus canonical ensemble: Universal structure of statistics and thermodynamics in a critical region of bose–einstein condensation of an ideal gas in arbitrary trap. *Journal of Statistical Physics*, 161(4):942–964, 2015.
- [79] Vitaly V Kocharovskiy and Vladimir V Kocharovskiy. Self-similar analytical solution of the critical fluctuations problem for the Bose–Einstein condensation in an ideal gas. *Journal of Physics A: Mathematical and Theoretical*, 43(22):225001, May 2010.
- [80] S. V. Tarasov. Self-similarity of the statistics in the critical region of Bose condensation of ideal gas in mesoscopic traps: Canonical and grand canonical ensembles. *Bulletin Of The Lebedev Physics Institute*, 43(4):143–147, APR 2016.
- [81] V. V. Kocharovskiy, V. V. Kocharovskiy, and K. E. Dorfman. Origin and universal structure of non-Gaussian statistics of Bose-Einstein condensate in a mesoscopic perfect gas. *Radiophysics and Quantum Electronics*, 52(5-6):422–434, May 2009.
- [82] Hongwei Xiong, Shujuan Liu, Guoxiang Huang, Zhijun Xu, and Cunyuan Zhang. Fluctuations of the condensate in ideal and interacting Bose gases. *Journal of Physics B: Atomic, Molecular and Optical Physics*, 34(21):4203, 2001.
- [83] Hongwei Xiong, Shujuan Liu, Guoxiang Huang, and Zaixin Xu. Canonical statistics of trapped ideal and interacting Bose gases. *Phys. Rev. A*, 65:033609, Feb 2002.
- [84] E. Megías, V.S. Timóteo, A. Gammal, and A. Deppman. Bose–einstein condensation and non-extensive statistics for finite systems. *Physica A: Statistical Mechanics and its Applications*, 585:126440, 2022.
- [85] Andrey S. Plyashechnik, Alexey A. Sokolik, and Yurii E. Lozovik. Bose-einstein condensation in a canonical ensemble with fixed total momentum. *Phys. Rev. A*, 110:013301, Jul 2024.
- [86] V I Yukalov. Number-of-particle fluctuations in systems with Bose-Einstein condensate. *Laser Physics Letters*, 2(3):156, nov 2004.
- [87] V. I. Yukalov. Fluctuations of composite observables and stability of statistical systems. *Phys. Rev. E*, 72:066119, Dec 2005.
- [88] J. W. Gibbs. *Collected Works*. Longmans, New York, 1931.
- [89] D. Ter Haar. *Elements of Statistical Mechanics*. Reinhart, New York, 1954.
- [90] D Ter Haar. Theory and applications of the density matrix. *Reports on Progress in Physics*, 24(1):304, jan 1961.
- [91] Vyacheslav I. Yukalov. Particle fluctuations in mesoscopic Bose systems. *Symmetry*, 11(5), 2019.
- [92] C.-H. Zhang. Number-of-particle fluctuations and stability of bose-einstein-condensed systems. *Phys. Rev. A*, 73:023601, Feb 2006.
- [93] M. Klaas, E. Schlottmann, H. Flayac, F. P. Laussy, F. Gericke, M. Schmidt, M. v. Helversen, J. Beyer, S. Brodbeck, H. Suichomel, S. Höfling, S. Reitzenstein, and C. Schneider. Photon-number-resolved measurement of an exciton-polariton condensate. *Phys. Rev. Lett.*, 121:047401, Jul 2018.
- [94] Nataliya Bobrovska and Michał Matuszewski. Adiabatic approximation and fluctuations in exciton-polariton condensates. *Phys. Rev. B*, 92:035311, Jul 2015.
- [95] Hassan Alnatah, Paolo Comaron, Shouvik Mukherjee, Jonathan Beaumariage, Loren N. Pfeiffer, Ken West, Kirk Baldwin, Marzena Szymańska, and David W. Snoke. Critical fluctuations in a confined driven-dissipative quantum condensate. *Sci. Adv.*, 10(12), March 2024.
- [96] Zhedong Zhang, Shixuan Zhao, and Danyuan Lei. Quantum statistical theory for an exciton-polariton condensate: Fluctuations and coherence. *Phys. Rev. B*, 106:L220306, Dec 2022.
- [97] Xuanhua Wang and Jin Wang. Full quantum theory of nonequilibrium phonon condensation and phase transition. *Phys. Rev. B*, 106:L220103, Dec 2022.
- [98] Christensen B. Mikkelsen. *Microcanonical Fluctuations in Interacting Bose-Einstein Condensates*. PhD thesis, Department of Physics and Astronomy, Aarhus University, 2020.
- [99] Nicholas Metropolis, Arianna W. Rosenbluth, Marshall N. Rosenbluth, Augusta H. Teller, and Edward Teller. Equation of state calculations by fast computing machines. *The Journal of Chemical Physics*, 21(6):1087–1092, June 1953.
- [100] Mirosław Brewczyk, Mariusz Gajda, and Kazimierz Rzażewski. Classical fields approximation for bosons at nonzero temperatures. *J. Phys. B: At. Mol. Opt. Phys.*, 40(2):R1, January 2007.
- [101] P. B. Blakie, A. S. Bradley, M. J. Davis, R. J. Ballagh, and C. W. Gardiner. Dynamics and statistical mechanics of ultra-cold Bose gases using c-field techniques. *Advances in Physics*, 57(5):363–455, 2008.
- [102] Emilia Witkowska, Mariusz Gajda, and Kazimierz Rzażewski. Monte Carlo method, classical fields and Bose statistics. *Opt. Commun.*, 283(5):671–675, March 2010.
- [103] J. Pietraszewicz and P. Deuar. Complex wave fields in the interacting one-dimensional Bose gas. *Phys. Rev. A*, 97:053607, 2018.
- [104] Krzysztof Gawryluk and Mirosław Brewczyk. Berezinskii–Kosterlitz–Thouless phase induced by dissipating quasisolitons. *Sci. Rep.*, 11(10773):1–10, May 2021.
- [105] Krzysztof Gawryluk and Mirosław Brewczyk. Mechanism for sound dissipation in a two-dimensional degenerate Fermi gas. *Sci. Rep.*, 14(10815):1–10, May 2024.
- [106] S. P. Cockburn, A. Negretti, N. P. Proukakis, and C. Henkel. Comparison between microscopic methods for finite-temperature Bose gases. *Phys. Rev. A*, 83:043619, Apr 2011.
- [107] Joanna Pietraszewicz and Piotr Deuar. Classical field records of a quantum system: Their internal consistency and accuracy. *Phys. Rev. A*, 92:063620, 2015.
- [108] J. Pietraszewicz and P. Deuar. Classical fields in the one-dimensional Bose gas: Applicability and determination of the optimal cutoff. *Phys. Rev. A*, 98:023622, 2018.
- [109] A. S. Bradley, P. B. Blakie, and C. W. Gardiner. Properties of the stochastic Gross–Pitaevskii equation: finite temperature ehrenfest relations and the optimal plane wave representation. *Journal of Physics B: Atomic, Molecular and Optical Physics*, 38(23):4259, 2005.
- [110] Przemysław Bienias, Krzysztof Pawłowski, Mariusz Gajda, and Kazimierz Rzażewski. Statistical properties of one-dimensional bose gas. *Phys. Rev. A*, 83:033610, Mar 2011.

- [111] Albert Einstein. *Zur Quantentheorie der Strahlung*, 1916.
- [112] Krzysztof Góral, Mariusz Gajda, and Kazimierz Rzażewski. Multi-mode description of an interacting Bose-Einstein condensate. *Opt. Express*, 8(2):92–98, 2001.
- [113] M. J. Davis, S. A. Morgan, and K. Burnett. Simulations of Bose fields at finite temperature. *Phys. Rev. Lett.*, 87:160402, 2001.
- [114] Mirosław Brewczyk, Mariusz Gajda, and Kazimierz Rzażewski. Classical fields approximation for bosons at nonzero temperatures. *Journal of Physics B: Atomic, Molecular and Optical Physics*, 40(2):R1, 2007.
- [115] C. W. Gardiner and M. J. Davis. The stochastic Gross-Pitaevskii equation: II. *Journal of Physics B: Atomic, Molecular and Optical Physics*, 36(23):4731, 2003.
- [116] S. J. Rooney, P. B. Blakie, and A. S. Bradley. Stochastic projected Gross-Pitaevskii equation. *Phys. Rev. A*, 86:053634, 2012.
- [117] J. Pietraszewicz, E. Witkowska, and P. Deuar. Continuum of classical-field ensembles in Bose gases from canonical to grand canonical and the onset of their equivalence. *Phys. Rev. A*, 96:033612, Sep 2017.
- [118] Alice Sinatra, Yvan Castin, and Carlos Lobo. A Monte Carlo formulation of the Bogolubov theory. *Journal of Modern Optics*, 47(14-15):2629–2644, 2000.
- [119] Janne Ruostekoski and Andrew D. Martin. *The Truncated Wigner Method for Bose Gases*, chapter 13, pages 203–214. Imperial College Press, 2013.
- [120] A. D. Martin and J. Ruostekoski. Quantum and thermal effects of dark solitons in a one-dimensional Bose gas. *Phys. Rev. Lett.*, 104:194102, 2010.
- [121] P. D. Drummond, P. Deuar, and K. V. Kheruntsyan. Canonical Bose gas simulations with stochastic gauges. *Phys. Rev. Lett.*, 92:040405, Jan 2004.
- [122] P. Deuar, A. G. Sykes, D. M. Gangardt, M. J. Davis, P. D. Drummond, and K. V. Kheruntsyan. Nonlocal pair correlations in the one-dimensional Bose gas at finite temperature. *Phys. Rev. A*, 79:043619, 2009.
- [123] Piotr Deuar, Alex Ferrier, Michał Matuszewski, Giuliano Orso, and Marzena H. Szymańska. Fully quantum scalable description of driven-dissipative lattice models. *PRX Quantum*, 2:010319, 2021.
- [124] Sigmund Heller and Walter T Strunz. Stochastic field equation for the canonical ensemble of an ideal Bose gas. *Journal of Physics B: Atomic, Molecular and Optical Physics*, 42(8):081001, 2009.
- [125] Sigmund Heller and Walter T. Strunz. Canonical ensemble of an interacting Bose gas: Stochastic matter fields and their coherence. *EPL (Europhysics Letters)*, 101(6):60007, 2013.
- [126] J. I. Cirac, M. Lewenstein, and P. Zoller. Quantum statistics of a laser cooled ideal gas. *Phys. Rev. Lett.*, 72:2977–2980, May 1994.
- [127] Y. Castin. Bose-Einstein Condensates in Atomic Gases: Simple Theoretical Results. In *Coherent atomic matter waves*, pages 1–136. Springer, Berlin, Germany, July 2002.
- [128] Yvan Castin. Bose-Einstein condensates in atomic gases: simple theoretical results. *arXiv*, May 2001.
- [129] M. Girardeau and R. Arnowitt. Theory of many-Boson systems: Pair theory. *Phys. Rev.*, 113:755–761, 1959.
- [130] Hongwei Xiong, Shujuan Liu, and Guoxiang Huang. Statistical properties of interacting Bose gases in quasi-two-dimensional harmonic traps. *Journal of Physics B: Atomic, Molecular and Optical Physics*, 35(9):2105, apr 2002.
- [131] Hongwei Xiong, Shujuan Liu, and Guoxiang Huang. Anomalous fluctuations of two-dimensional Bose-Einstein condensates. *Phys. Rev. A*, 67:055601, May 2003.
- [132] Shujuan Liu, Hongwei Xiong, Guoxiang Huang, and Zhi-jun Xu. Anomalous particle-number fluctuations in a three-dimensional interacting Bose-Einstein condensate. *Phys. Rev. A*, 68:065601, Dec 2003.
- [133] Liu Shu-Juan, Xiong Hong-Wei, Xu Zhi-Jun, and Huang Lin. Roles of collective excitations in the anomalous fluctuations of one-dimensional interacting Bose-condensed gases. *Chinese Physics Letters*, 20(10):1672, oct 2003.
- [134] Alexander Yu. Cherny. Condensate fluctuations in the dilute Bose gas. *Phys. Rev. A*, 71:043605, Apr 2005.
- [135] V I Yukalov. Particle fluctuations in nonuniform and trapped Bose gases. *Laser Physics Letters*, 6(9):688, May 2009.
- [136] F. Meier and W. Zwerger. Anomalous condensate fluctuations in strongly interacting superfluids. *Phys. Rev. A*, 60:5133–5135, Dec 1999.
- [137] A Minguzzi and M P Tosi. Linear density response in the random-phase approximation for confined Bose vapours at finite temperature. *Journal of Physics: Condensed Matter*, 9(46):10211, nov 1997.
- [138] Z. Idziaszek, Ł. Zawitkowski, M. Gajda, and K. Rzażewski. Fluctuations of a weakly interacting Bose-Einstein condensate. *Europhysics Letters*, 86(1):10002, apr 2009.
- [139] Elliott H. Lieb and Werner Liniger. Exact analysis of an interacting Bose gas. I. The general solution and the ground state. *Phys. Rev.*, 130:1605–1616, May 1963.
- [140] Elliott H. Lieb. Exact analysis of an interacting Bose gas. II. The excitation spectrum. *Phys. Rev.*, 130:1616–1624, May 1963.
- [141] C. N. Yang and C. P. Yang. Thermodynamics of a One-Dimensional System of Bosons with Repulsive Delta-Function Interaction. *J. Math. Phys.*, 10(7):1115–1122, July 1969.
- [142] K. V. Kheruntsyan, D. M. Gangardt, P. D. Drummond, and G. V. Shlyapnikov. Pair correlations in a finite-temperature 1d Bose gas. *Phys. Rev. Lett.*, 91:040403, Jul 2003.
- [143] K. V. Kheruntsyan, D. M. Gangardt, P. D. Drummond, and G. V. Shlyapnikov. Finite-temperature correlations and density profiles of an inhomogeneous interacting one-dimensional Bose gas. *Phys. Rev. A*, 71:053615, 2005.
- [144] A. G. Sykes, D. M. Gangardt, M. J. Davis, K. Viering, M. G. Raizen, and K. V. Kheruntsyan. Spatial nonlocal pair correlations in a repulsive 1d Bose gas. *Phys. Rev. Lett.*, 100:160406, 2008.
- [145] Joanna Pietraszewicz and Piotr Deuar. Mesoscopic density grains in a 1d interacting Bose gas from the exact Yang-Yang solution. *New Journal of Physics*, 19(12):123010, dec 2017.
- [146] Matthew L. Kerr, Giulia De Rosi, and Karen V. Kheruntsyan. Analytic thermodynamic properties of the Lieb-Liniger gas. *SciPost Phys. Core*, 7:047, 2024.
- [147] Werner Krauth. Quantum Monte Carlo calculations for a large number of bosons in a harmonic trap. *Phys. Rev. Lett.*, 77:3695–3699, Oct 1996.
- [148] D. M. Ceperley. Microscopic simulations in physics. *Rev. Mod. Phys.*, 71:S438–S443, Mar 1999.
- [149] Jens O. Andersen. Theory of the weakly interacting Bose gas. *Rev. Mod. Phys.*, 76:599–639, Jul 2004.
- [150] Iacopo Carusotto and Yvan Castin. Condensate statistics in one-dimensional interacting Bose gases: Exact results. *Phys. Rev. Lett.*, 90:030401, Jan 2003.
- [151] K. E. Dorfman, M. Kim, and A. A. Svidzinsky. Condensate statistics and thermodynamics of weakly interacting Bose gas: Recursion relation approach. *Phys. Rev. A*, 83:033609, Mar 2011.

- [152] S. V. Tarasov, Vl. V. Kocharovskiy, and V. V. Kocharovskiy. Bose-Einstein-condensate fluctuations versus an interparticle interaction. *Phys. Rev. A*, 102:043315, Oct 2020.
- [153] Sergey Tarasov, Vladimir Kocharovskiy, and Vitaly Kocharovskiy. Anomalous statistics of Bose-Einstein Condensate in an interacting gas: An effect of the trap's form and boundary conditions in the thermodynamic limit. *Entropy*, 20(3), 2018.
- [154] S.V. Tarasov. Effect of boundary conditions on fluctuations of the Bose condensate of interacting atoms. *Quantum Electronics*, 50(6):525, jun 2020.
- [155] S. V. Tarasov, Vl. V. Kocharovskiy, and V. V. Kocharovskiy. Dependence of the Bose-condensate population fluctuations in a gas of interacting particles on the system size: Numerical analysis. *Radiophysics and Quantum Electronics*, 63(4):288–297, SEP 2020.
- [156] S. V. Tarasov, Vl. V. Kocharovskiy, and V. V. Kocharovskiy. Crossover of quasiparticles and statistics of Bose-Einstein condensate with increasing interaction: from an ideal gas to a Thomas-Fermi regime. the case of a one-dimensional flat trap. *Radiophysics and Quantum Electronics*, 62(4):293–310, SEP 2019.
- [157] P. Bienias, K. Pawłowski, M. Gajda, and K. Rzażewski. Statistical properties of one-dimensional attractive bose gas. *Europhysics Letters*, 96(1):10011, sep 2011.
- [158] Ji-Xuan Hou. Microcanonical condensate fluctuations in one-dimensional weakly-interacting bose gases. *Modern Physics Letters B*, 34(35):2050410, 2020.
- [159] Nick P Proukakis and Brian Jackson. Finite-temperature models of Bose–Einstein condensation. *Journal of Physics B: Atomic, Molecular and Optical Physics*, 41(20):203002, 2008.
- [160] Sangita Bera, Mantile Leslie Lekala, Barnali Chakrabarti, Satadal Bhattacharyya, and Gaotsiwe Joel Rampho. Statistical properties and condensate fluctuation of attractive bose gas with finite number of particles. *Physica A: Statistical Mechanics and its Applications*, 481:79–89, 2017.
- [161] H. Touchette. Ensemble equivalence for general many-body systems. *EPL (Europhysics Letters)*, 96(5):50010, 2011.
- [162] Tiziano Squartini, Joey de Mol, Frank den Hollander, and Diego Garlaschelli. Breaking of ensemble equivalence in networks. *Phys. Rev. Lett.*, 115:268701, Dec 2015.
- [163] Marco Baldovin. Physical interpretation of the canonical ensemble for long-range interacting systems in the absence of ensemble equivalence. *Phys. Rev. E*, 98:012121, Jul 2018.
- [164] Francois Huveneers and Elias Theil. Equivalence of ensembles, condensation and glassy dynamics in the Bose-Hubbard Hamiltonian. *Journal of Statistical Physics*, 177(5):917–935, DEC 2019.
- [165] Tomotaka Kuwahara and Keiji Saito. Gaussian concentration bound and ensemble equivalence in generic quantum many-body systems including long-range interactions. *Annals of Physics*, 421:168278, 2020.
- [166] J.-C. Jaskula. *Création et étude de sources d'états non classiques pour l'optique atomique quantique*. PhD thesis, Université de Paris-Sud, December 2010.
- [167] Mick Kristensen, M. Gajdacz, P. L. Pedersen, Carsten Klempt, J. F. Sherson, J. J. Arlt, and A. J. Hilliard. Sub-atom shot noise Faraday imaging of ultracold atom clouds. *J. Phys. B: At., Mol. Opt. Phys.*, 50(3):034004, January 2017.
- [168] Alessio Chiocchetta and Iacopo Carusotto. Quantum langevin model for nonequilibrium condensation. *Phys. Rev. A*, 90:023633, 2014.
- [169] Oliver Penrose and Lars Onsager. Bose-Einstein condensation and liquid helium. *Phys. Rev.*, 104:576–584, Nov 1956.
- [170] Jan Klaers, Julian Schmitt, Frank Vewinger, and Martin Weitz. Bose-Einstein condensation of photons in an optical microcavity. *Nature*, 468(7323):545–548, November 2010.
- [171] F. Gerbier, J. H. Thywissen, S. Richard, M. Hugbart, P. Bouyer, and A. Aspect. Experimental study of the thermodynamics of an interacting trapped Bose-Einstein condensed gas. *Phys. Rev. A*, 70(1):013607, jul 2004.
- [172] R. Meppelink, R. A. Rozendaal, S. B. Koller, J. M. Vogels, and P. van der Straten. Thermodynamics of Bose-Einstein-condensed clouds using phase-contrast imaging. *Phys. Rev. A*, 81(5):053632, May 2010.
- [173] Naaman Tammuz, Robert P. Smith, Robert L. D. Campbell, Scott Beattie, Stuart Moulder, Jean Dalibard, and Zoran Hadzibabic. Can a Bose gas be saturated? *Phys. Rev. Lett.*, 106(23):230401, jun 2011.
- [174] F. Gerbier, J. H. Thywissen, S. Richard, M. Hugbart, P. Bouyer, and A. Aspect. Critical temperature of a trapped, weakly interacting Bose gas. *Phys. Rev. Lett.*, 92(3):030405, jan 2004.
- [175] Robert P. Smith, Robert L. D. Campbell, Naaman Tammuz, and Zoran Hadzibabic. Effects of interactions on the critical temperature of a trapped Bose gas. *Phys. Rev. Lett.*, 106(25):250403, jun 2011.
- [176] Franco Dalfovo, Stefano Giorgini, Lev P. Pitaevskii, and Sandro Stringari. Theory of Bose-Einstein condensation in trapped gases. *Rev. Mod. Phys.*, 71(3):463–512, apr 1999.
- [177] Matthew J. Davis and P. Blair Blakie. Critical temperature of a trapped Bose gas: Comparison of theory and experiment. *Phys. Rev. Lett.*, 96(6):060404, feb 2006.
- [178] Robert P. Smith, Naaman Tammuz, Robert L. D. Campbell, Markus Holzmann, and Zoran Hadzibabic. Condensed fraction of an atomic Bose gas induced by critical correlations. *Phys. Rev. Lett.*, 107(19):1–5, 2011.
- [179] J. Esteve, J.-B. Trebbia, T. Schumm, A. Aspect, C. I. Westbrook, and I. Bouchoule. Observations of density fluctuations in an elongated bose gas: Ideal gas and quasicondensate regimes. *Phys. Rev. Lett.*, 96:130403, Apr 2006.
- [180] Thibaut Jacqmin, Julien Armijo, Tarik Berrada, Karen V. Kheruntsyan, and Isabelle Bouchoule. Sub-poissonian fluctuations in a 1d bose gas: From the quantum quasicondensate to the strongly interacting regime. *Phys. Rev. Lett.*, 106:230405, Jun 2011.
- [181] C.-S. Chuu, F. Schreck, T. P. Meyrath, J. L. Hanssen, G. N. Price, and M. G. Raizen. Direct observation of sub-Poissonian number statistics in a degenerate Bose gas. *Phys. Rev. Lett.*, 95:260403, Dec 2005.
- [182] D. S. Petrov, G. V. Shlyapnikov, and J. T. M. Walraven. Regimes of quantum degeneracy in trapped 1d gases. *Phys. Rev. Lett.*, 85:3745–3749, 2000.
- [183] D. S. Petrov, G. V. Shlyapnikov, and J. T. M. Walraven. Phase-fluctuating 3d bose-einstein condensates in elongated traps. *Phys. Rev. Lett.*, 87:050404, Jul 2001.
- [184] S. Dettmer, D. Hellweg, P. Rytty, J. J. Arlt, W. Ertmer, K. Sengstock, D. S. Petrov, G. V. Shlyapnikov, H. Kreutzmann, L. Santos, and M. Lewenstein. Observation of Phase Fluctuations in Elongated Bose-Einstein Condensates. *Phys. Rev. Lett.*, 87(16):160406, October 2001. arXiv: [cond-mat/0105525](https://arxiv.org/abs/cond-mat/0105525) Publisher: American Physical Society Genre: Statistical Mechanics.
- [185] Louise Wolswijk, Carmelo Mordini, Arturo Farolfi, Dimitris Trypogeorgos, Franco Dalfovo, Alessandro Zenesini, Gabriele Ferrari, and Giacomo Lamporesi.

- Measurement of the order parameter and its spatial fluctuations across bose-einstein condensation. *Phys. Rev. A*, 105:033316, Mar 2022.
- [186] T Vibel, M B Christensen, R M F Andersen, L N Stokholm, K Pawłowski, K Rzażewski, M A Kristensen, and J J Arlt. Atom number fluctuations in Bose gases—statistical analysis of parameter estimation. *Journal of Physics B: Atomic, Molecular and Optical Physics*, 57(19):195301, sep 2024.
- [187] Miroslav Gajdacz, Poul Lindholm Pedersen, Troels Mørch, Andrew Hilliard, Jan Arlt, and Jacob Sherson. Non-destructive Faraday imaging of dynamically controlled ultracold atoms. *Rev. Sci. Instrum.*, 84(8):083105, August 2013.
- [188] G. Reinaudi, T. Lahaye, Z. Wang, and D. Guery-Odelin. Strong saturation absorption imaging of dense clouds of ultracold atoms. *Opt. Lett.*, 32(21):3143, July 2007.
- [189] Klaus Hueck, Niclas Luick, Lennart Sobirey, Jonas Siegl, Thomas Lompe, Henning Moritz, Logan W. Clark, and Cheng Chin. Calibrating high intensity absorption imaging of ultracold atoms. *Opt. Express*, 25(8):8670–8679, Apr 2017.
- [190] Romain Veyron, Vincent Mancois, Jean-Baptiste Gerent, Guillaume Baclet, Philippe Bouyer, and Simon Bernon. Quantitative absorption imaging: The role of incoherent multiple scattering in the saturating regime. *Phys. Rev. Research*, 4(3):033033, July 2022.
- [191] T. Vibel, M. B. Christensen, M. A. Kristensen, J. J. Thuesen, L. N. Stokholm, C. A. Weidner, and J. J. Arlt. Spatial calibration of high-density absorption imaging. *Journal of Physics B: Atomic, Molecular and Optical Physics*, 57(14):145301, June 2024.
- [192] J. Szczepkowski, R. Gartman, M. Witkowski, L. Tracewski, M. Zawada, and W. Gawlik. Analysis and calibration of absorptive images of Bose-Einstein condensate at nonzero temperatures. *Rev. Sci. Instrum.*, 80(5):053103, May 2009.
- [193] Wolfgang Ketterle, D. S. Durfee, and D. M. Stamper-Kurn. Making, probing and understanding Bose-Einstein condensates. In M Inguscio, S Stringari, and C E Wieman, editors, *Proceedings of the International School of Physics “Enrico Fermi”*. Società Italiana di Fisica, 1999.
- [194] Wolfgang Muessel, Helmut Strobel, Maxime Joos, Eike Nicklas, Ion Stroescu, Jiří Tomkovič, David B. Hume, and Markus K. Oberthaler. Optimized absorption imaging of mesoscopic atomic clouds. *Appl. Phys. B*, 113(1):69–73, Oct 2013.
- [195] D. Genkina, L. M. Ayccock, B. K. Stuhl, H.-I. Lu, R. A. Williams, and I. B. Spielman. Feshbach enhanced s-wave scattering of fermions: Direct observation with optimized absorption imaging. *New J. Phys.*, 18(1):013001, December 2015.
- [196] Andika Putra, Daniel L. Campbell, Ryan M. Price, Subhadeep De, and I. B. Spielman. Optimally focused cold atom systems obtained using density-density correlations. *Rev. Sci. Instrum.*, 85(1):013110, January 2014.
- [197] M. Pappa, P. C. Condylis, G. O. Konstantinidis, V. Bolpasi, A. Lazoudis, O. Morizot, D. Sahagun, M. Baker, and W. von Klitzing. Ultra-sensitive atom imaging for matter-wave optics. *New J. Phys.*, 13(11):115012, November 2011.
- [198] Munekazu Horikoshi, Aki Ito, Takuya Ikemachi, Yukihito Aratake, Makoto Kuwata-Gonokami, and Masato Koashi. Appropriate probe condition for absorption imaging of ultracold 6li atoms. *J. Phys. Soc. Jpn.*, 86(10):104301, oct 2017.
- [199] Bernd Lücke. Multi-particle entanglement in a spinor Bose-Einstein condensate for quantum-enhanced interferometry. PhD thesis, Gottfried Wilhelm Leibniz Universität Hannover, 2014.
- [200] C. F. Ockeloen, A. F. Tauschinsky, R. J. C. Spreeuw, and S. Whitlock. Detection of small atom numbers through image processing. *Phys. Rev. A*, 82(6):061606, December 2010.
- [201] Linxiao Niu, Xinxin Guo, Yuan Zhan, Xuzong Chen, W. M. Liu, and Xiaoji Zhou. Optimized fringe removal algorithm for absorption images. *Appl. Phys. Lett.*, 113(14):144103, October 2018.
- [202] Gal Ness, Anastasiya Vainbaum, Constantine Shkedrov, Yanay Florshaim, and Yoav Sagi. Single-exposure absorption imaging of ultracold atoms using deep learning. *Phys. Rev. Applied*, 14(1):014011, July 2020.
- [203] Bo Song, Chengdong He, Zejian Ren, Entong Zhao, Jeongwon Lee, and Gyu-Boong Jo. Effective statistical fringe removal algorithm for high-sensitivity imaging of ultracold atoms. *Phys. Rev. Applied*, 14(3):034006, September 2020.
- [204] Jan Klaers, Julian Schmitt, Tobias Damm, Frank Vewinger, and Martin Weitz. Statistical physics of Bose-Einstein-condensed light in a dye microcavity. *Phys. Rev. Lett.*, 108:160403, Apr 2012.
- [205] Julian Schmitt, Tobias Damm, David Dung, Frank Vewinger, Jan Klaers, and Martin Weitz. Observation of grand-canonical number statistics in a photon Bose-Einstein condensate. *Phys. Rev. Lett.*, 112:030401, Jan 2014.
- [206] E. C. I. van der Wurff, A.-W. de Leeuw, R. A. Duine, and H. T. C. Stoof. Interaction effects on number fluctuations in a bose-einstein condensate of light. *Phys. Rev. Lett.*, 113:135301, Sep 2014.
- [207] Fahri Emre Öztürk, Frank Vewinger, Martin Weitz, and Julian Schmitt. Fluctuation-dissipation relation for a bose-einstein condensate of photons. *Phys. Rev. Lett.*, 130:033602, Jan 2023.
- [208] Fahri Emre Ozturk, Tim Lappe, Göran Hellmann, Julian Schmitt, Jan Klaers, Frank Vewinger, Johann Kroha, and Martin Weitz. Fluctuation dynamics of an open photon bose-einstein condensate. *Phys. Rev. A*, 100:043803, Oct 2019.
- [209] Jिंगgang Xiang, Enid Cruz-Colón, Candice C. Chua, William R. Milner, Julius de Hond, Jacob F. Fricke, and Wolfgang Ketterle. In situ imaging of the thermal de Broglie wavelength in an ultracold Bose gas. *arXiv*, November 2024.
- [210] Joris Verstraten, Kunlun Dai, Maxime Dixmierias, Bruno Peaudecerf, Tim de Jongh, and Tarik Yefsah. In-situ Imaging of a Single-Atom Wave Packet in Continuous Space. *arXiv*, April 2024.
- [211] Ruixiao Yao, Sungjae Chi, Mingxuan Wang, Richard J. Fletcher, and Martin Zwierlein. Measuring pair correlations in bose and fermi gases via atom-resolved microscopy. *arXiv*, 2024.
- [212] Cosetta Baroni, Giacomo Lamporesi, and Matteo Zaccanti. Quantum mixtures of ultracold gases of neutral atoms. *Nature Reviews Physics*, 6(12):736–752, November 2024.
- [213] Lauriane Chomaz, Igor Ferrier-Barbut, Francesca Ferlaino, Bruno Laburthe-Tolra, Benjamin L Lev, and Tilman Pfau. Dipolar physics: a review of experiments with magnetic quantum gases. *Reports on Progress in Physics*, 86(2):026401, dec 2022.
- [214] Miłosz Panfil and Jean-Sébastien Caux. Finite-temperature correlations in the lieb-liniger one-dimensional bose gas. *Phys. Rev. A*, 89:033605, Mar 2014.
- [215] Igor Ferrier-Barbut, Holger Kadau, Matthias Schmitt, Matthias Wenzel, and Tilman Pfau. Observation of quantum droplets in a strongly dipolar bose gas. *Phys.*

- Rev. Lett., 116:215301, May 2016.
- [216] L. Chomaz, S. Baier, D. Petter, M. J. Mark, F. Wächtler, L. Santos, and F. Ferlaino. Quantum-fluctuation-driven crossover from a dilute bose-einstein condensate to a macrodroplet in a dipolar quantum fluid. Phys. Rev. X, 6:041039, Nov 2016.
- [217] Mingyang Guo, Fabian Böttcher, Jens Hertkorn, Jan-Niklas Schmidt, Matthias Wenzel, Hans Peter Büchler, Tim Langen, and Tilman Pfau. The low-energy Goldstone mode in a trapped dipolar supersolid. Nature, 574:386–389, October 2019.
- [218] L. Chomaz, D. Petter, P. Ilzhöfer, G. Natale, A. Trautmann, C. Politi, G. Durastante, R. M. W. van Bijnen, A. Patscheider, M. Sohmen, M. J. Mark, and F. Ferlaino. Long-lived and transient supersolid behaviors in dipolar quantum gases. Phys. Rev. X, 9:021012, Apr 2019.
- [219] Shai Ronen and John L. Bohn. Dipolar bose-einstein condensates at finite temperature. Phys. Rev. A, 76:043607, Oct 2007.
- [220] Christopher Ticknor. Finite-temperature analysis of a quasi-two-dimensional dipolar gas. Phys. Rev. A, 85:033629, Mar 2012.
- [221] R. N. Bisset, D. Baillie, and P. B. Blakie. Finite-temperature trapped dipolar bose gas. Phys. Rev. A, 86:033609, Sep 2012.
- [222] Krzysztof Pawłowski, Przemysław Bienias, Tilman Pfau, and Kazimierz Rzǎżewski. Correlations of a quasi-two-dimensional dipolar ultracold gas at finite temperatures. Phys. Rev. A, 87:043620, Apr 2013.
- [223] Abdelâali Boudjemâa. Theory of excitations of dipolar Bose–Einstein condensate at finite temperature. J. Phys. B: At. Mol. Opt. Phys., 48(3):035302, January 2015.
- [224] E. Aybar and M. Ö. Oktel. Temperature-dependent density profiles of dipolar droplets. Phys. Rev. A, 99(1):013620, January 2019.
- [225] D. S. Petrov. Quantum mechanical stabilization of a collapsing bose-bose mixture. Phys. Rev. Lett., 115:155302, Oct 2015.
- [226] Renate Landig, Lorenz Hruby, Nishant Dogra, Manuele Landini, Rafael Mottl, Tobias Donner, and Tilman Esslinger. Quantum phases from competing short- and long-range interactions in an optical lattice. Nature, 532(7600):476–479, Apr 2016.
- [227] Ferdinand Brennecke, Tobias Donner, Stephan Ritter, Thomas Bourdel, Michael Köhl, and Tilman Esslinger. Cavity qed with a Bose–Einstein condensate. Nature, 450(7167):268–271, 2007.
- [228] Kristian Baumann, Christine Guerlin, Ferdinand Brennecke, and Tilman Esslinger. Dicke quantum phase transition with a superfluid gas in an optical cavity. Nature, 464(7293):1301–U1, APR 29 2010.
- [229] J. Kasprzak, M. Richard, S. Kundermann, A. Baas, P. Jeambrun, J. M. J. Keeling, F. M. Marchetti, M. H. Szymanska, R. Andre, J. L. Staehli, V. Savona, P. B. Littlewood, B. Deveaud, and Le Si Dang. Bose-einstein condensation of exciton polaritons. Nature, 443(7110):409–414, SEP 28 2006.
- [230] R. Balili, V. Hartwell, D. Snoke, L. Pfeiffer, and K. West. Bose-einstein condensation of microcavity polaritons in a trap. Science, 316(5827):1007–1010, MAY 18 2007.
- [231] Esther Wertz, Lydie Ferrier, Dmitry D. Solnyshkov, Pascale Senellart, Daniele Bajoni, Audrey Miard, Aristide Lemaître, Guillaume Malpuech, and Jacqueline Bloch. Spontaneous formation of a polariton condensate in a planar gas microcavity. Applied Physics Letters, 95(5):051108, 08 2009.
- [232] Isabelle Bouchoule and Jérôme Dubail. Generalized hydrodynamics in the one-dimensional bose gas: theory and experiments. Journal of Statistical Mechanics: Theory and Experiment, 2022(1):014003, jan 2022.
- [233] A. Sinatra, Y. Castin, and E. Witkowska. Nondiffusive phase spreading of a bose-einstein condensate at finite temperature. Phys. Rev. A, 75:033616, Mar 2007.